Tekniska Högskolan i Lund
Avdelningen för Bärande Konstruktioner

Lund Institute of Technology
Department of Structural Engineering

Lund 1995

Rapport TVBK-5074

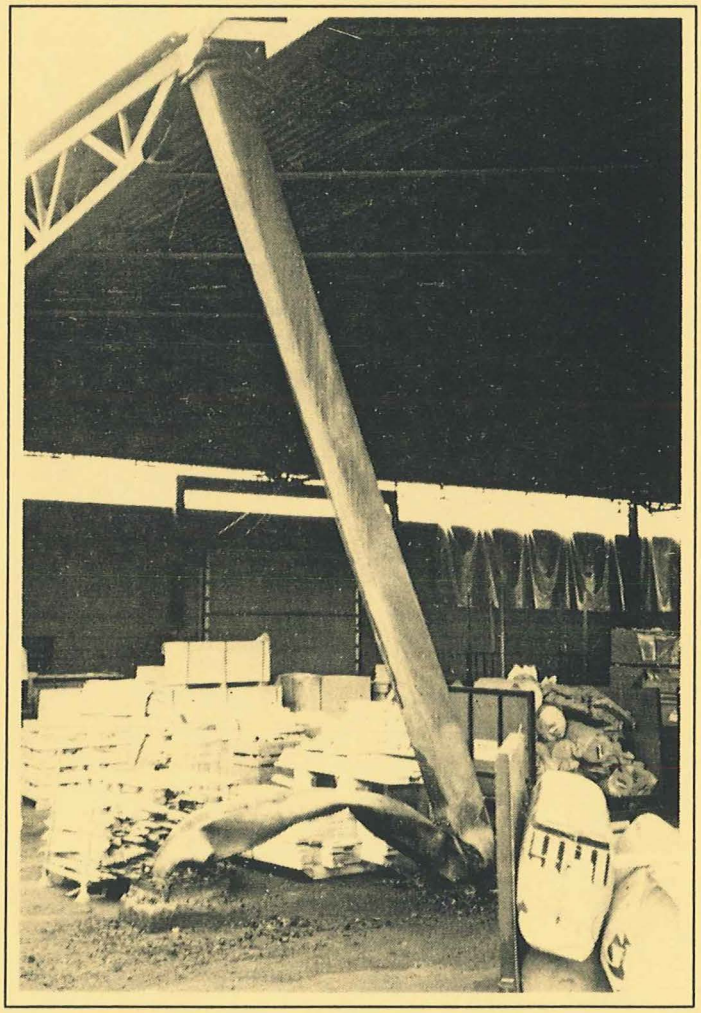

Steel Columns Under Partial Fire Exposure

A Theoretical Study

Jens Oredsson

Rapport TVBK-5074
ISSN 0349-4969
ISRN: LUTVDG/TVBK--5074-SE

Steel Columns Under Partial Fire Exposure

A Theoretical Study

EXAMENSARBETE TVBK-5074

Handledare: Sven Thelandersson

LUND Januari1995

Jens Oredsson

CONTENTS

Summary

In conformity with all sorts of construction design, the fire engineering design is a very important part in the planning of a construction project. Thus it is essential to know the performance of structures, exposed to fire, under various combinations of adjoining parameters. This issue has to be incorporated in the structural design procedure in order to get a satisfactory coverage of the accidental situation of fire.

The adopted fire engineering design methods for steel structures of today are based on the generalisation that cross-sectional temperatures remain constant in the cross-section plane, however increasing continuously with time. From computer simulations and tests though, it is known that the real temperature distribution diverges substantially from this assumption, when the fire exposes limited parts of the circumference. The simplification is of considerable importance, especially in design of steel columns, since the imposed cross-sectional temperature gradient will render a bending of the column. This bending is very crucial to columns since they carry axial loads that interact with the lateral deflection and hence will produce a bending moment in the column.

In order to assess a more comprehensive foundation for future improvements of the structural design of steel structures, Dr. Yngve Anderberg, Fire Safety Design AB, has initiated a project study in the field of; "Partially fire exposed steel columns". This report is one of the "fruits" of the mentioned initiative.

The purpose of the report is to investigate the effects of partial fire exposure on columns, and to determine the accuracy of the generalised assumption of constant cross-sectional temperatures, applied in present codes. In order to accomplish this, a parameter study was made to illuminate the behaviour of steel columns due to various types of fire exposure. Two degrees of fire exposure, viz. 83% and 100% of the circumference, were selected. These two conditions have been studied for various combinations of adjoining parameters, such as: time temperature relationship, degree of loading, slenderness, eccentricity and restrained elongation. The investigation is performed by means of computer simulations.

The results obtained, have shown the interesting phenomenon, that for the present case of partial fire exposure (i.e. 83% of the circumference) and under the combined influence of the adjoining parameters adopted, partial fire exposure is more disadvantageous to a column´s load-bearing capacity than the corresponding case, with fire exposure on all faces. Hence considering cross-sections with a large temperature gradient, it is unacceptable to assume constant cross-sectional temperatures when designing for axially loaded columns.

The results are presented in terms of computer calculated failure predictions (i.e. points of time when the column, according to the computer program, fails to carry the applied initial axial load), displacement time charts, cross-section stress charts and cross-section strain charts.

There is a need for a further extension of this study to encompass a greater variety of partial fire exposures and axial restraints.

A modernisation of the present design code is thus necessary to undertake, that these effects from partial fire exposure can be compensated for and involved in the code. This way the original intention of a design code will be fulfilled, viz. always to provide a conservative design value.

Acknowledgements

The project was initiated and financed by Dr. Yngve Anderberg, Fire Safety Design AB, Lund Sweden. Formulation of parametrical study was mutually agreed on by Dr. Anderberg and the author.

Computer equipment and software as well as literature and office space has been supplied by Fire Safety Design AB.

The author would like to express his gratitude to the management and all employees at Fire Safety Design AB.

During the progress of the project assistance in solving theoretical obstacles has been provided by Professor Sven Thelandersson, Department of Structural Engineering at Lund Institute of Technology.

Detailed and fundamental technical support in theoretical matters as well as in the managing of the software, has been offered by MSc in Civil Engineering, Fredrik Holst, former employee at Fire Safety Design AB, to whom the author owes the answer of many questions.

Thanks are also due to everybody who have read and pointed out issues that needed to be corrected.

In projects there are always times that are bothersome, thus it´s a great asset to have in your possession a never ceasing source of encouragement and support; for this I thank Carola Joelsson.

Lund in January, 1995

Jens Oredsson

Symbols

symbols	definition	dimension
A	cross section area	mm^2
E	Youngs modulus of elasticity at room temperature	$N\ mm^{-2}$
E(T)	Youngs modulus of elasticity at elevated temperature	$N\ mm^{-2}$
G	shear modulus	$N\ mm^{-2}$
I	moment of inertia	m^4
L	member length	m
L_c, l_c	system length	m
M	moment	N m
M_{Sd}	design moment	N m
$M_{fi,t,Rd}$	design moment resistance with respect to temperature	N m
N	axial load	N
N_{cr}	buckling load according to the Euler buckling theory	N
$N_{c,Rd}$	design compression resistance	N
$N_{b,Rd}$	design buckling resistance of a compression member	N
N_{Sd}	axial design load	N
$N_{fi,t,Rd}$	axial design resistance with respect to temperature	N
T	temperature	°C
T_g	gas temperature	°C
T_b	boundary temperature	°C
Q	generated heat	$W\ m^{-3}$
W	elastic section modulus	m^3
b	cross section width	mm
c	specific heat	$J\ kg^{-1}\ °C^{-1}$
d_f	flange thickness	mm
d_w	web thickness	mm
e	eccentricity	mm
e_0	initial out of straightness	mm
f_y	yield stress at room temperature	Pa
$f_y(T)$	yield stress at elevated temperatures	Pa
f_p	proportional stress limit	Pa
f_u	ultimate strength	Pa
h	height of cross section	mm
i	radius of gyration	mm
$k_{x,y}$	thermal conductivity	$W\ m^{-1}\ °C^{-1}$
q_n	heat flow at the boundary	$W\ m^{-2}$
t	time	min
u	displacement in x direction	mm
w	displacement in z direction	mm
x	x-axis	mm
y	y-axis, distance from neutral layer to considered cross sectional position	mm
z	z-axis	mm
α	expansion coefficient	$°C^{-1}$
α_k	convection heat transfer coefficient	$W\ m^{-2}\ °C^{-1}$
β_M	equivalent uniform moment factor	-
γ	factor of restrained thermal elongation	-
γ_{M1}	partial safety factor	-

Symbols

symbols	definition	dimension
A	cross section area	mm^2
E	Youngs modulus of elasticity at room temperature	$N\ mm^{-2}$
E(T)	Youngs modulus of elasticity at elevated temperature	$N\ mm^{-2}$
G	shear modulus	$N\ mm^{-2}$
I	moment of inertia	m^4
L	member length	m
L_c, l_c	system length	m
M	moment	N m
M_{Sd}	design moment	N m
$M_{fi,t,Rd}$	design moment resistance with respect to temperature	N m
N	axial load	N
N_{cr}	buckling load according to the Euler buckling theory	N
$N_{c,Rd}$	design compression resistance	N
$N_{b,Rd}$	design buckling resistance of a compression member	N
N_{Sd}	axial design load	N
$N_{fi,t,Rd}$	axial design resistance with respect to temperature	N
T	temperature	°C
T_g	gas temperature	°C
T_b	boundary temperature	°C
Q	generated heat	$W\ m^{-3}$
W	elastic section modulus	m^3
b	cross section width	mm
c	specific heat	$J\ kg^{-1}\ °C^{-1}$
d_f	flange thickness	mm
d_w	web thickness	mm
e	eccentricity	mm
e_0	initial out of straightness	mm
f_y	yield stress at room temperature	Pa
$f_y(T)$	yield stress at elevated temperatures	Pa
f_p	proportional stress limit	Pa
f_u	ultimate strength	Pa
h	height of cross section	mm
i	radius of gyration	mm
$k_{x,y}$	thermal conductivity	$W\ m^{-1}\ °C^{-1}$
q_n	heat flow at the boundary	$W\ m^{-2}$
t	time	min
u	displacement in x direction	mm
w	displacement in z direction	mm
x	x-axis	mm
y	y-axis, distance from neutral layer to considered cross sectional position	mm
z	z-axis	mm
α	expansion coefficient	$°C^{-1}$
α_k	convection heat transfer coefficient	$W\ m^{-2}\ °C^{-1}$
β_M	equivalent uniform moment factor	-
γ	factor of restrained thermal elongation	-
γ_{M1}	partial safety factor	-

ΔT	temperature difference	°C,K
ΔL	elongation	m
ΔL_{lim}	space available for elongation	m
$\Delta\sigma$	additional stress contribution due to restrained elongation	Pa (N m^2)
ε_{tot}	total strain	-
ε_{th}	thermal strain	-
ε_{σ}	stress related strain	-
ε_{cr}	creep strain	-
ε_{pl}	plastic strain	-
ε_{y}	yield strain	-
ε_{ρ}	resulting emissivity	-
λ	slenderness ratio	-
λ	thermal conductivity	W m^{-1} K^{-1}
ν	Poisson´s ratio	-
ρ	density	kg m^{-3}
σ	stress	Pa (N m^2)
σ	Stefan-Bolzman constant	-
χ	empirical correction factor for the buckling phenomenon	-

1 INTRODUCTION

1.1 Background

The occurrence of a fire can be devastating and accordingly has to be prevented if possible. However, regardless of the extent of preventive measures taken, fires will occasionally occur and thus the importance of a sophisticated fire protection engineering design should be emphasised. This kind of protective action is called passive fire protection. Its obligation is to keep the building functional for a certain length of time, so that people located in the building will be able to rescue themselves.

The fire engineering design methods employed today are based on the assumption that the cross-sectional temperature is constant across the height of the cross-section, during the progress of fire. In accordance with knowledge obtained from advanced computer simulations however, it has been concluded that the temperature will not be constant but vary in the cross-section. The error made by the assumption will increase if the fire exposes a limited part of the circumference. This is due to the enhancement of the temperature gradient that will take part. The problem is most essential when considering axially loaded steel columns, since the temperature gradient will cause bending and an eccentricity to the axial load. The cross-sectional temperature enhancement will also reduce the material parameters of yield strength and modulus of elasticity. This means that in order to determine the stiffness of the structure an integration across the cross-section has to be undertaken.

The facts pointed out above underline the importance of modernising and continuing the development of a more detailed design guide for steel columns. In order to accomplish this, the lack of studies on this aspect of fire design has to be compensated for and the research must be intensified that these effects from partial fire exposure can be quantified and incorporated in the design procedure.

1.2 Purpose and scope of investigation

The purpose of the investigation presented, is to study the effects of unsymmetrical fire exposure. The calculations undertaken in this study are intended to illuminate how a member exposed to fire on a limited part of the circumference compare to a member that is exposed to fire on all faces. Any differences between these two cases, under any combination of adjoining parameters, are very interesting. Of particular interest are cases where a limited degree of fire exposure would be the more disadvantageous situation. It has been a prevailing point of view that fire exposure on all faces render the most disadvantageous circumstances, since the temperature is spread a lot faster in the cross-section. The present design code is based on that reasoning and results opposing this would therefore be important to put forward and involve in the design process.

Additional parameters that were considered to have a special influence on the columns behaviour, have been included in the study.

These are:

- time-temperature relationship
- degree of loading,
- slenderness
- eccentricity
- restrained elongation

The investigation has been accomplished by means of a combination of literature studies and computer simulations. In the computer simulations, use have primarily been made of two finite element programs, viz. Super-Tempcalc and Steelfire. For verification of these two computer programs the reader is referred to /4/ and /11/ in the reference list.

The material model and the material data are all in accordance with Eurocode, as are partial safety coefficients and miscellaneous other reduction factors and calculations. The material steel and its properties are presented in chapter two together with a characterisation of stresses and strains. In chapter three the effect of a temperature variation in the cross-section is introduced. Chapter four summarises the significations of steel columns. Simulations and analyses of results are dealt with in chapters five and six. Conclusions are given in chapter seven. In the appendix the graphical results from the simulations can be found among other things.

Figures, equations and tables are numbered with a numeral combination where the first figure coincides with the current chapter and the following is a number of the figure/equation/table in consecutive order within each chapter.

1.3 Limitations and assumptions

The cross-section of all columns studied is a hot rolled profile, type HEB 300.

Out of the instability effects only flexural buckling has been considered, and hence measures are presumed to be taken against other modes of buckling. Furthermore the column is asumed to be braced against buckling around the weak axis.

No creep strain is regarded, in accordance with suggestions in Eurocode.

It is assumed that the cross-section temperature is constant along the length of the column. The Bernoulli assumption is expected to hold, i.e. plane cross-sections remain plane and perpendicular to the H-beam axis during the progress of deformation. Angles of deformation are taken to be small, hence $\tan\alpha \approx \alpha$ (α equal to angle of deformation).

2 PROPERTIES OF STEEL

Knowing the characteristics of the material used, is of great significance in the design work of a structure. In this chapter the properties of steel will be presented at room temperature and as a function of the temperature.

2.1 Chemical composition

Steel is an alloy with iron being the main "ingredient". Carbon, silicon, manganese, phosphorus and sulphur compose the remaining components, their part range from round about 1% to a few hundredths percent each. Thus the material consists of a great many chemical components with different properties and abilities. It is therefore possible to control the properties of the steel in a desirable way by adjusting the dozes of the components included. Out of the chemicals mentioned above carbon is the one that has the greatest influence on the final product and with which significant alterations of great importance can be accomplished. For instance, the ability of steel to harden is only achievable at a minimum contents of carbon of 0.3%. Hot rolled structural steel is not hardened. It contains between 0.1 and 0.2% of carbon.

2.2 Design values of material coefficients

The material coefficients adopted in the present calculations for steel are, according to Eurocode:

- $E=210\ 000\ N/mm^2$ modulus of elasticity (Young´s modulus)
- $G=E/(2(1+\nu))\ N/mm^2$ shear modulus
- $\nu=0.3$ Poisson´s ratio
- $\rho=7850\ kg/m^3$ density

Coefficients omitted here require a more thorough introduction and will be dealt with further on in the report.

2.3 Stress - strain relations

Stress and strain are, in the proportional range, related to each other through Hooke´s law.

$$\sigma = E*\varepsilon \qquad \text{(eq 2.1)}$$

Fig 2.1 shows how a steel specimen responds when exposed to a certain magnitude of stress at 20 degrees Celsius (eq 2.1 applies to the linear part of the curve). As will be shown later on in this chapter, this curve changes when the effects of an elevated temperature are involved. There will also be a decrease in steel strength and Young´s modulus with increasing temperature.

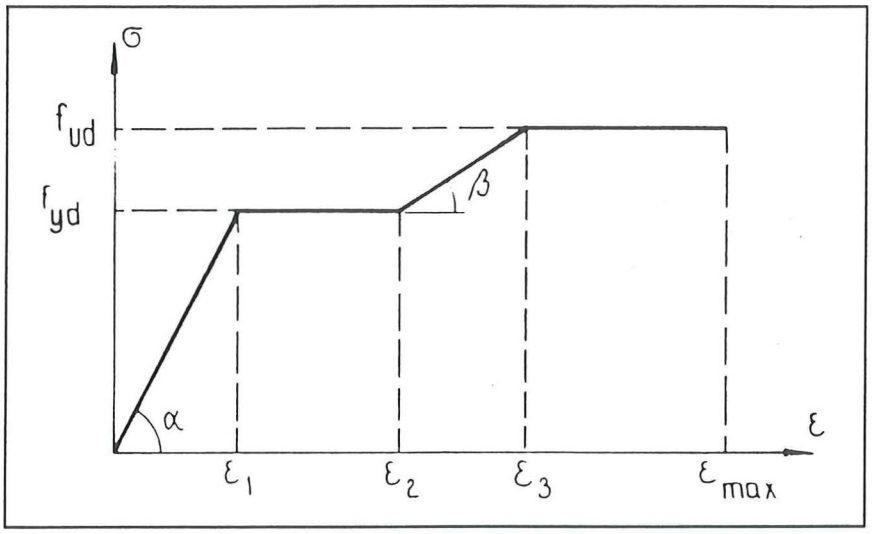

Fig 2.1 Strength-strain relationship for steel at room temperature /10/.

2.3.1 Cross-sectional forces

Cross-sectional forces and moments are the resultants to the stress distribution in the cross-section. Knowing the magnitude of stress, it is possible to decide whether or not the proportional or the yield limit of fig 2.1 has been exceeded.

For a given value of the axial force, N, and the moment, M, the stress, σ, is in the elastic phase obtained by Navier´s formula (eq 2.2).

$$\sigma = \frac{N}{A} + \frac{M}{I} * y \qquad \text{(eq 2.2)}$$

where y is the distance from the neutral axis to the considered position in the cross-section. A is the cross-sectional area and I is the moment of inertia of the cross-section.

Fig 2.2 illustrates the stress distribution due to axial force and moment, the sum of them determine the total stress distribution.

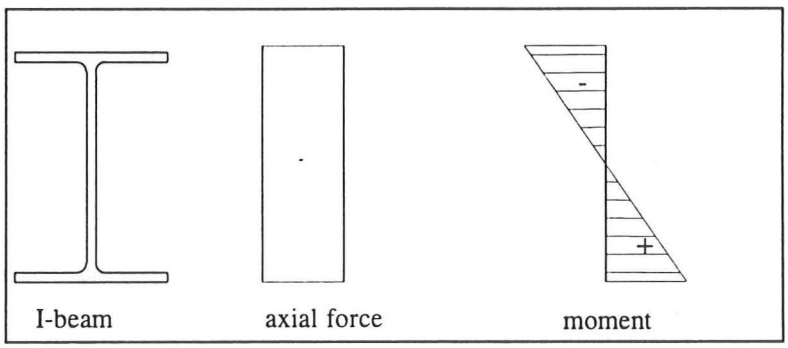

Fig 2.2 Stress contribution from axial force and moment.

2.3.2 Kinematic relation

Strain is defined as elongation per unit length. It occurs either when the structure is exposed to external forces or when thermal expansion is regarded. In accordance with eq 2.1, the shape of the strain distribution is equal to the shape of the corresponding stress distribution (fig 2.2). The total strain is related to the displacements of the beam axis by:

$$\varepsilon(y)_{tot} = \frac{du}{dx} - y^* \frac{d^2 w}{dx^2} \qquad \text{(eq 2.3)}$$

where

y = the distance between the neutral axis and the cross-sectional position regarded.

u = the axial displacement

w = the deflection perpendicular to the beam axis

2.3.3 Initial stresses

Depending on the method of manufacturing, initial stresses will occur in a structural element. As for hot rolling, which is the most usual way of producing I-beams, these are due to the time difference in cooling, over the cross-section. The regions cooling off first will be in compression and those cooling off later will be in tension. This is illustrated in fig 2.3.

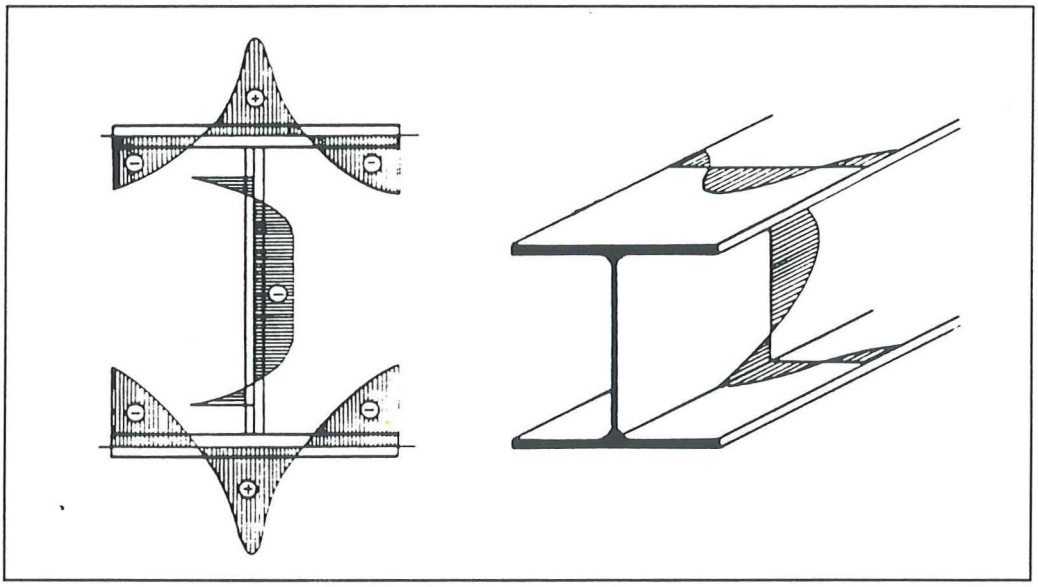

Fig 2.3 Illustration of initial stresses in a hotrolled I-beam /10/.

The effect of initial stresses will not affect the capacity in the fully plastic state. Considering slender structures like columns, the critical failure phenomenon is more likely to be from flexural buckling then from the plasticity, and thus the initial stresses have to be taken into account (c.f. chapter four).

2.3.4 Effects of temperature

Steel is very sensitive to increasing temperatures and its strength in compression and tension is dramatically reduced when exposed to fire. Thus all sorts of insulation, coating or other protectional measures normally should be taken to prevent the heat from penetrating the structure.

Considering the influence of temperature, the total strain, ε_{tot}, can now be expressed in components of stress related strain, ε_{σ}, and thermal strain, ε_{th}, (eq 2.4).

$$\varepsilon_{tot} = \varepsilon_{\sigma} + \varepsilon_{th} \qquad \text{(eq 2.4)}$$

It should be emphasised that for a statically determined beam element the stress related strain only experiences changes when the thermal strain is distributed in a nonlinear way. If not, the expansion is a pure rigid body motion which causes no stress, provided that the boundary conditions permit the structure an unrestrained expansion and rotation. The analytical expression of thermal strain is defined in section 2.4. The stress related strain is the component that is connected to the stress through the stress-strain relation (cf. fig 2.4).

Creep strain (ε_{cr}) is a time and temperature depending strain component, which for temperatures below 400 degrees Celsius can be disregarded. This component is omitted in the design principle given in Eurocode, and will not be dealt with in this report.

In fig 2.4 a modified version of fig 2.1 (stress-strain relationship) for higher temperatures is presented. Note that the higher the temperature, the flatter the slope of the elastic part of the curve, i.e. Young´s modulus decreases due to the temperature rise. Furthermore the yield stress limit, which was very significant at room temperature, tends to vanish as the temperature is increased. Hence it is not relevant to talk about a yield limit when considering elevated steel temperatures. For the design procedure however some sort of acceptable stress limit has to be defined. In Eurocode this limit has been set to the stress level that results in 2% residual strain (see indication in fig 2.4). Henceforth when the yield limit is mentioned for the case of elevated temperatures, this residual strain level is referred to.

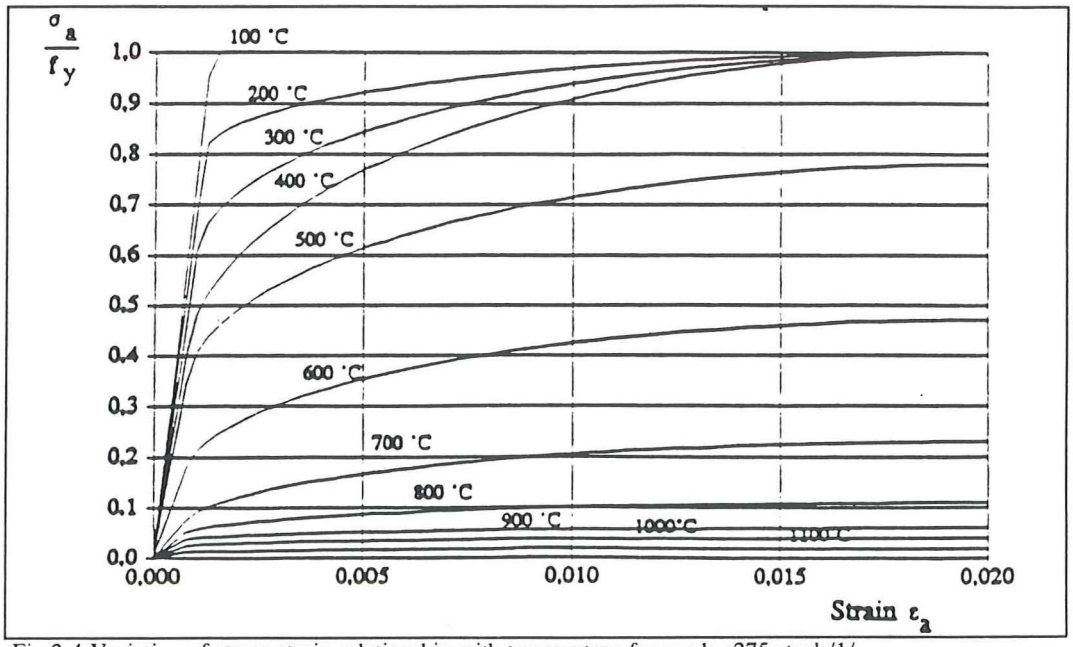

Fig 2.4 Variation of stress-strain relationship with temperature for grade s275 steel /1/.

Relating strength and Young´s modulus to its magnitudes at room temperature, the influence of the temperature is very clear and the chart in fig 2.5 expresses the decrease as a percentage.

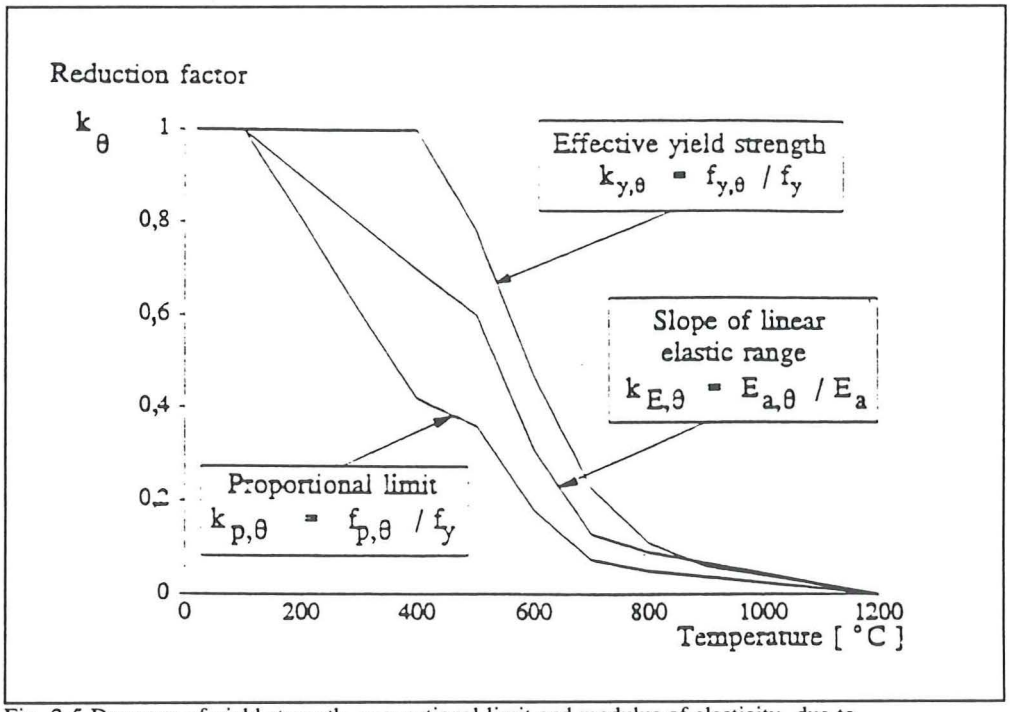

Fig. 2.5 Decrease of yield strength, proportional limit and modulus of elasticity, due to elevated temperatures, as represented in Eurocode. The strength is based on 2% residual strain / 1/.

The increase in temperature will result in a decrease in strength and modulus of elasticity. The curve for strength depends on the chosen level of residual strain. This is illustrated in fig 2.6 where the curves for 0.2%, 0.5%, 0.75% and 2.0% are displayed.

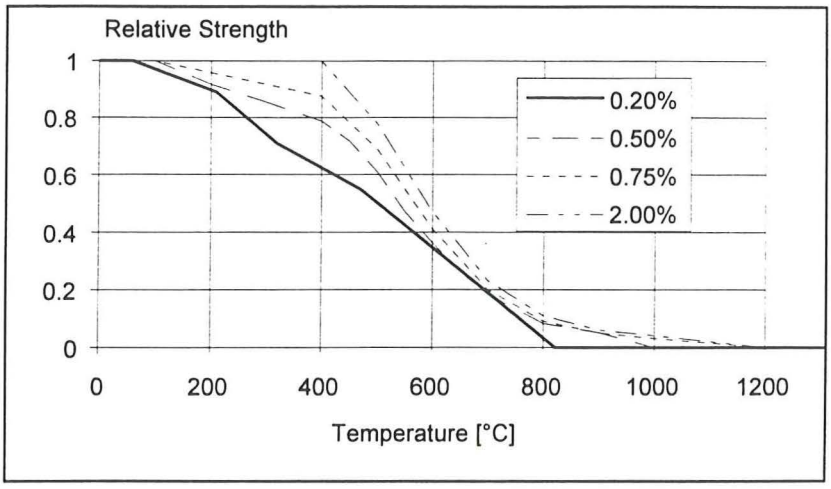

Fig 2.6 Relative strength as function of temperature for various magnitudes of residual strain /1/.

When using steel as a construction material, it is always of great importance to set the allowable degree of residual strain at an appropriate level, having considered the sensitivity of the structure. When designing for room-temperature, it is customary to allow a residual strain of 0.2%, meaning that a permanent deformation of 0.2% is acceptable. The opinions about the most accurate estimate of residual strain level at elevated temperatures are somewhat divided. In Eurocode 3 the 2%-criteria is maintained although there have been objections about this level of residual strain, saying that it is overestimating the capacity of the material. This applies especially to columns since their sensitivity to buckling and deflection is of great importance. It should however be emphasised that using this definition of stress has required the introduction of an empirical reduction factor (division by 1.2) in design of columns. This factor includes the effect of temperature increase on the buckling phenomenon, due to a more rapid decrease in the magnitude of Young´s modulus than in the yield limit (cf. fig 2.5).

Another general effect of the temperature is that the initial stresses, discussed previously, will be relaxed when the temperature increases. Including them in the analysis however, is being "on the safe side", since they disappear gradually and are not completely eliminated until there have been a significant raise in temperature.

2.4 Thermal expansion

Steel, being an isotropic material, has the same properties in all directions. One of these is the ability to expand when exposed to a temperature elevation. This expansion will cause a strain in the material. The thermal expansion can be described by:

$$\varepsilon_{th} = \alpha * \Delta T \qquad \text{(eq 2.5)}$$

The variable α can be expressed in many ways, for instance as a constant or as a linear variation of the temperature or as a polynomial function of the temperature. In Eurocode it has been given the following form (T in °C):

$$\varepsilon_{th} = 1.2*10^{-5}*T + 0.4*10^{-8}*T^2 - 2.416*10^{-4} \qquad 20°C \le T < 750°C$$
$$\varepsilon_{th} = 1.1*10^{-2} \qquad 750°C \le T \le 860°C$$
$$\varepsilon_{th} = 2*10^{-5}*T - 6.2*10^{-3} \qquad 860°C < T \le 1200°C$$

(eq 2.6)

In fig 2.6, equation 2.6 is represented in a chart.

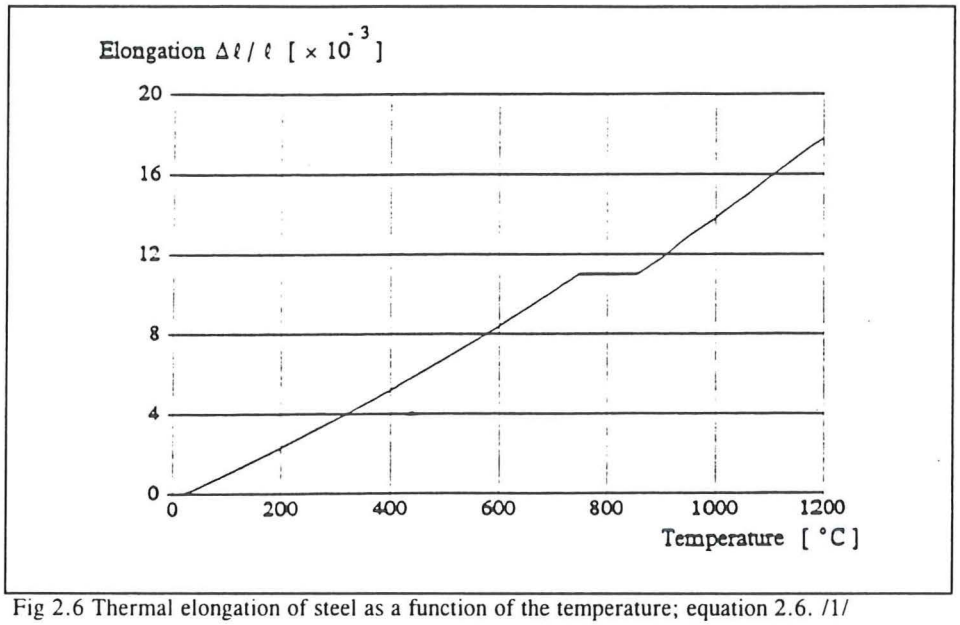

Fig 2.6 Thermal elongation of steel as a function of the temperature; equation 2.6. /1/

In simple calculation methods the ratio between thermal expansion and steel temperature change may be considered to be constant. In this case the value of the constant is set to $14*10^{-6}$ in Eurocode, and hence the equation will be:

$$\varepsilon_{th} = 14*10^{-6}(T - 20) \qquad \text{(eq 2.7)}$$

2.5 Miscellaneous thermally related parameters

The two most important thermal properties of steel are specific heat and conductivity. These are shown in fig 2.7 and fig 2.8 below, as they are presented in Eurocode.

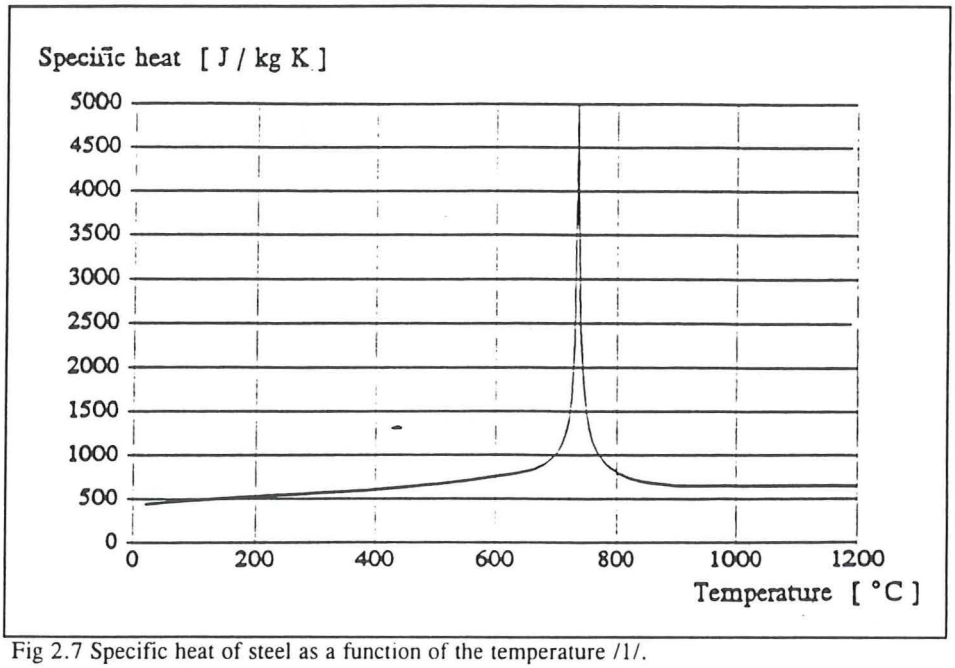

Fig 2.7 Specific heat of steel as a function of the temperature /1/.

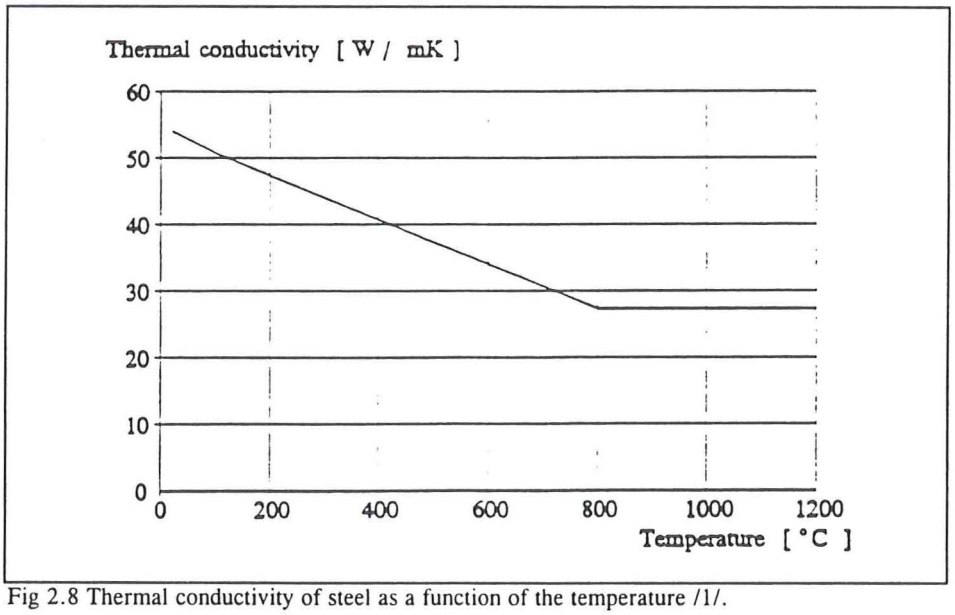

Fig 2.8 Thermal conductivity of steel as a function of the temperature /1/.

3 EFFECTS OF TEMPERATURE DISTRIBUTION IN THE CROSS-SECTION

The following types of temperature distributions over the cross-section will be considered in this section:

- constant
- linear
- nonlinear

It should be stressed that only the third gives a fully correct description of reality. A real temperature distribution can always be separated into a combination of the three. Regardless of the fire exposure on the profile´s circumference, a nonlinear distribution will be obtained in the cross-section. Normally the temperature in a member exposed to fire on the entire circumference will be approximated as constant, and a partly exposed member will be given a linear temperature distribution. This is not correct but may be a rather good approximation in many situations.

The cross-sectional temperature distributions along the length of the column is always assumed to be constant in this report.

In section 2.3.4 general effects from temperature elevations are discussed. Apart from these there are structural effects as well, depending on the appearance of the temperature distribution, which will be further looked into now from an elastic point of view.

3.1 Constant temperature distribution

For a constant temperature distribution the expansion of the structure is uniform, and accordingly a pure axial translation. No stress will be developed in the material provided that the expansion is unrestrained.

3.1.1 Restrained structures

If the structure is restrained axially, a constraint force will act on the member. In section 2.4 the properties of steel concerning thermal expansion were given. Considering axially loaded steel columns subjected to fire, it is important not to forget that the magnitude of the strain, that originates in the loading, will increase as the temperature reduces the value of Young´s modulus. In other words the column can expand an additional distance compared to the original expansion restriction (cf. second term of eq 3.1). The mathematical expression for the total elongation of axially loaded steel columns is given in eq 3.1; formulas retrieved from /7/.

$$\Delta L = \alpha \Delta T L - \frac{NL}{A}\left(\frac{1}{E(T)} - \frac{1}{E_0}\right) \qquad \text{(eq 3.1)}$$

$$\Delta\sigma = \frac{\Delta L}{L} * E(T) * (1-\gamma) \qquad \text{(eq 3.2)}$$

In order to define the restraint elongation, the parameter γ is introduced, which is the percentage of the desired elongation that is available for expansion. The remaining part $(1-\gamma)$ causes the constraint. In eq 3.3 the formula for the limited allowable expansion is shown.

$$\Delta L_{lim} = \gamma \Delta L \qquad \text{(eq 3.3)}$$

ΔL_{lim} = space available for unrestrained elongation

The effects of this parameter has been studied in the simulations and is presented in chapter 5.

The phenomenon is by no means exclusive to this type of temperature distribution, but will be present in all problems, presumed that the expansion restrictions are conserved.

3.2 Linear temperature distribution

Assuming a linear temperature distribution over the cross-section, the cross-sectional expansion will also be linear. This expansion is not subjected to any constraint in any way, because every fibre in the cross-section is extending exactly as much as is desired. A new stage of equilibrium has simply been reached, based on the present temperature conditions in the studied structure. The rate of expansion is larger in one flange than the other, thus in order to fulfil the Bernoulli assumption, that plane cross-sections remain plane and perpendicular to the bending axis during loading, this will cause a bowing of the structure. Most building materials thermally expand when exposed to a fire, this applies to metals, concrete and masonry. Being an exception though is timber, reacting in the exact opposite way due to shrinkage from loss of moisture. Fig 3.1 illustrates the bowing of a column. Eq 3.4 presents an approximation of the magnitude of the total deflection due to unrestrained thermal bowing, the expression assuming:

- Bernoulli's assumption applicable
- small angles of deformation ($\tan\alpha \approx \alpha$)
- linear temperature gradient

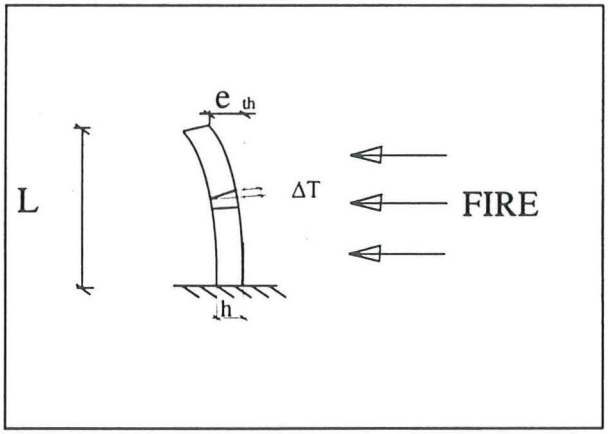

$$e_{th} = \alpha \Delta T L^2 / 2h \qquad \text{(eq 3.4)}$$

e_{th}: total thermal deflection

L: length

Fig 3.1 Unrestrained thermal bowing of a column due to a cross-sectional temperature gradient.

A non constant temperature distribution in the cross-section will also affect the stiffness of the structure, since the Young´s modulus is a temperature depending parameter. The total modified stiffness is shown in eq 3.5, where an integration over the cross-section is undertaken.

$$E^*I^* = \int E(y)y^2 dA \qquad \text{(eq 3.5)}$$

where

E^*I^* =modified temperature related stiffness

E(y) =E(T(y)); the variable y being the location in the cross-section.

T(y) =cross-sectional temperature at location y

3.3 Nonlinear temperature distribution

Imposing a nonlinear temperature gradient across the height of the cross-section, phenomena that have not been dealt with before will arise. There will be a conflict between the desire of the material to expand, according to the temperature, and the requirement that Bernoulli's assumption must hold. This conflict is of great significance and will in fact result in a new stress component, that originates in the cross-sectional constraint that will occur when the member is maintaining the shape of the cross-section. The constraint stress is self-balancing, i.e. the sum of compression and tension along the cross-section is equal to zero. In fig 3.2 and 3.3 the cross-sectional thermal strain is given for three-sided and four-sided fire exposure respectively. Indicated is also a line illustrating the "average thermal strain distribution", which in reality will be the appearance of the deformed cross-section. The shaded areas represent the constraint strain. Based on the magnitude of the constraint strain the constraint stress can be derived utilising the stress-strain relation of fig 2.4.

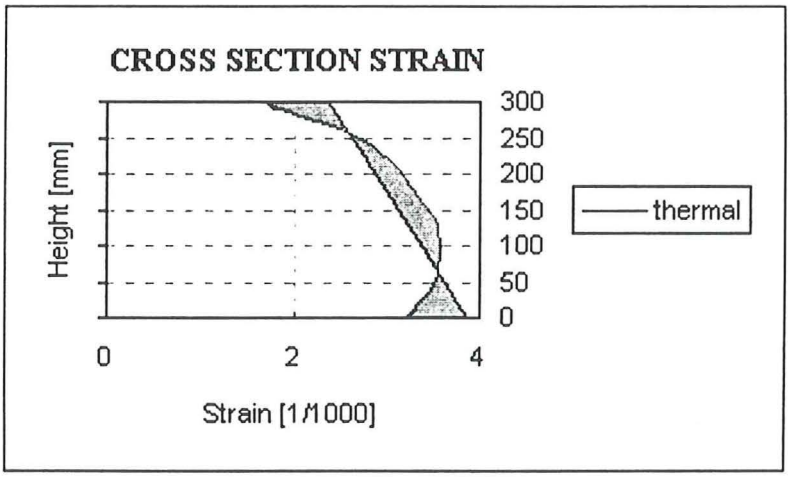

Fig 3.2 Thermal strain distribution from a three-sided fire exposure (unsymmetrical fire exposure) on an I-beam. Shaded areas represent the constraint strain. * Upper flange unexposed.

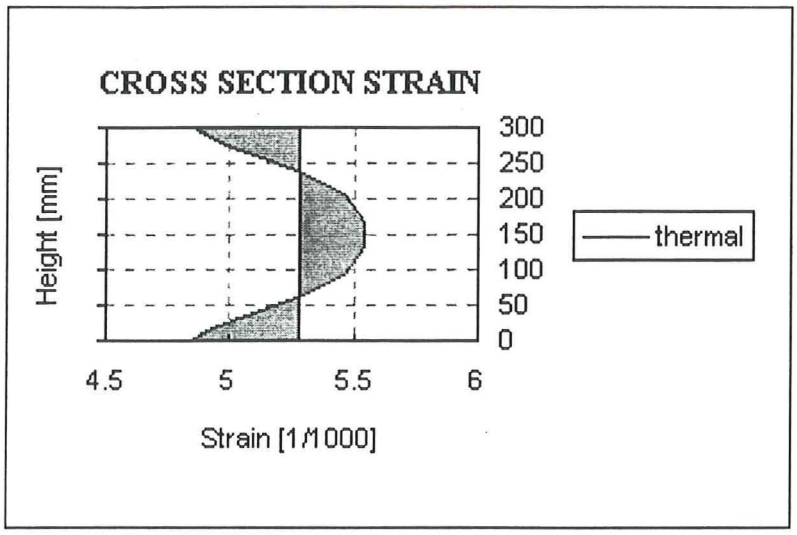

Fig 3.3 Thermal strain distribution from a four-sided fire exposure (symmetrical fire exposure) on an I-beam. Shaded areas represent the constraint strain.

It is recalled that the contributions to the total stress distribution from moment and axial force, both are of linear or constant nature. Considering the aspects of nonlinear temperature variation across the height, the stress component that was newly made acquaint with, is simply superposed to the others. Note the curvature on the stress distribution, due to the nonlinear form of the cross-sectional temperature. The stress components are illustrated in fig 3.4 and the shape of the temperature distribution corresponding to the cross-sectional constraint can be identyfied in fig 3.3.

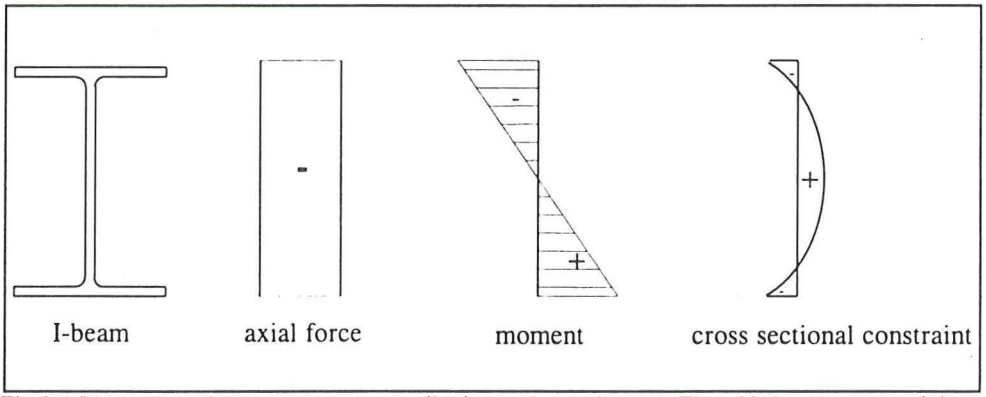

Fig 3.4 Illustration of the components contributing to the total stress. The added component originates in the cross-sectional constraint from temperature variation across the height.

Focusing on the differences between linear and nonlinear temperature distribution, it is found that the nonlinearity causes an additional stress component (cf. fig 3.4). Furthermore the change in stiffness according to eq 3.5 is emphasised. Following this reasoning, the phenomenon of bowing, discussed in the previous section, will of course be present here as well, presuming that the temperature distribution is unsymmetrical. If not, the elongation will simply be translational.

It should be emphasised that even if a profile is exposed to fire on all faces, the thermal strain distribution will not be uniform, but have the appearance of fig 3.3. It is clear that there is a gradient but it is symmetrically distributed and will cause no severe effects on the instability.

It is important to distinguish the differences between nonlinear temperature distributions that are symmetrical, and those that are not symmetrical. Unsymmetricallity will enhance the effects of instability and give the cross-section an eccentricity in stiffness as well as in strength, and of course in addition to that, there is the thermal bow, as mentioned before.

4 STEEL COLUMNS

Columns differ significantly from other structures, being subjected to effects from instability. This means that failure generally occurs from the axial load reaching the critical load (eq 4.3), and not from the cross-sectional strain attaining the yield limit. The main task of a column is generally to transfer loads vertically down to the foundation, i.e. columns in structures are carrying axial loads. This makes the column a very essential part of a structure.

Combining the load-bearing task with the extreme geometrical proportions of a column makes it easy to understand that instability problems will arise. In this report it is assumed that measures have been taken against all sorts of instability but flexural buckling, which is the most critical. This may sound as to rough a simplification, but as a matter of fact this type of structural modelling is a very realistic and common situation in practical building production of today.

Steel cross-sections are generally divided into four classes depending on their ability to form a plastic hinge. The method is practically the same in all design codes; here the Eurocode version is represented.

4.1 Slenderness

Slenderness is an important parameter in design of columns. It expresses the degree of sensitivity to the buckling phenomenon (flexural buckling), and links the strength, the length, the stiffness and the cross-section dimensions together. The slenderness ratio, λ, is defined in eq 4.1. The ratio relates the characteristic compression resistance, $N_{c.R}$, to the critical axial buckling force, N_{cr}, according to the Euler buckling theory.

$$\lambda = \sqrt{\frac{A^* f_y}{N_{cr}}} = \frac{l_c}{\pi i}\sqrt{\frac{f_y}{E}} \qquad \text{(eq 4.1)}$$

$$N_{c.R} = A^* f_y \qquad \text{(eq 4.2)}$$

$$N_{cr} = \frac{\pi^2 EI}{l_c^2} \qquad \text{(eq 4.3)}$$

where

l_c = a modification of the member length according to the rigidity of the actual end condition.

As in all design work it is customary always to design for the worst possible combination of loads. Equation 4.1, above, can be interpreted similarly, indicating the turning point between two different modes of failure. Values of λ exceeding 1.0 applies to a buckling failure in accordance with eq 4.3 (flexural buckling). For lower values of λ it is acceptable to disregard from effects of buckling and hence the failure will come from the cross-sectional stress reaching the yield strength. Relating the loading to the characteristic compression resistance and making it a function of the slenderness ratio, the chart shown in fig 4.1 will be obtained. The chart displays exactly what happens when the slenderness value of 1.0 is attained.

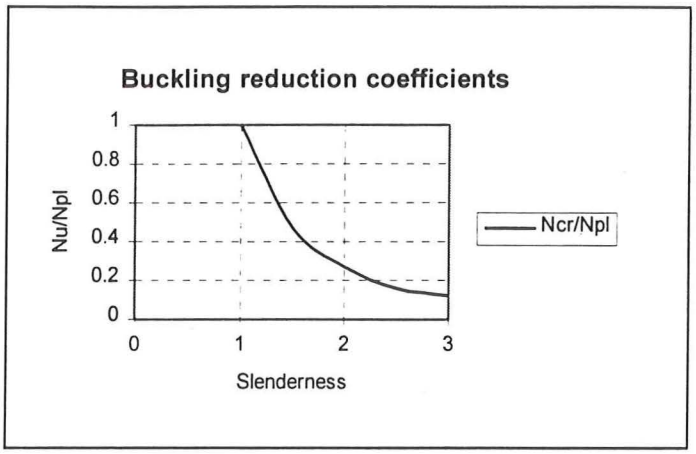

Fig 4.1 Load-bearing capacity for steel columns as function of the slenderness ratio.

In the previous text the following issues have not been regarded:

- initial out of straightness
- unintentional eccentricity
- secondary geometrical effects
- initial stresses
- plasticizing during the buckling process

which all are affecting steel columns in one way or another. Taking these effects into account, a somewhat smoother and as well lower curve is obtained. This curve is shown in fig 4.2, and its values should be taken as the most reliable and the best possible estimate of a column´s relative load-bearing capacity, manufactured and erected using customary production methods.

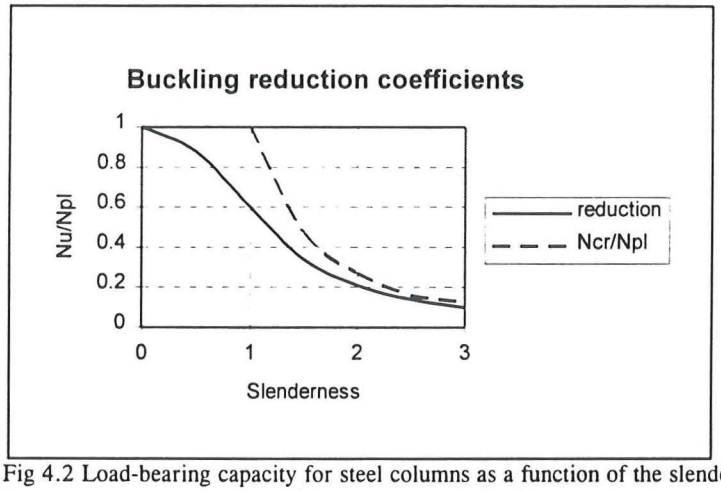

Fig 4.2 Load-bearing capacity for steel columns as a function of the slenderness ratio.
Realistic version of fig 4.1, with numerous reducing factors taken into account.

The reduction parameter in fig 4.2 is denoted χ. It is defined by the ratio between the characteristic buckling compression resistance and the characteristic plastic compression resistance (eq 4.2). The magnitude is based on empirical investigations and is therefore rather difficult to derive. The dependence on the factors listed above however is known. The ratio, being a reduction factor, must never exceed the magnitude of 1.0, for obvious reasons.

Now that the relationship between the slenderness ratio and the reduction in load-bearing capacity due to flexural buckling is known, the characteristic buckling resistance of a compression member can be defined as:

$$N_{b.R}=\chi N_{c.R} \qquad \text{(eq 4.4)}$$

Slenderness and stiffness, defined as the product EI, are two essential parameters concerning columns. Studying eq 4.1 and switching the radius of gyration (i) for the expression $(I/A)^{0.5}$ it is found that the stiffness and the slenderness are inversely proportional to each other. Hence a decrease in stiffness will cause an increase in slenderness, and vice versa. Focusing on the main issue of this report, viz. the aspect of fire exposure, it is repeated once again that this will decrease the magnitude of the Young´s modulus and thus the stiffness, which will lead to an increase in slenderness.

4.2 Miscellaneous stress enlarging factors

In modern design work the most disadvantageous situation possible is usually designed for. There are many stress enlarging factors that affects the column, such as eccentricity, degree of loading, initial stresses, restrained elongation and cross-sectional constraint. Considering these and above all the extreme situation of the united action of them, the design load combination has been found. The last three of the listed factors have been dealt with before. For initial stresses see section 2.3.3, restrained elongation see section 3.1.1 and cross-sectional constraint section 3.3. All factors mentioned above have been studied in the simulations (chapter five).

Refering once again to fig 3.4 , where the stress components are displayed separately, adding the initial stresses and imagining that the contribution from moment includes effects from eccentricity and second order theory, the most disadvantageous situation has been obtained. It is then noted that the largest stress is located on the compression side of the cross-section, where the strength is highest, since the temperature is lower here. This is advantageous.

4.2.1 Eccentricities and its effects on the design procedure

Columns are sensitive to eccentricities since these, as seen in eq 4.5, will implicate a moment due to the axial load.

$$M=N*e \qquad \text{(eq 4.5)}$$

Three sorts of eccentricities have been mentioned so far in this report; initial out of straightness, thermal bending and unintentional eccentricity. It is possible to divide these into two categories, where on one hand there is the initial out of straightness and thermal bending, and on the other the intentional and unintentional eccentricity. Characterising the two categories it is found that when it comes to initial out of straightness and thermal bowing, the eccentricity will vary along the length of the column, while intentional and unintentional eccentricity will denote a constant level of eccentricity. The shape of the initial out of straightness is commonly described with a sine curve, where the maximum magnitude, the amplitude, at the top of the column is represented by the ratio between the system length, l_c, and a standard figure based on the actual buckling curve and the type of analysis. In this report the standard figure is taken to be 400 according to Eurocode. As for thermal bending, equation 3.4 is referred to, where an expression for e_{th} is given. Similarly for the

initial out of straightness it is notable that the eccentricity here is a function of the length and hence is equal to zero at the boundary end condition.

The two categories discussed will, following the shape of the eccentricity, generate two different types of moment distributions along the column, viz. the one that is constant and the one that is a reflected image of the deflection curve. In fig 4.3 two examples of eccentricity with corresponding moment distribution are shown.

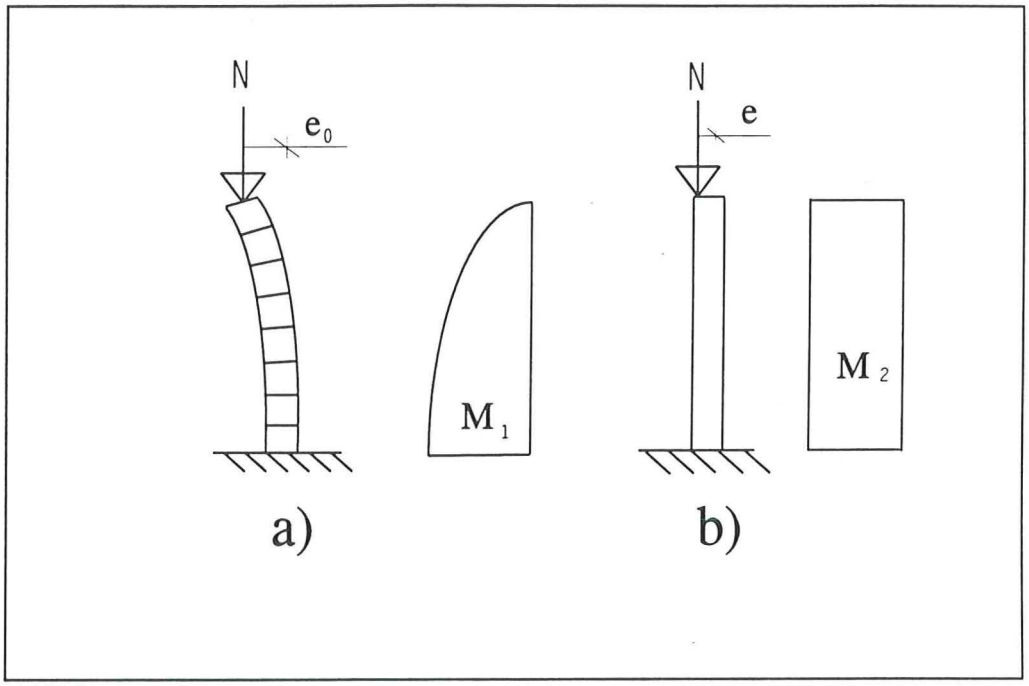

Fig 4.3 Deflection/eccentricity with corresponding moment distribution. a) Enlarging eccentricity along the length of the column. b) Constant eccentricity rendering a constant moment distribution.

The reader is reminded of section 3.1 which states that effects of initial out of straightness and unintentional eccentricity is included in the correction factor, χ, and thus no additional measures have to be taken in order to correct for these phenomena. Concerning intentional eccentricity and thermal bowing, no stress enlarging effects have been taken into account. The stress enlargement originates in the previously discussed moment, which is obtained from the combination of axial force and eccentricity (eq 4.5). An interaction between axial force and moment is thus necessary to undertake. The procedure and the analytical expressions are retrieved from Eurocode. Members with cross-sections of class one and two, subjected to a combination of bending and axial compression, shall satisfy eq 4.6.

$$\frac{N_{Sd}}{\chi N_{fi,t,Rd}} + \frac{kM_{Sd}}{M_{fi,t,Rd}} \leq 1.0 \qquad \text{(eq 4.6) /2/}$$

where

$$k = 1 - \frac{\mu N_{Sd}}{\chi \gamma_{M1} N_{fi,t,Rd}} \qquad k \leq 1.5$$

$$\mu = \lambda(2\beta_M - 4) + \frac{W_{pl} - W}{W} \qquad \mu \leq 0.90$$

N_{sd} =axial design load; [N]
M_{sd} =design moment; [Nm]
$N_{fi,t,Rd}$ =axial design resistance with respect to temperature; [N]
$M_{fi,t,Rd}$ =design moment resistance with respect to temperature; [Nm]
χ =buckling reduction coefficient, cf. fig 4.2
γ_{M1} =partial safety coefficient
β_M =equivalent uniform moment factor

Apart from the eccentrical effects dealt with above, it should be emphasised that there are effects similar to these concerning strength. A nonlinear temperature distribution will imply an eccentricity to the cross-sectional strength, since the temperature related strength reduction varies over the cross-section. For the yield stress this means that fibres subjected to higher temperatures can take a lower magnitude of stress before attaining the yield limit, then less temperature affected areas.

4.2.2 Degree of utilisation concerning loading

Dealing with stress enlarging factors, the magnitude of the applied axial load is of course a very important issue. When designing for columns it is observed that the axial load not only results in a uniform stress component but also determines the magnitude of the moment, which as well contributes to the stress distribution.

The degree of utilisation is a somewhat vague parameter. It is therefore of great importance that it is clearly and unmistakably defined, that no misunderstandings can occur. In this report the degree of utilisation is determined from the ratio between applied load and the characteristic buckling compression resistance load at room temperature, 20°C (eq 4.4).

4.2.3 United action of stress enlarging factors

As mentioned several times before in this report, it is always the most disadvantageous load combination that is relevant to the design engineer. Therefore the action of all possible stress enlarging factors have to be added together in order to obtain this maximum. All these stress contributing factors have been examined above and it is now possible to list them all, together with the origination of them, and illustrate the extreme situation in a figure (fig 4.4). Factors that will enlarge the cross-sectional stress are:

- degree of loading ⇔ design option
- initial out of straightness ⇔ manufacturing
- initial stresses ⇔ manufacturing
- unintentional eccentricity ⇔ production stage
- intentional eccentricity ⇔ design option
- global constraint ⇔ expansion restrictions
- thermal bowing ⇔ cross-sectional temperature gradient
- cross-sectional constraint ⇔ nonlinear cross-sectional temperature distribution

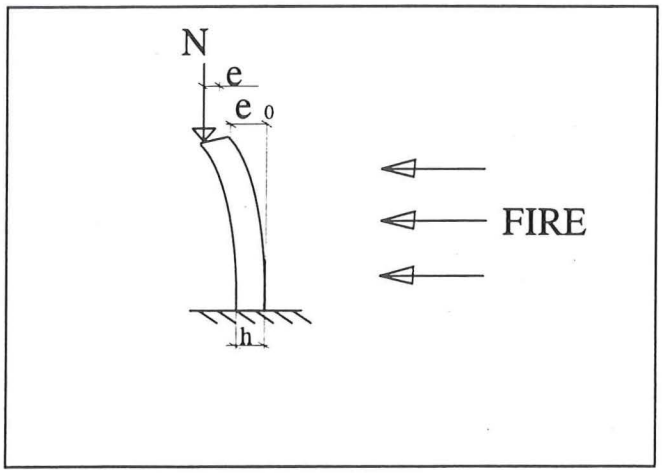

Fig 4.4 The united action of all possible disadvantageous stress contributing factors.

5 COMPUTER SIMULATIONS

Totally 60 calculations have been undertaken. Out of these 36 have been studied in detail and the remaining 24 have confirmed the results and tendencies obtained from the more thoroughly studied. In section 5.2 the complete matrix of studied parameters is included along with a description of each one of them. The overall intention has been to focus on the effects of unsymmetrical/partial fire exposure, and this aspect is illustrated for a variety of different parameter combinations.

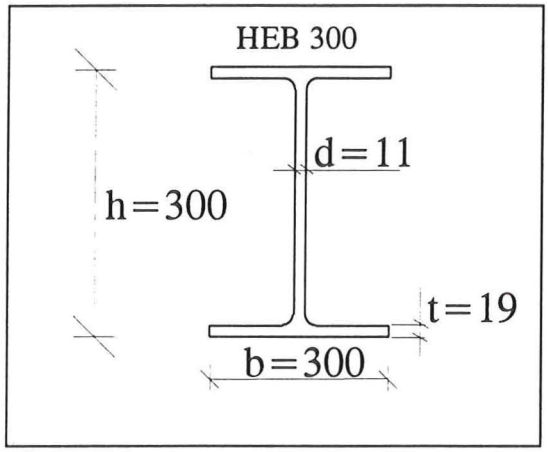

In all simulations the considered cross-section has been the same. It was decided that HEB 300 would be an appropriate profile (fig 5.1).

Section 5.1 contains an introduction to the computer software that have been very beneficial in the simulations.

Fig 5.1 Dimensions of HEB 300.

5.1 Programs and macros

As mentioned in the previous text, the selected cross-section is an HEB 300. Taking advantage of the computer programs illustrated in fig 5.2, it is important to be alert on their cross-sectional definitions and thus note that there is a conflict between the standardised list of HEB profiles and the one that has been defined in the calculations. The standard list is composed of hot rolled I-beams and hence the intersection between web and flange is somewhat smooth. Defining this in the computer programs is not possible and thus the model will be confined to make use of rectangular coordinates. As long as the user is aware of this dilemma it is not a problem, since the required magnitudes for area and moment of inertia (the change in the radius of gyration is negligible) easily can be recalculated, resulting in slightly different values then those given in the tables.

The computer programs used in the simulations are; Super-Tempcalc, Steelfire and Microsoft Excel. In order to make these compatible and convert output data from one program into input data to another, use have been made of a couple of conversion programs, namely Sfconv and Sfxl. Fig 5.2 illustrates how the entire array of programs are linked together and that it is possible to cover the process of action from fire exposure on a structure to graphical presentations of deflection, cross-sectional stresses and strains and any other parameter desirable. In the last stage where the charts have been produced, use have been made of a macro, Sfxl.xlm, that has simplified this work substantially.

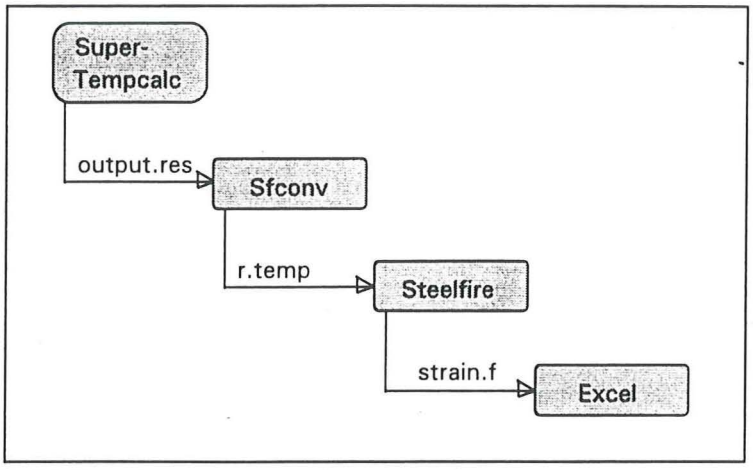

Fig 5.2 Computer programs used in the simulations.

5.1.1 Super-Tempcalc

In this program the cross-section to be studied is defined and then exposed to a standard fire of some sort, e.g. ISO 834. The temperature field of the member is calculated as the fire scenario continues for a certain period of time. Analysis of structures comprising several different materials are possible to accomplish. By applying fire protectional coating on the member, it is possible to adjust the time-temperature curve in any way desired. There are a variety of different coating products available for selection in the database, from which Hensotherm 4KS 2 has been chosen in the present study.

Super-Tempcalc is based on the finite element method (FEM), where the cross-section of a structure is divided into small (finite) elements. Two dimensional problems are regarded and the governing nonlinear transient heat conduction equation is given in eq 5.1. The variation of thermal properties with temperature in the considered materials are incorporated.

$$\frac{\partial}{\partial x}(k_x \frac{\partial T}{\partial x}) + \frac{\partial}{\partial y}(k_y \frac{\partial T}{\partial y}) + Q = \rho c \frac{\partial T}{\partial t} \qquad \text{(eq 5.1)}$$

where

T	=	temperature [°C]
k_x, k_y	=	thermal conductivity [W/m°C]
c	=	specific thermal capacity [J/kg °C]
ρ	=	density [kg/m^3]
Q	=	internal heat generation [W/m^3]

Two different boundary conditions are available; prescription of surrounding temperature and prescribed heat flow at the boundary. Considering the first option, the heat flow at the boundary is based on convection and radiation following eq 5.2.

$$q_n = \alpha_k (T_g - T_b) + \varepsilon_r \sigma (T_g^4 - T_b^4) \qquad \text{(eq 5.2)}$$

where

q_n	=	heat flow at the boundary [W/m^2]
T_g	=	gas temperature [°C]
T_b	=	boundary temperature [°C]

α_k = convection heat transfer coefficient [W/m^2°C]
ε_r = resulting emissivity
σ = Stefan-Boltzman constant [W/m^{2}K^4]

As for "prescribed heat flow at the boundary", the magnitude of the heat flow is simply given by the current time dependent value, thus the flow, $q_b = q(t)$.

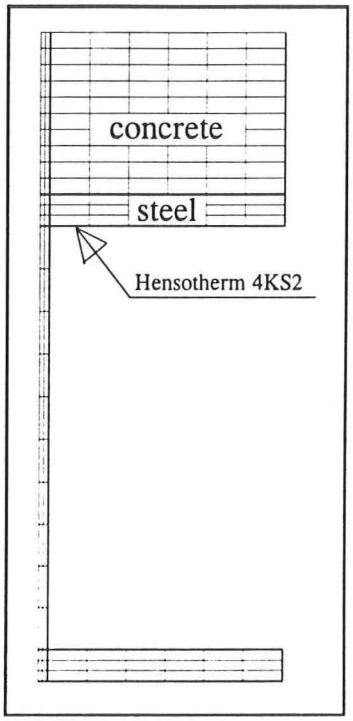

Fig 5.3 Finite element mesh of half an I-cross-section as modelled in Super-Tempcalc.

In fig 5.3 an example of a finite element mesh is presented. Note that due to symmetry only half the cross-section is modelled. The center line is being interpreted as an adiabatic boundary, with zero heat transfer. The outer boundary of the steel, except for the symmetri line, is covered with the fire protectional coating Hensotherm 4KS.

Super-Tempcalc was developed at Fire Safety Design AB, Lund Sweden.

5.1.2 Steelfire

Steelfire is a nonlinear finite element method (FEM) program that calculates stresses, strains and displacements. The calculations require characteristic input data, such as considered case of loading, cross-sectional measures, material data, rigidity of boundary end condition, temperature distribution in the members and so on. As mentioned before, when defining a cross-section in the program the modelling is confined to the use of an idealised ditto, where the intersection between web and flange forms a 90 degree angle and not a smooth curvature as is the case for real hot rolled I-beams. It is important to be aware of this phenomenon, that no mistakes occur when calculating a standardised profile, where the tabulated magnitudes of area and moment of inertia differ from those calculated by the program.

The possibility to impose a temperature gradient across the height of considered cross-section members, makes the program very useful. The program is intended for analysis of steel frames and is thus of perfect assistance in the study of fire-exposed columns. The calculations are applicable, both to geometrical and material nonlinearities. The structure is being constructed out of straight beam elements and the FEM theory is based on the displacement formulation.

In the current version of Steelfire the material- and the mechanical properties are employed in accordance with the suggestions in Eurocode; chapter 3 of reference /1/.

The material model is defined by eq 5.3.

$$\varepsilon_{tot}(\sigma,T)=\varepsilon_{\sigma}(\sigma,T)+\varepsilon_{th}(T) \qquad \text{(eq 5.3) /5/}$$

where

ε_{σ} = stress related strain
ε_{th} = thermal strain
σ = stress
T = temperature

Steelfire was developed in 1983 by Dr. N E Forsén, presently employed by Multiconsult AS, Consulting Engineers Oslo.

5.1.3 Sfconv

Sfconv is a conversion utility that converts Super-Tempcalc temperature output to Steelfire input. The temperatures reported from the Super-Tempcalc calculation represent every node of the finite element mesh. This format however does not comply with the request of input data to Steelfire, and thus a conversion is necessary. Sfconv calculates average temperatures from the node points and rearranges them in a way that agrees with the input format to Steelfire.

Sfconv was developed at Fire Safety Design AB, Lund Sweden in 1992.

5.1.4 Sfxl and Sfxl.xlm

Sfxl converts and rearranges Steelfire output to a comma separated value format in order to enable the use of graphical Excel functions. The output produced by Sfxl is designed primarily to work smoothly with the Excel macros collection; Sfxl.xlm. Working with this utility is very convenient and it opens up a great many options of diagrams that are useful when presenting the results of a calculation.

These programs were developed at Fire Safety Design AB, Lund Sweden.

5.2 Parameter study

Apart from the main task of the study, viz. effects of partial (unsymmetrical) fire exposure, a few other parameters that were considered to have an interesting influence on columns were selected.

These, of whom most have been mentioned in previous sections, are listed in tables 5.1, 5.2 and 5.3.

	R30, R60, R90 ISO 834 (e_0)		
	HEB20	HEB40	HEB60
lambda=0.5	83% / 100%	83% / 100%	83% / 100%
lambda=1.0	83% / 100%	83% / 100%	83% / 100%

Table 5.1 Three series of calculations with various time-temperature curves; R30, R60 and R90. Each and one of the shaded cells represents two calculations per series; 83% and 100%, i.e. all in all 36 calculations in this table. The significations of the abbreviations are given below.

The calculations in table 5.1 are all accomplished with the mandatory eccentricity e_0, the initial out of straightness, in accordance with Eurocode. Turning the attention to table 5.2 it is noted that the next set of calculations follow the same procedure as obtained in table 5.1. Here, the time-temperature scenarios of R30 and R90 have been omitted and an additional eccentricity (e_1) is included.

	R60 (e_1) ISO834		
	HEB20	HEB40	HEB60
lambda=0.5	83% / 100%	83% / 100%	83% / 100%
lambda=1.0	83% / 100%	83% / 100%	83% / 100%

Table 5.2 This series of calculations corresponds with series R60 of table 5.1, only here the effects of an additional eccentricity are taken into account. Each and one of the shaded cells represents two calculations; 83% and 100%, i.e. all in all 12 calculations in this table.
The significations of the abbreviations are given below.

In the last one of the parameter study tables, table 5.3, the effects of restrained elongation is considered for the time-temperature scenario of R60. The expansion is restricted to allow only 90% of the unrestrained elongation, and hence the remaining 10% will result in an additional axial load component.

	R60 (γ0.9) ISO834		
	HEB20	HEB40	HEB60
lambda=0.5	83% / 100%	83% / 100%	83% / 100%
lambda=1.0	83% / 100%	83% / 100%	83% / 100%

Table 5.3 This series as well, comply with the calculations in series R60 of table 5.1. Here though it has been imposed with a restricted elongation, whereas only 90% of the desired extension is allowed. Each and one of the shaded cells represents two calculations; 83% and 100%, i.e. all in all 12 calculations in this table. The significations of the abbreviations are given below.

The abbreviations for the parameters above are:

- R30/60/90 =fire safety class, the figures represent the time in minutes to attainment of critical temperature in the steel core
- 83% / 100% =percentage of fire exposure on the faces of the circumference
- lambda (λ) =slenderness

- HEB20/40/60 =degree of loading, the figures represent the applied percentage of the axial design load, defined by eq 4.4.
- e_1 =additional eccentricity in excess of the initial out of straightness
- e_0 =initial out of straightness
- $\gamma 0.9$ =restrained thermal elongation, only 90% of the desired expansion is allowed for; the remainder will cause an additional axial force

In this report results from the calculations referred to in table 5.2, table 5.3 and the R60 series of table 5.1, are presented. As for the results of the R30 and R90 series of table 5.1, these have been analysed and found to confirm the conclusions from the more thoroughly studied calculations but are omitted in this report.

5.2.1 Time-temperature relationship in the steel

In order to determine effects from varying rate of temperature elevation, three different time-temperature curves (R30,R60, R90) have been incorporated in the study. These define the number of minutes that have passed when critical temperature is reached in any location of the cross-section in the material of the member. The critical temperatures for the three degrees of loading are obtained from figure 2.5 by reading off the chart at 20, 40 and 60% of the relative strength. By altering the amont of passive fire protection (Hensotherm 4KS 2) applied the critical temperature can be attained at specified desired point of time; e.g. 30, 60 and 90 minutes. Note that the critical temperature alters with the degree of loading. In computer simulations of this kind, it is customary to use the standard fire exposure curve, ISO 834 at the heat exposed boundary.

The product of fire protection coating considered in the simulations, is called Hensotherm 4KS 2. Its material properties, with the aspects of elevated temperatures incorporated, are shown in fig 5.4 and 5.5 where the characteristic performance of coating materials is observed.

Fig 5.4 illuminates the most important ability of a fire protection material; the ability to prevent heat from entering the member. Hence the conductivity of the insulating material is characterised by exceptionally low magnitudes. It should be emphasised that the chart displayed in fig 5.4 denotes a fictitious temperature dependent development of the conductivity, assessed by iterative computer simulations, that involve aspects of adjoining parameters and thus should not be refered to as a pure conductivity. It is noted that the curve can be divided in three different phases. The middle phase is distinguishable and represents the stage where the purpose of the coating is fulfilled, viz. almost no heat is permitted to penetrate the coating. The two adjacent phases illustrate how the material reacts when first exposed to a fire, and what happens when the temperature has reached a magnitude of above 800 degrees Celsius. In the first stage, the coating is developing its advantageous conductivity properties by expanding and turning into an insulating layer. The expansion is fully completed when the temperature has reached 200°C. This also reflects on the time-temperature curves provided in the appendix, where it is observed that the rate of temperature increase is diminishing when the temperature level of 200°C has been attained. As for temperatures above 800°C the coating is physically terminated by means of sublimation.

From fig 5.5 it can be concluded that the capacitivity is equal to 1000 KJ/m^3°C, regardless of the temperature.

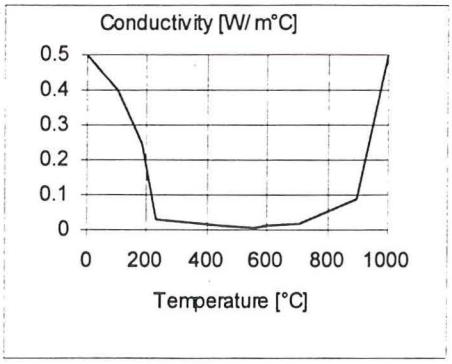

Fig 5.4 Conductivity as a function of temperature for Hensotherm 4KS 2.

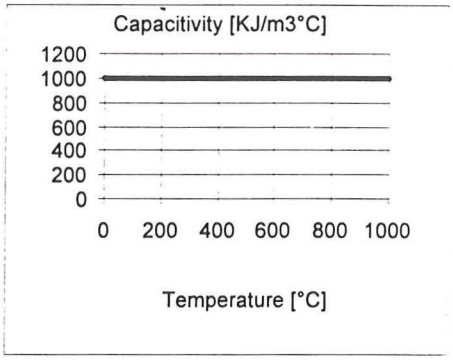

Fig 5.5 Capacitivity as a function of temperature for Hensotherm 4KS 2.

The standard fire curve given by ISO 834 provides the gas temperature-time relationship, which then imposes the heat onto the member through emission and convection. This transferation of heat is taken care of by Super-Tempcalc (section 5.1.1). The gas temperature-time curve presented by ISO 834 is displayed in fig 5.6.

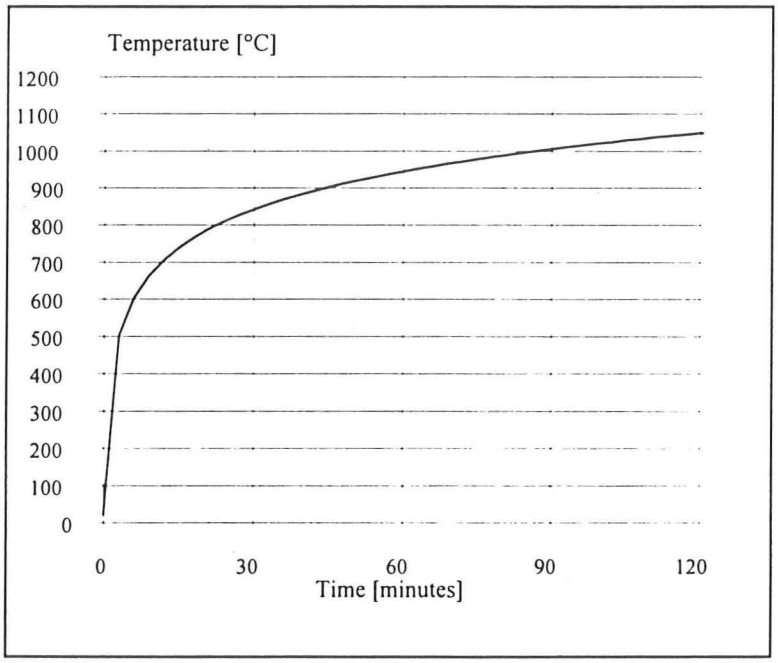

Fig 5.6 Gas temperature-time curve in accordance with ISO 834.

There is obviously a firm connection between the degree of axial load and the critical temperature. A column subjected to a tiny load is resistant to a higher temperature and so forth. The critical temperature corresponding to a given percentage of the design compression resistance is found through fig 2.5.

5.2.2 Definition of 83% and 100% fire exposure

In the previous section it was discussed how the critical temperature would be obtained. Following that reasoning and in order to define two types of fire exposure that are comparable, the thickness

of the Hensotherm layer is derived corresponding to the 100% case and then use is made of the same thickness when simulating the 83% case.

The difference between the two cases is the modelling technique in the temperature simulations. 83% fire exposure implies that 17% of the circumference is not in contact with the fire. This has been attained by surrounding the upper part of one flange with concrete. Fig 5.7 illustrates how 83% and 100% exposure are being modelled in the temperature calculation.

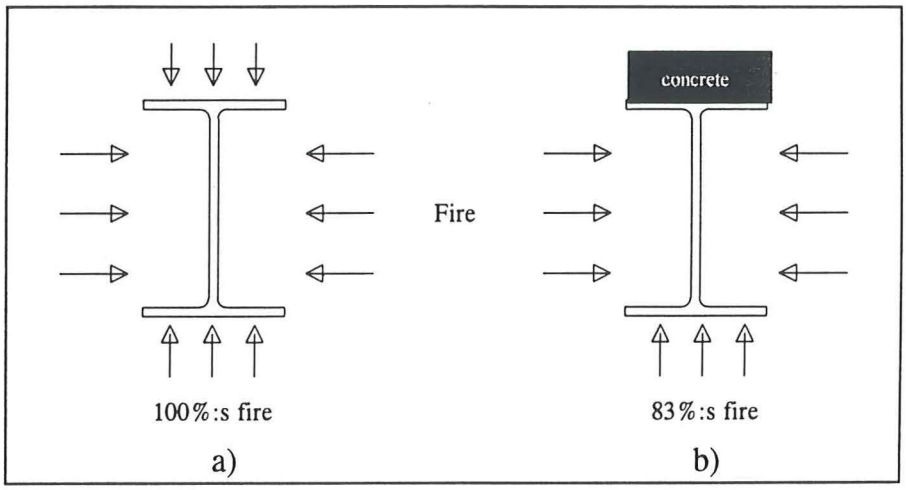

Fig 5.7 Boundary conditions for temperature calculations of 100% (a) and 83% fire exposure (b).

5.2.3 Definition of slenderness

The parameter slenderness has been defined in section 4.1. Here in the simulation chapter the content is confined to concern the derivation of slenderness for the parameter study. Two magnitudes of slenderness have been studied, viz. $\lambda=1.0$ and $\lambda=0.5$. Since the cross-section profile has been selected and the material parameters are determined, eq 4.1 will provide the system length that corresponds to the considered magnitude of slenderness. From the system length the member length is easily obtained, knowing the type of boundary end condition, and then the column can be divided into elements. The element size has been conserved through out the simulations and thus the number of elements was set to 16 and 8 for $\lambda=1.0$ and $\lambda=0.5$ respectively.

5.2.4 Degree of loading

The degree of loading is taken as a percentage of the axial design load, represented by the expression defined in eq 4.4, which is repeated here.

$$N_{b.R}=\chi N_{c.R}$$

where

$$N_{c.R} = Af_y$$

and $\chi(\lambda)$ can be obtained from fig 4.2, the continous curve.

Appropriate magnitudes of loading were found to be 20%, 40% and 60%. They are referred to as HEB20, HEB40 and HEB60.

5.2.5 Eccentricity

Two sorts of modelled eccentricities are incorporated in the simulations; initial out of straightness and an applied intentional eccentricity. The initial out of straightness is modelled, as mentioned before, using a sine curve with half the amplitude taken as the system length divided by 400 (cf. fig 5.9).

The intentional eccentricity is derived from the criteria that its magnitude shall, when interacting with the axial force, produce a moment that on the tension side will be large enough to equalise the normal stress, originating in the axial force. In other words the stress distribution, with the eccentricity taken into account, shall have the appearance displayed in fig 5.8

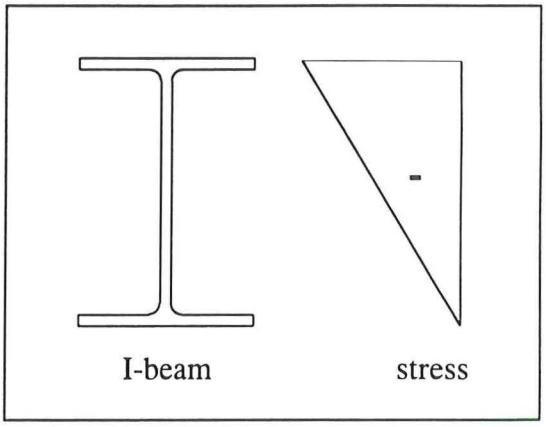

Fig 5.8 Original stress distribution when the intentional eccentricity is taken into account.

5.2.6 Axially restrained expansion

In section 3.1.1 restrained structures has been regarded. It should be stressed, in order to avoid misunderstandings, that the percentage expresses the part of the desired expansion that is allowed, and not the degree of restraint.

In this report the value of the parameter γ to be simulated was set to 0.9.

In order to accomplish the simulations with effects of restrained expansion incorporated, calculations would be undertaken for the case of unrestrained elongation. Determining from the output of these calculations the total expansion obtained. Entering 90% of this expansion as an allowable displacement in the input file of a new calculation, and the desired simulation has been achieved.

5.2.7 Structural model

In this section the structural model that has been referred to in the previous text, is displayed in fig 5.9. Initial out of straightness and axial load is applied. Elements and nodal points are indicated for the case of a slenderness equal to 0.5.

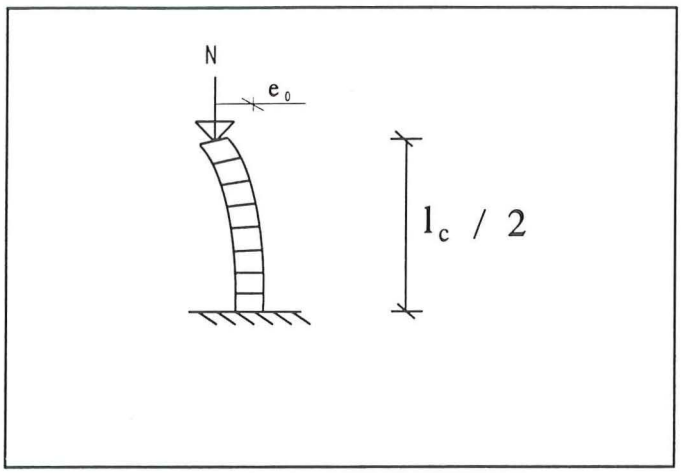

Fig 5.9 Structural model of a steel column with eight elements, which corresponds to a slenderness of 0.5 in the present simulation series. The system length (l_c) is twice the modelled length for the current type of end condition. The initial out of straightness is illustrated by the bowing of the column.

In the cases studied where there are more than one factor contributing to the bending of the column (ex. 83%:s fire exposure and e_1), these have been arranged in a manner that unites their action.

6 RESULT FROM COMPUTER SIMULATIONS

For each and one of the calculations, a number of charts and diagrams have been developed to simplify the analysis of effects from partial fire exposure. The variety of chart combinations are listed below.

- Displacement-Time
- Time-Temperature
- Cross-sectional stress at three points of time
- Cross-sectional strain at the same three points of time

In the charts, that display cross-sectional stress, a curve indicating temperature reduced yield stress, defined by figure 2.5, is entered. Including this curve in the cross-sectional study of the member, makes it possible to get a more profound survey of the situation and to make a better estimate of the degree of utilisation of the member´s capacity. This function is of particular importance when calculating cross-sections where an elevated temperature has been imposed across the height, and hence the yield stress is varying. The studying of the charts makes it possible to determine which parameter combination is the most disadvantageous. A closer analysis of the parameters incorporated, based on the graphical results, is accomplished in section 6.2.

All charts are listed and put together in a logical way in the appendix. The formulation of the charts in the appendix is performed with the intention to illustrate the differences between 83% and 100% fire exposure. References are occasionally made to charts in the appendix. These will easily be found through the appendix list.

Apart from detailed studying of the charts, there is of course the point of time when the computer analysis is interrupted, which provides a lot of information about the structure´s sensitivity to the involved parameters. Section 6.1 displays the points of time when the analysis has been interrupted.

6.1 Predicted failure

When the computer analysis is interrupted the column has failed to bear the applied loads, due to escalating eccentricity and diminishing strength and stiffness, that originates in the elevated temperature. By trying to establish general effects based on the specification of the failure time results, it is possible to find a pattern of how the differences in fire exposure and combined influence from other parameters, go together.

It should be emphasised, in order to avoid misunderstandings, that the fire resistance times of the three selected degrees of loading (20%, 40% and 60%) are not comparable. As the loading is elevated there is simultaneously a change in time-temperature curves, which is recalled from section 5.2.1 where the concept for obtaining the critical temperatures corresponding to each degree of loading is given. In other words it is not necessarily so that a higher degree of loading renders a shorter fire resistance time, since the time-temperature curves used in the simulations, are not equal and hence the results are not comparable.

Similarly, it is not possible to compare the results from the two magnitudes of slenderness, since the loads differ in accordance with the reduction factor χ, introduced in equation 4.4. However the comparisons of the effects from different fire exposures will always be adequate and make it

possible to map how the differences in load-bearing capacity between the two cases of fire exposure, respond to alterations in slenderness and degree of loading.

Table 6.1 shows the results corresponding to selected parts of table 5.1, viz. the R60 series.

	R60 (e_0)					
	HEB20		HEB40		HEB60	
	83%	100%	83%	100%	83%	100%
lambda=0.5	47.52	51.36	50.40	51.36	36.96	37.92
lambda=1.0	48.48	51.36	40.80	50.40	20.64	37.92

Table 6.1 Specification of the times of failure [minutes] for the R60 (e_0) series. The table corresponds to the parameter matrix of table 5.1; results obtained from the output of the structural FEM program, Steelfire.

The conclusions drawn from table 6.1 are summarized and expressed in terms of slenderness, degree of loading and type of fire exposure.

Comparing the two types of fire exposure (83% and 100% of the circumference of the member) to each other, it is noted that the 83% exposure without exception fails before the 100% ditto. There is also a tendency, observed for the slenderness of 1.0, that the higher the degree of loading the greater the differences in collapse time between the two cases of fire exposure.

In table 6.2 the results corresponding to the parameter combination of table 5.2 is given. In accordance with the results listed in table 6.1, it is noted that the 83% case is ruling in all simulations regardless of degree of loading and slenderness. Tendencies similar to those found in the previous set of calculations are observed. These being the enhancement of the difference in collapse time between 83% and 100% fire exposure, which is more characteristic for the slenderness of 1.0 and of course the decrease in fire resistance due to elevated degree of loading.

It is also emphasised that the additional eccentricity consistently render a shorter fire resistance time, compared to the results obtained from simulations with a pure initial out of straightness (table 6.1).

As seen in table 6.2 there is a void in the cells belonging to the calculations of 60% loading at a slenderness of 0.5. Accordingly the column has not been able to cope with the applied load at the present magnitude of eccentricity at room temperature.

	R60 (e_1+e_0)					
	HEB20		HEB40		HEB60	
	83%	100%	83%	100%	83%	100%
lambda=0.5	45.60	48.48	40.80	42.16	-	-
lambda=1.0	48.48	49.44	32.16	39.84	7.20	17.76

Table 6.2 Specification of the calculation results [minutes] concerning additional eccentricity. The table corresponds to the parameter matrix of table 5.2; results obtained from the output of the structural FEM program, Steelfire.

	R60 (γ0.9, e_0)					
	HEB20		HEB40		HEB60	
	83%	100%	83%	100%	83%	100%
lambda=0.5	46.56	51.36	50.40	58.08	36.96	54.24
lambda=1.0	50.40	52.32	54.24	60.96	20.64	61.92

Table 6.3 Specification of the calculation results [minutes] concerning restrained elongation. The table corresponds to the parameter matrix of table 5.3; results obtained from the output of the structural FEM program, Steelfire.

Table 6.3 specifies the results obtained in the simulations of partially restrained elongation. A closer look and comparison with the results concerning unrestrained elongation (Table 6.1, apart from the restraint same conditions apply) may seem a bit confusing. It is clear that the computer analysis continues longer when considering restrained elongation than when unrestrained elongation is considered. This is in opposition to the facts that were introduced before and calls for an explanation. The answer can be found in the structural computer program, Steelfire. As the effects of partially restrained axial elongation is simulated, the restrained degree of freedom and the allowable elongational distance are input data. During the progress of the fire scenario the column will extend axially and eventually attain the allowable expansion. Then the elevation of the axial force starts, and continues till a maximum has been reached and from there on the load will decrease. The decreasing path proceeds and passes the magnitude of the initial axial load. Thus a tension effect will be obtained that enables the analysis to continue for a few more minutes, despite the enlarged deflection.

The deflectional enlargement, considering restrained elongation, is confirmed in section 6.2, where graphical results are presented. Following the reasoning in the previous text, the most accurate way to deal with this, would probably be to regard the point of time where the axial load has regained its initial magnitude as a better estimate than the values in table 6.3. Therefore table 6.3 has been rearranged in table 6.4 and the values updated in accordance with the new definition of time. The procedure has been chosen since it would be incorrect to assume that tension forces always occur in a real situation.

	R60 (γ0.9, e_0) $N=N_{initial}$					
	HEB20		HEB40		HEB60	
	83%	100%	83%	100%	83%	100%
lambda=0.5	41	43	40	51	35	37
lambda=1.0	48	51	42	46	16	36

Table 6.4 Specification of results [minutes] based on simulations performed in accordance with the parameter matrix of table 5.3 concerning restrained elongation. The calculations are equal to those in table 6.3, however here a new definition of time is introduced as described above.

6.2 Graphical presentation of effects from partial fire exposure

In this section the final analysis of the results will be presented and graphical illustration will be used in order to illuminate the differences between partial fire exposure and a completely surrounding fire. Adequate parameters that are affecting this phenomenon, are dealt with one by one in the following. The effects from partial fire exposure are lined out by means of time-temperature curves for various cross-sectional parts, displacement-time curves, cross-sectional stress and cross-sectional strain for various points of times.

In appendices A, B, C, D, E, F, G, H and I, the produced charts are collected and put together in a structured way that is easy to survey. In the report though, only selected parts will be presented in order to illuminate interesting phenomena, and occasionally references will be made to the more extensive collection in the appendices. Section 6.2.1 contains graphical illustrations of the results obtained from the calculations concerning 60% loading, slenderness of 1.0 and no additional eccentricity (apart from the initial out of straightness). Section 6.2.2 presents the results that correspond to involvement of additional eccentricity. Finally section 6.2.3 refers to the results concerning partially restrained axial elongation.

6.2.1 60% loading and slenderness equal to 1.0

The graphical results that have been selected for a more detailed study here, correspond to, as the headline implies, the simulations that have been performed with 60%´s loading, slenderness equal to 1.0, no additional eccentricity for the axial load and no restrained elongation. In the appendix collection, results from other parameter combinations are specified. Appendix A and appendix B refer to different degrees of loading, 20% and 40% respectively. Appendix A, B and C also contain the graphical results from simulations with the slenderness parameter equal to 0.5.

One of the most important things to know, when performing a structural analysis under the influence of elevated temperatures is of course the temperature distribution as a function of time in the studied specimen. In figure 6.1 and figure 6.2 these time-temperature relationships are presented and it is noted that partial fire exposure renders a significant temperature gradient across the height of the profile.

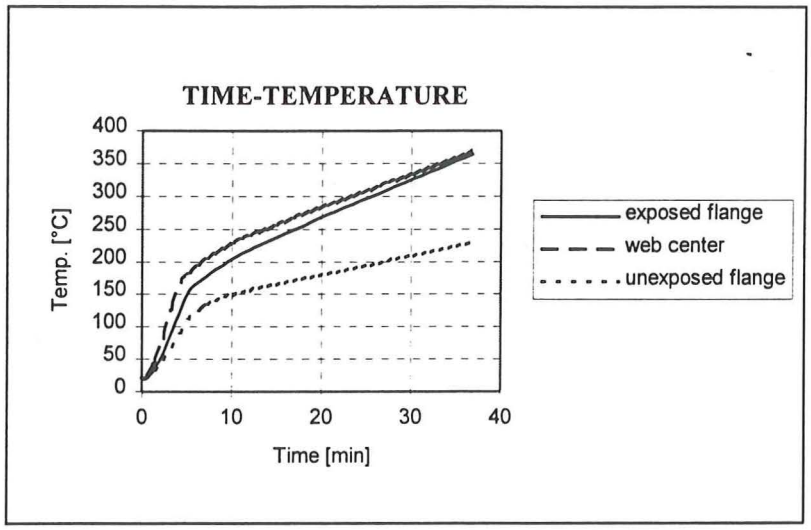

Fig 6.1 Time temperature curve in various locations of the steel profile for the case of partial fire exposure (83%). Note the elevating temperature gradient between the two flanges.

Studying fig 6.1 makes it easy to understand that the simplified assumption, with constant temperatures across the height of the cross-section, is very coarse.

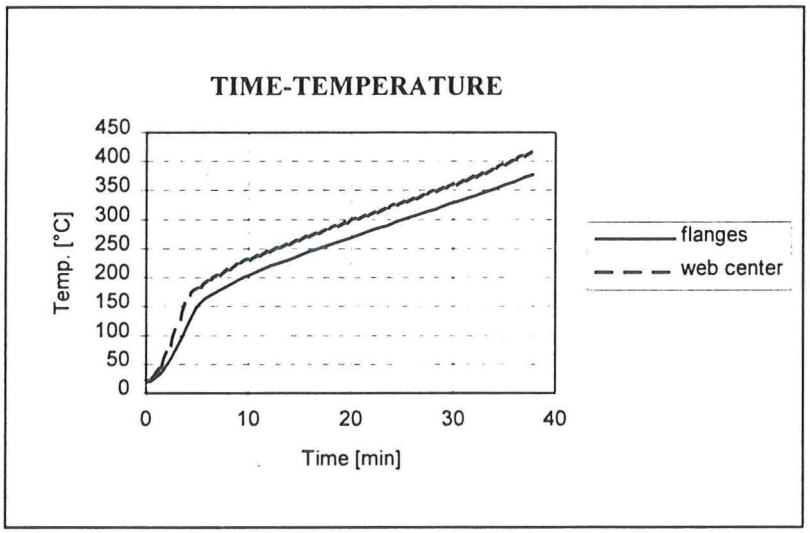

Fig 6.2 Time temperature curve in various locations of the steel profile, for the case of fire exposure on the entire circumference (100%.) Note the similarity in temperature elevation between the flanges and the web center.

With this mode of fire exposure, the simplification of constant cross-sectional temperatures, applied in the design guide, would be more acceptable.

Studying columns, another issue that will be very important is the lateral deflection. Axially loaded columns will have a moment distribution along the length and accordingly higher magnitudes of stress will be imposed in the cross-sectional material. As pointed out repeatedly in this report, the deflection will have a substantially greater magnitude (5-6 times greater) when subjected to fire exposure on limited parts of the circumference, than when all faces are exposed. This is confirmed by the charts presented in fig 6.3 and fig 6.4.

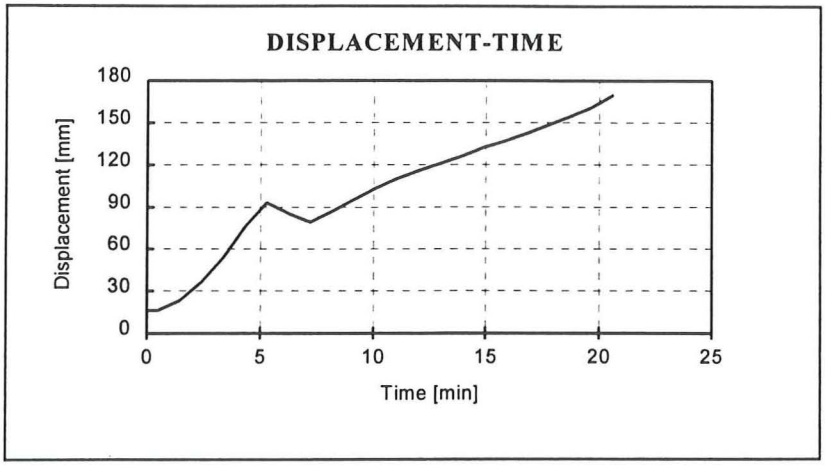

Fig 6.3 Displacement time curve corresponding to the top of a steel column subjected to partial fire exposure (83%). Observe the difference in magnitude between this chart and the chart displayed in fig 6.4.

The loading is 60% of the design compression load at room temperature, the slenderness is equal to 0.5.

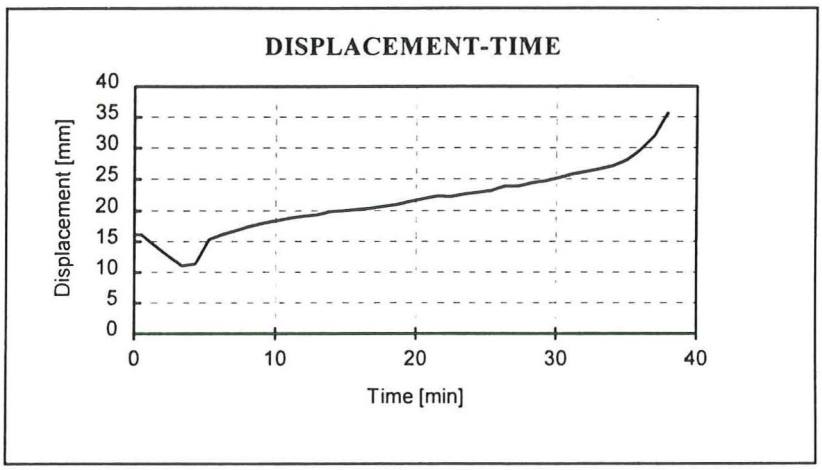

Fig 6.4 Displacement time curve corresponding to the top of a steel column subjected to fire exposure on all faces (100%).

Otherwise same conditions apply as defined in fig 6.3.

A lot of information is provided by the two charts of deflection (fig 6.3 and fig 6.4). In fig 6.3 partial fire exposure is considered. Here the deflection is elevating continuously as a function of time. Thermal bowing and elevating magnitude of moment are contributing to the accomplishment of this appearance. Contemplating fig 6.4 the deflection is rather constant during the introductory 35 minutes. During this period of time, the modulus and strength parameters decrease as the steel temperature is elevated. Finally the parameters have reach a critical magnitude and the column fails to carry the applied loads.

In the following the development of cross-sectional stress and cross-sectional strain will be given for three points of time. First in the chronological order is the time, t=0, i.e. the calculations are performed in room temperature and hence there is no difference between partial and complete fire exposure. This comparison makes the differences between partial and complete fire exposure distinguishable. The dashed line, included in the figures displaying cross-section stress, illustrates the actual magnitude of the temperature related yield strain based on the 2.0% criteria, defined in Eurocode. The reduction due to temperature starts at 400°C, which is why the line is constant in some figures.

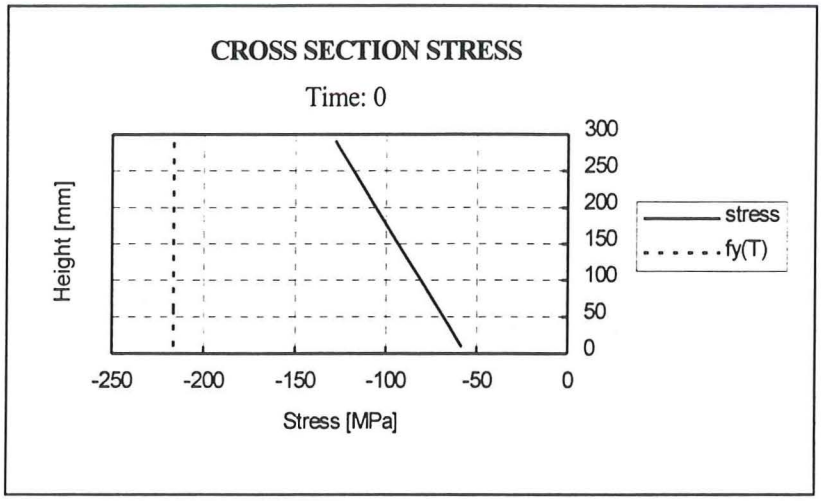

Fig 6.5 Initial stress distribution in the cross-section, equal to both kinds of fire exposure.

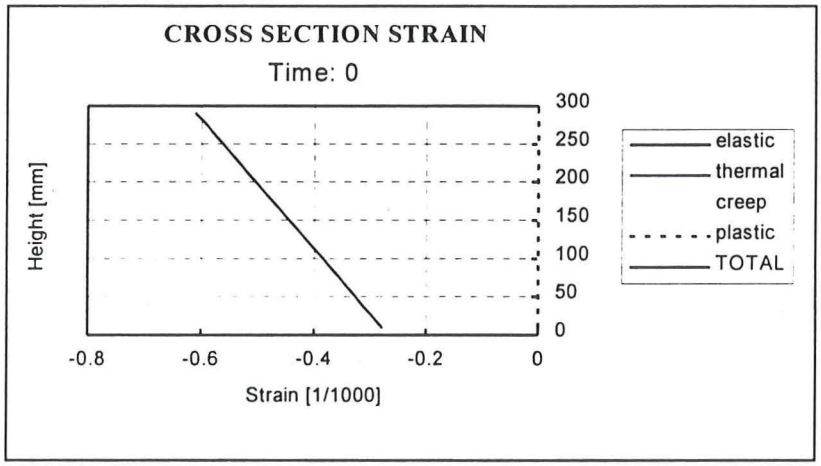

Fig 6.6 Initial strain distribution in the cross-section, equal to both kinds of fire exposure.

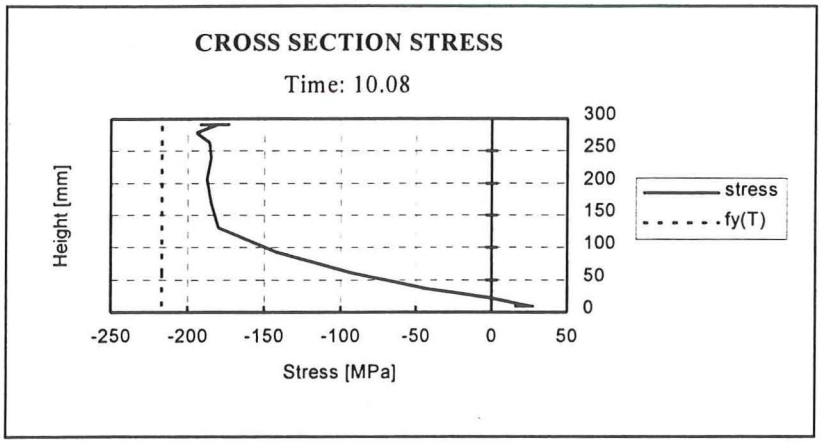

Fig 6.7 Stress distribution in the cross-section after 10.08 minutes, partial fire exposure (83%).

Comparing fig 6.7 with fig 6.8, it is noted that the upper part of the cross-section is subjected to a lot higher magnitude of stress when this flange is protected from fire exposure. Comparing with the corresponding charts of strain, fig 6.11 and 6.12, the influence of the temperature related modulus of elasticity (E(T)) is clear. Considering in fig 6.11 the curve displaying elastic strain, the cross-section stress (fig 6.7) is obtained from multiplication with the temperature related modulus of elasticity. Studying the shape of the cross-section stress it is observed that the upper part of the cross-section lacks the reduction in magnitude obtained in fig 6.11. This is due to the cross-sectional temperature gradient that implies a reduction of the modulus of elasticity, that will vary in the cross-section. Thus the strain decrease in the upper part of the flange is compensated by a higher magnitude of the modulus of elasticity, and the final temperature related stress distribution in this part will be rather constant.

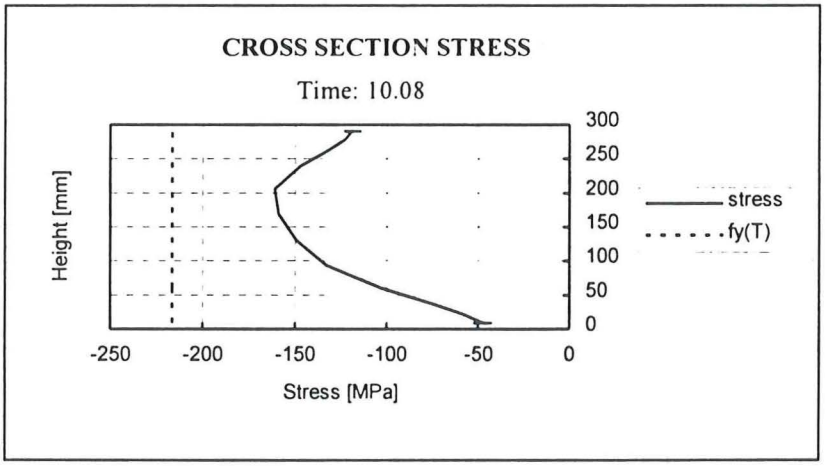

Fig 6.8 Stress distribution in the cross-section after 10.08 minutes, fire exposure on all faces (100%).

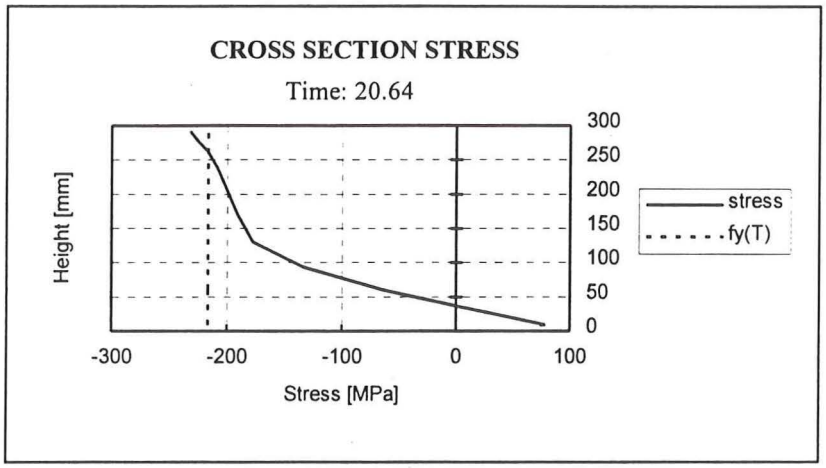

Fig 6.9 Cross-section stress after 20.64 minutes, partial fire exposure (83%).

Fig 6.9 displays the cross-section stress about 10 minutes later than the point of time shown in fig 6.7. The development of the stress distribution that is influenced by partial fire exposure, has now lead to the intersection between stress and strength in the upper part of the cross-section. Simultaneously the stress magnitude in the lower part of the cross-section is approaching 100 MPa tension stress.

The stress distribution in fig 6.10 is not by near utilising the material capacity as much as is the case in fig 6.9. It is then possible to conclude that partial fire exposure affect the cross-section in a more disadvantageous way then fire exposure on all faces. It is once again emphasised that the only difference between the calculations corresponding to the results in figures 6.9 and 6.10 is the mode of temperature exposure (83%/100% of the circumference).

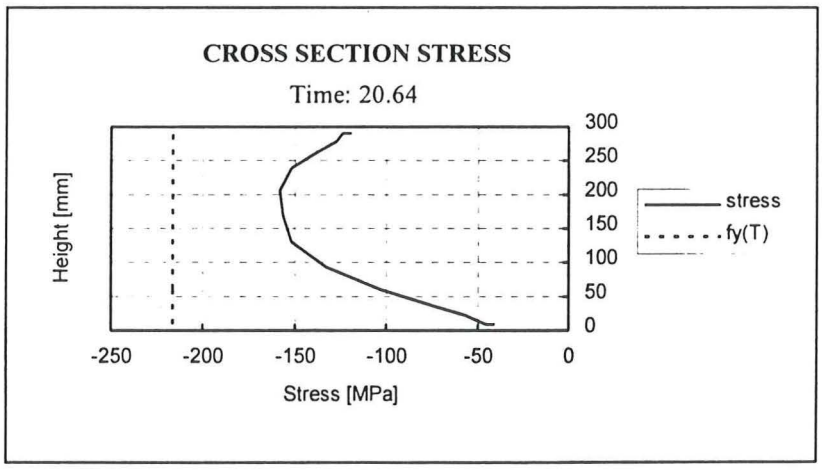

Fig 6.10 Cross-section stress after 20.64 minutes, fire exposure on all faces (100%).

Referring to appendix A fig A9 and A10, higher temperatures in the steel core are regarded and thus the dashed line, indicating temperature related yield strength, forms a curvature. The reason why this dashed line shows a constant appearance in the previous figures could be explained through consultation of fig 2.5. The temperature related yield strength reduction does not start until the cross-sectional temperature has attained 400°C, and thus $f_y(T)$ will remain unaffected during the first time period of the fire scenario. It is easy to distinguish the one that represents partial fire exposure from the one of that represents fire exposure on all faces. Fire exposure on all faces will render a completely symmetrical strength reduction (fig A10).

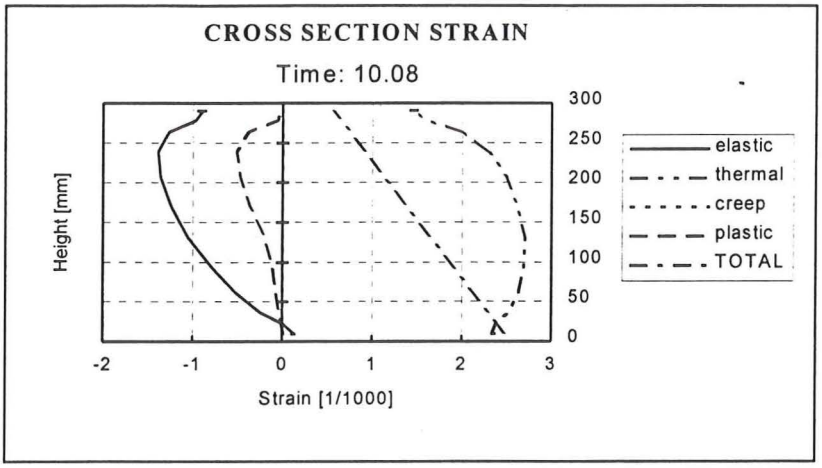

Fig 6.11 Cross-section strain after 10.08 minutes; partial fire exposure (83%).

The thermal strain component of fig 6.11 corresponds to partial fire exposure and is hence, in contradistinction to fig 6.12, unsymmetrically distributed over the cross-section.

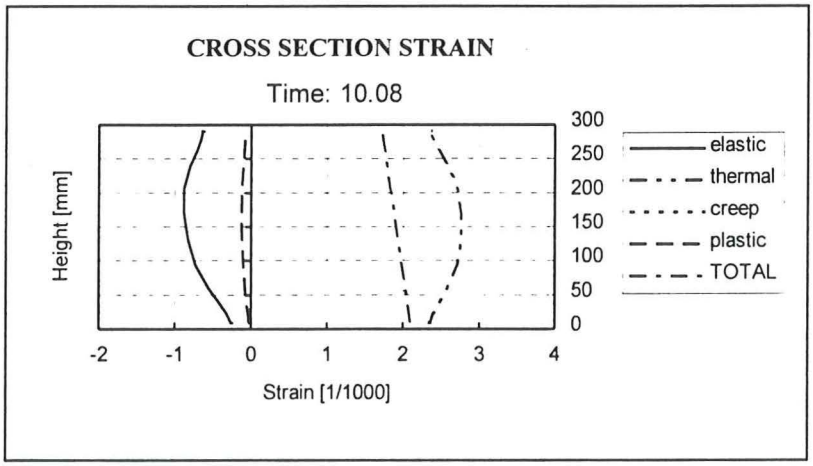

Fig 6.12 Cross-section strain after 10.08 minutes; fire exposure on all faces (100%).

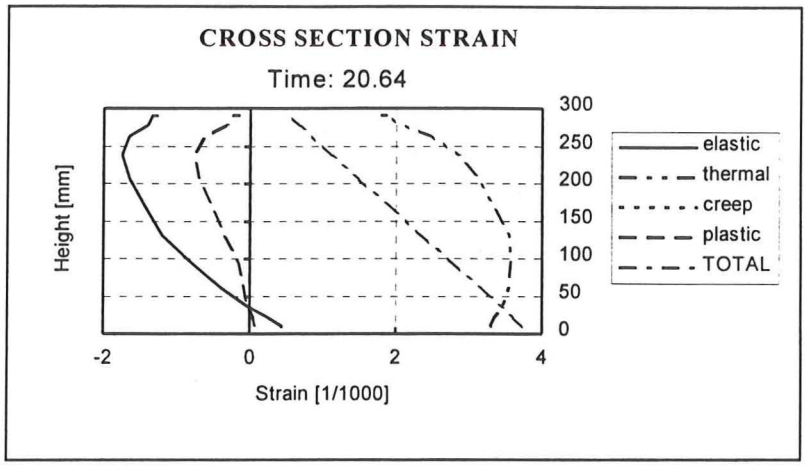

Fig 6.13 Cross-section strain after 20.64 minutes; partial fire exposure (83%).

As the fire scenario continues the steel core temperatures increase and the difference, between partial fire exposure and fire on all faces, grows larger. This also translates to the stresses and strains, which is confirmed by comparing the results displayed in the charts presented in this section.

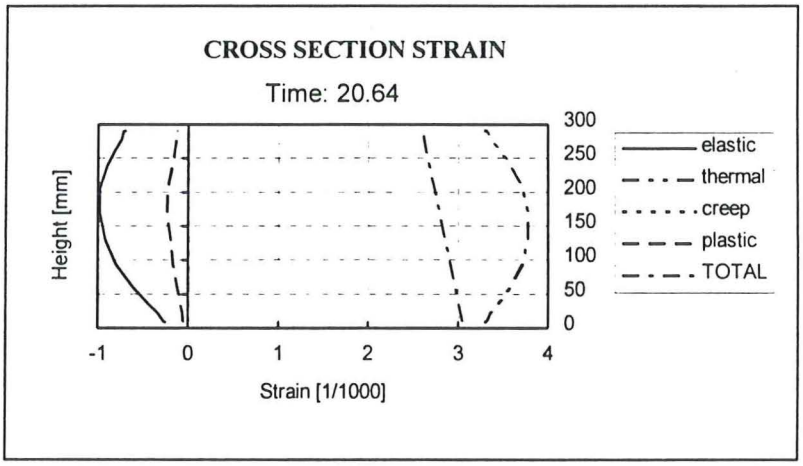

Fig 6.14 Cross-section strain after 20.64 minutes; fire exposure on all faces (100%).

6.2.2 40% loading, slenderness equal to 1.0 and additional eccentricity

This section displays the results obtained when the effects from an additional eccentricity have been involved. Graphical results concerning 20%:s loading and as well 60%:s loading can be obtained from appendix D and appendix F.

The magnitude of the additional eccentricity is defined as described in section 5.2.3, with the cross-sectional stress equal to zero in the least stress affected flange. This parameter is the only one that has been altered, compared to the previous section, and hence the charts may very well be compared to each other in order to illuminate the influence from additional eccentricity.

The graphical illustration in this section is not as comprehensive as the material lined out in the previous section. Here the presentation is confined to illustrate stresses and strains at one point of time only.

The charts will follow in the order adopted before; time temperature relationship, displacement, cross-sectional stress and cross-sectional strain. Hence in figures 6.15 and 6.16 the time temperature curves, applying to partial fire exposure and fire exposure on all faces, are displayed.

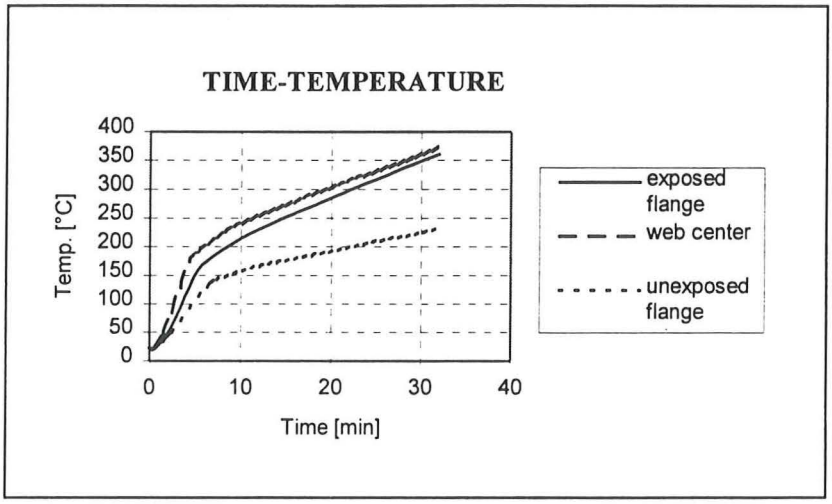

Fig 6.15 Time temperature curve in various locations (exposed flange, web center and unexposed flange) of the steel profile for the case of partial fire exposure (83%). Note the elevating temperature gradient between the to flanges.

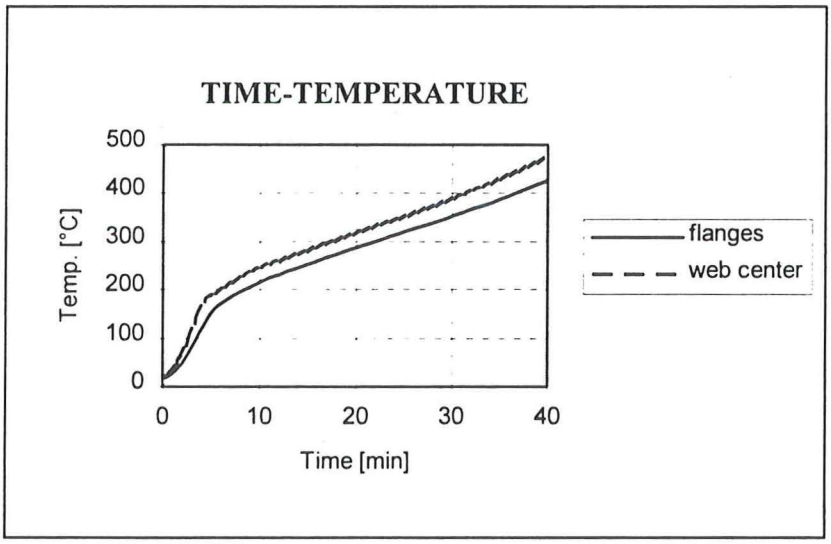

Fig 6.16 Time temperature curve in the flanges and in the web center, for the case of fire exposure on all faces (100%).

Studying figure 6.16, the similarity between the temperature development in flanges and web center is observed. Accordingly it would here be justifiable to approximate the cross-section temperature as constant. The corresponding development in figure 6.15 though, where only three of the faces are exposed to fire, displays a completely different time temperature scenario, with huge differences between the two flanges and obviously an assumption of constant cross-sectional temperatures, is in this case to serious a simplification to accept.

In figures 6.17 and 6.18 the time displacement curves are shown. Comparing with the corresponding calculation in appendix B, figures B15 and B16, where no additional eccentricity has been applied, the influence of the moment distribution that develops along the column is clear. A considerably larger magnitude of the displacement is obtained, when fire exposure on all faces is regarded. As for the case of partial fire exposure the enhancement in displacement is rather modest, and only a limited increase has been found compared to the calculation where no additional eccentricity has been imposed.

Thus the lateral displacement ratio between partial fire exposure and fire exposure on all faces is not as striking as was the case when no additional eccentricity was regarded.

Between the two figures, 6.17 and 6.18, it is noted that for the latter part of the scenario the magnitudal difference could be expressed by a multiplying factor of 4-5.

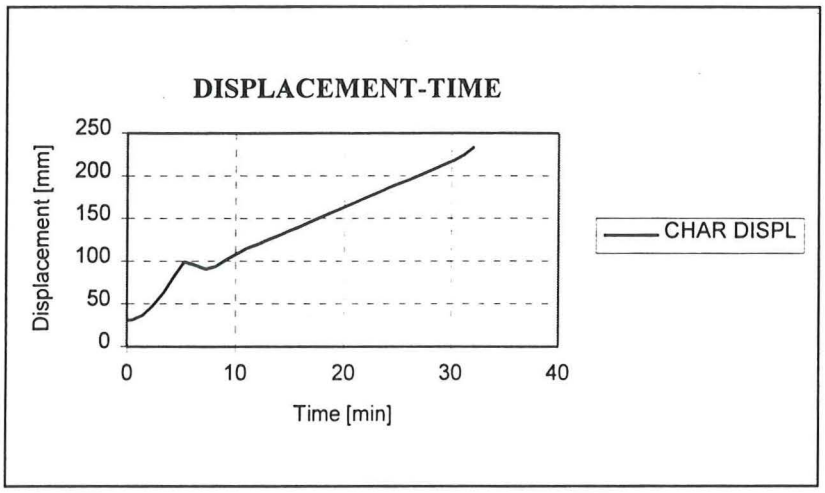

Fig 6.17 Characteristic lateral displacement at the top of an axially loaded steel column. Partial fire exposure (83%).

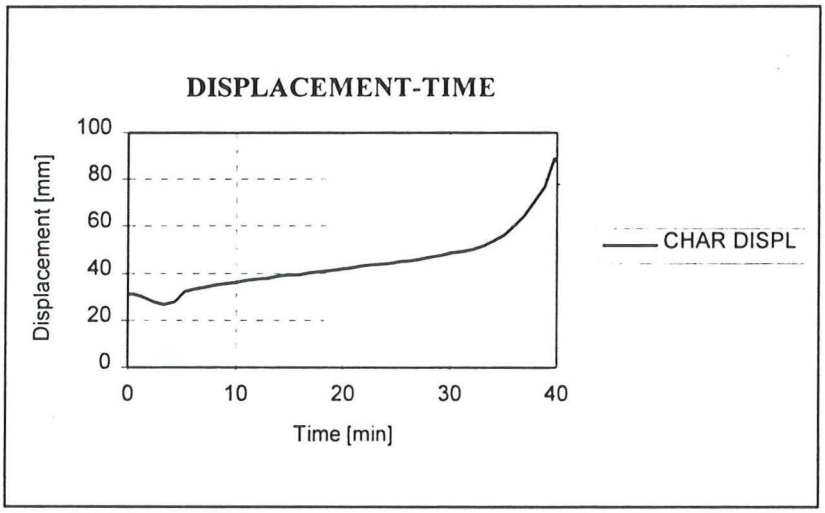

Fig 6.18 Characteristic lateral displacement at the top of an axially loaded steel column. Fire exposure on all faces (100%).

The enlarged magnitude of deflection result in a greater moment, that will render an enhancement in the cross-sectional stress, as seen in figures 6.19 and 6.20.

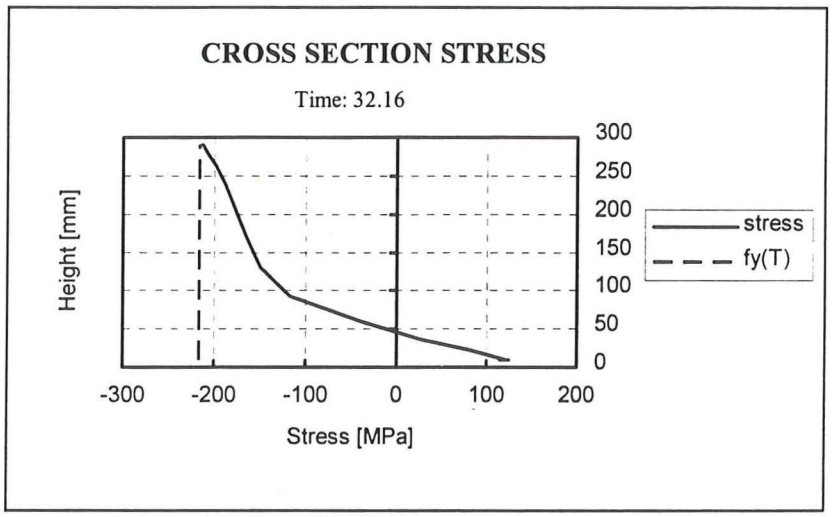

Fig 6.19 Cross-section stress distribution in the critical cross-section, i.e. the end condition (see figure 5.8). Partial fire exposure (83%).

Comparing figure 6.19 with figure B21 of appendix B, it is observed that the stress distributions are very similar. The difference however is that this loading situation is obtained approximately 10 minutes earlier when effects from additional eccentricity are involved.

It is concluded that the stress relationship between partial fire exposure and fire exposure on all faces, is pretty much the same, comparing influence from additional eccentricity to the case where no additional eccentricity is applicable, only higher magnitudes are obtained faster when additional eccentricity is considered.

Studying the two stress charts of figures 6.19 and 6.20, the appearance is recognised from before and the message is clear; partially fire exposed steel columns utilise the material capacity to a greater extent then those exposed to fire on all faces.

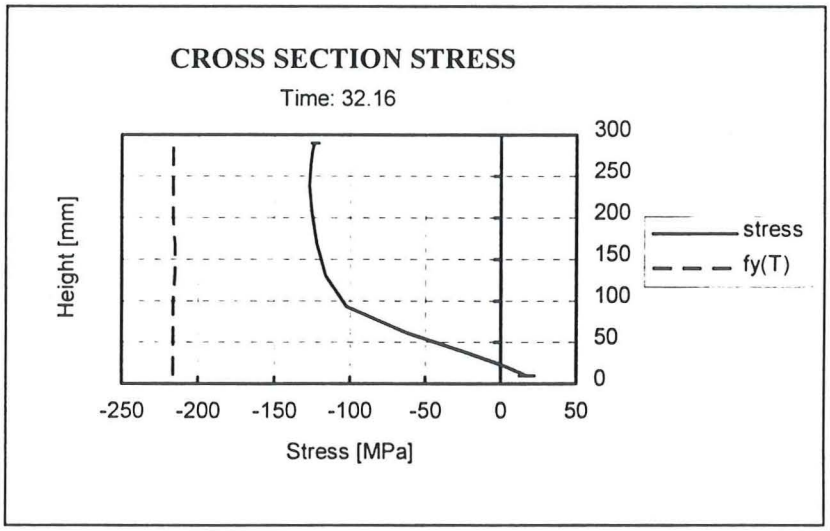

Fig 6.20 Cross-section stress distribution in the critical cross-section, i.e. the end condition (see figure 5.8). Fire exposure on all faces (100%).

The cross-sectional strain distributions that correspond to, the in figures 6.19 and 6.20 shown stress distributions, are presented in figures 6.21 and 6.22.

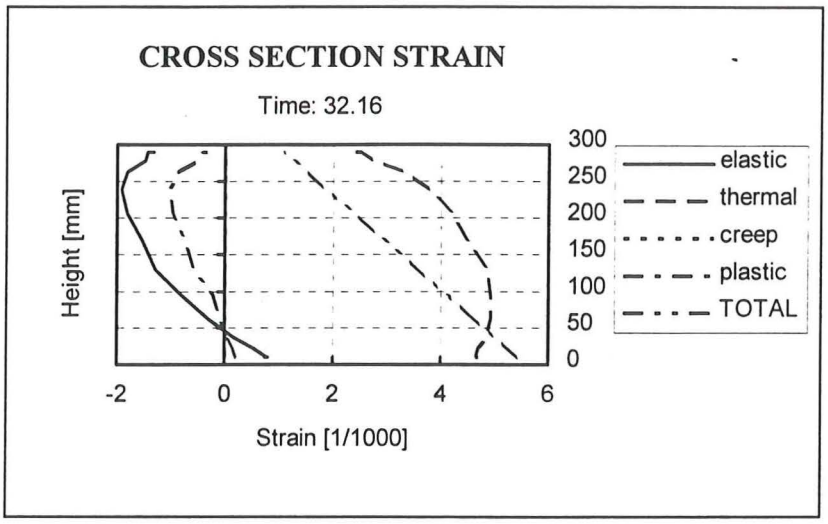

Fig 6.21 Cross-section strain distribution in the critical cross-section, i.e. the end condition (see figure 5.8). Partial fire exposure (83%).

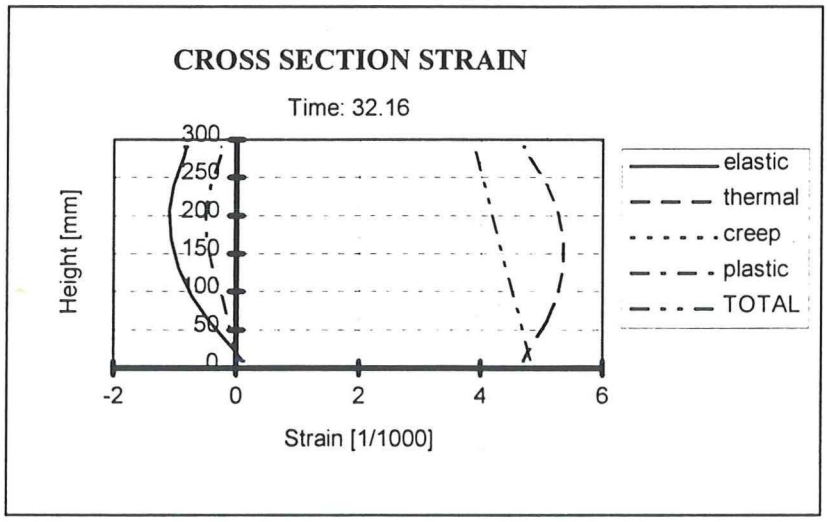

Fig 6.22 Cross-section strain distribution in the critical cross-section, i.e. the end condition (see figure 5.8). Fire exposure on all faces (100%).

6.2.3 60% loading, slenderness equal to 1.0 and restrained elongation

In this section the parameter restrained elongation is taken into account. The definition is described in section 5.2.6. In this report partial elongation has been studied by means of a restricted allowable elongation distance. 90% of the desired elongation was decided to be an appropriate magnitude of this parameter, hence $\gamma=0.9$.

The results obtained for 20% and 40% loading are presented in appendix G and appendix H.

Studying the results of the computer simulations concerning restrained elongation, there is one item, discussed in section 6.1, that has to be kept in mind. This thing being the fact that, when simulating partially restrained elongation, the structural computer program will develop a tension force by the end of the fire scenario. It would be incorrect to take advantage of this favourable tension force, since it can not be confirmed that it will exist in a real fire situation. Therefore a new definition of critical point of time was introduced in table 6.4, which should be kept in mind here. Accordingly the charts in this section are not applicable after 16 minutes, for the case of

partial fire exposure, and after 36 minutes when fire exposure on all faces is regarded, cf. table 6.4.

Generally speaking, the restrained elongation has the same kind of influence on the deflection and the cross-sectional stress as the additional eccentricity.

The two time temperature relationships are displayed in figures 6.23 and 6.24. The displacement time curves for 83%´s and 100%´s fire exposure are shown in figures 6.25 and 6.26 respectively. Cross-section stresses and strains for a fixed point of time are presented in figures 6.27-6.30.

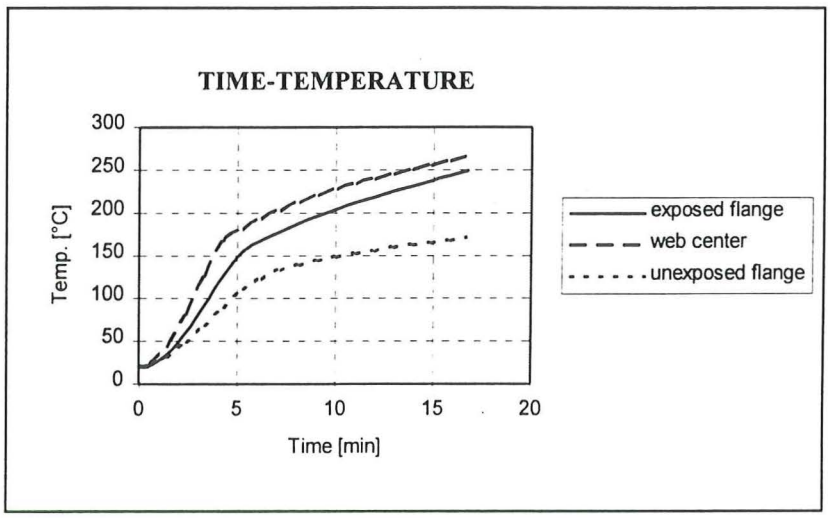

Fig 6.23 Time temperature curve in various locations (web center, exposed and unexposed flange) of the steel profile for the case of partial fire exposure (83%). Note the elevating temperature gradient between the to flanges.

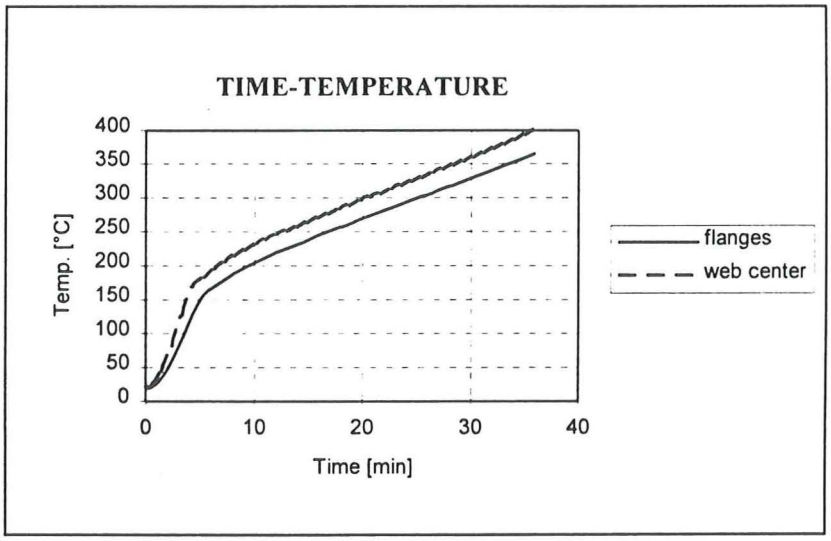

Fig 6.24 Time temperature curve in various locations of the steel profile, for the case of fire exposure on the entire circumference (100%.) Note the similarity in temperature elevation between the flanges and the web center.

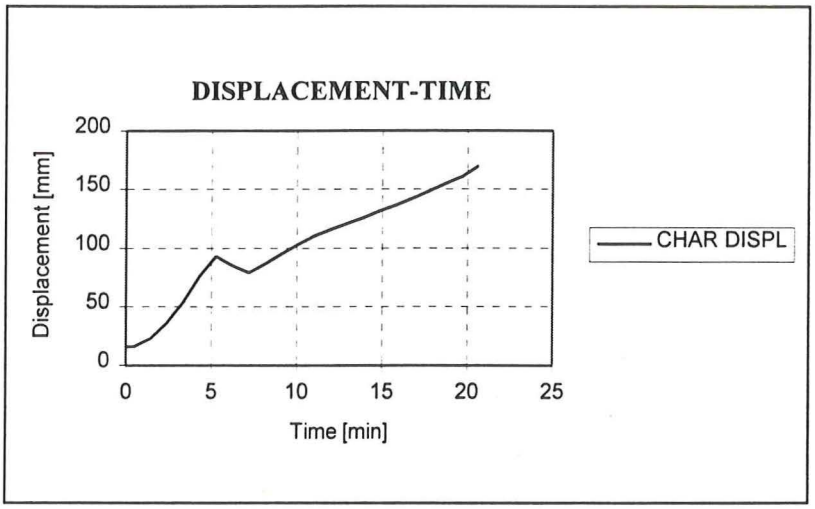

Fig 6.25 Characteristic lateral displacement at the top of an axially loaded steel column. Partial fire exposure (83%). The curve is only applicable to the first 16 minutes.

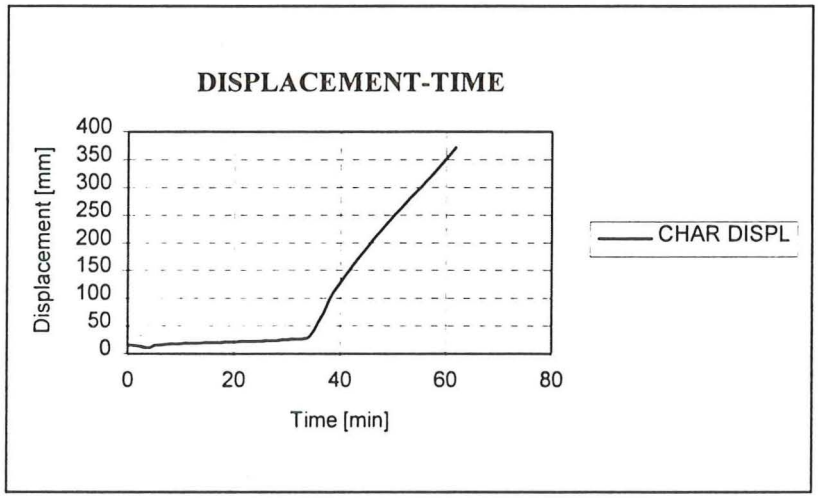

Fig 6.26 Characteristic lateral displacement at the top of an axially loaded steel column. Fire exposure on all faces. The chart applies to the first 36 minutes only.

Comparing figure 6.26 with figure 6.4, the deflection development is the same till the allowable elongation is attained, this happens after 33 minutes. Then a constraint force is developing and the deflection is increasing. The progress could be followed in the detailed output of Steelfire. When the axial force has reached a peak value it starts to decrease and regains it is initial value at 36 minutes. After that the reduction process proceeds and a tensional effect is developing that takes the analysis further.

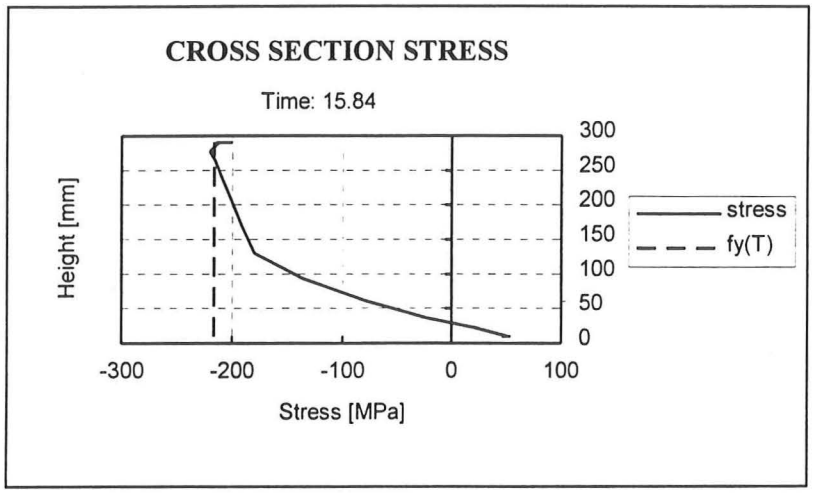

Fig 6.27 Cross-section stress at critical time (table 6.4). Partial fire exposure (83%).

Analysing the chart in figure 6.27 it is noted that the stress has attained the temperature related yield strain limit ($f_y(T)$) at the upper flange. If the distribution is compared with the cross-section stress in figure C21 of appendix C (unrestrained elongation) it is seen that they look very similar. The difference though is that for the case of restrained elongation this stress distribution is obtained 5 minutes earlier.

Once again the vast difference between the stress distribution at partial fire exposure and fire exposure on all faces, is emphasised, c.f figures 6.27 and 6.28.

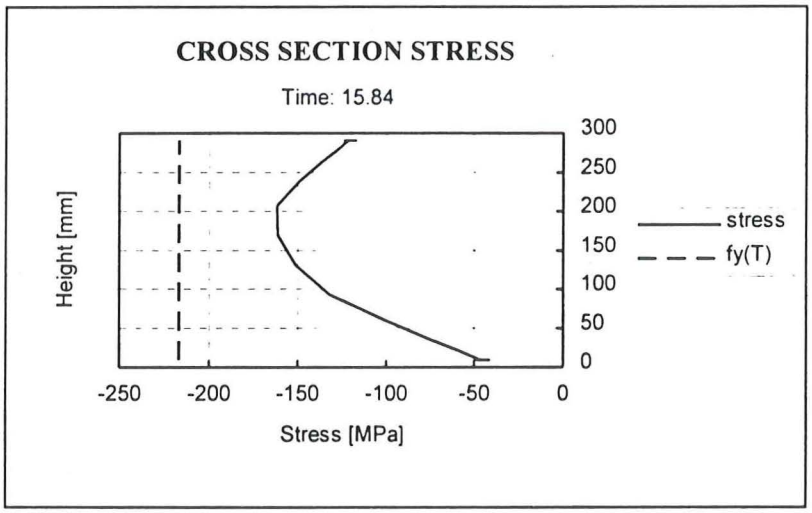

Fig 6.28 Cross-section stress 15.84 minutes after the temperature elevation was initiated. Fire exposure on all faces (100%).

The cross-sectional strain that corresponds to the stress distributions showed in figures 6.27 and 6.28 are presented in figures 6.29 and 6.30. The difference between these charts is the temperature related modulus of elasticity.

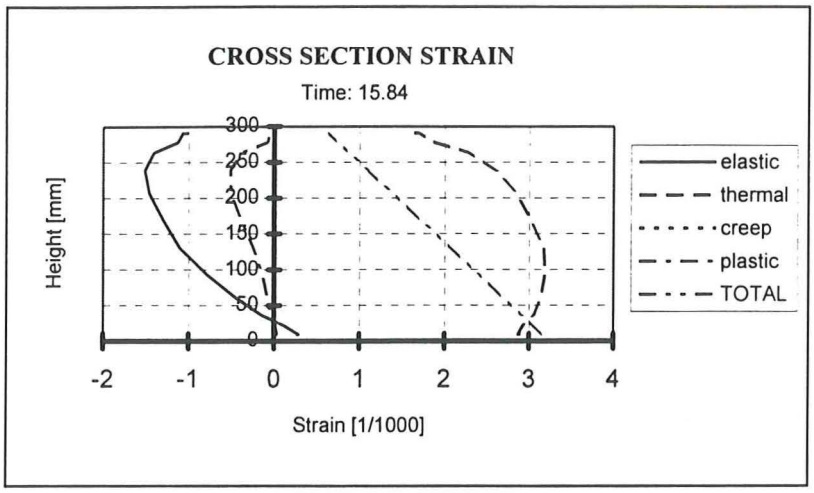

Fig 6.29 Cross-section strain at 15.84 minutes. Partial fire exposure (83%).

A glance on the shape of the thermal strain component of figure 6.29 implies that only a limited part of the circumference is exposed to fire. As for figure 6.30, the fire exposes all faces and thus the distribution of the thermal strain component is symmetrical across the height of the cross-section.

The elastic strain component is obtained by subtracting the thermal strain from the total strain. The creep strain is omitted in Eurocode calculations, and could have been left out in the description of lines. Plastic strain refers to the part of the deformation that is irreversible.

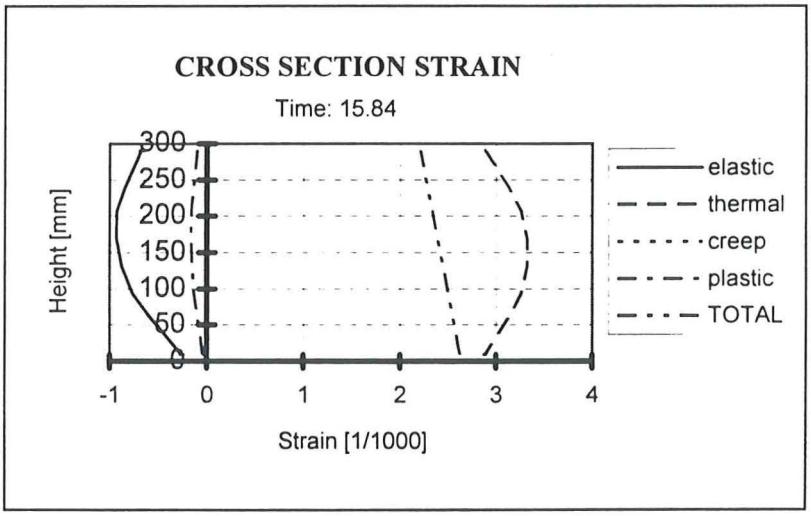

Fig 6.30 Cross-section strain at 15.84 minutes. Fire exposure on all faces (100%).

7 CONCLUSION

In the previous chapter the results of the simulations undertaken in this report was analysed. Based on the facts lined out there, it is possible to conclude that there evidently exist situations when partial fire exposure is more disadvantageous to a column´s load-bearing capacity then fire exposure on all faces.

The results obtained, apply to the presented selection of parameter combinations and under the assumptions adopted, and are by no means general to this phenomenon under different circumstances. However, the fact that this study has revealed a degree of partial fire exposure that is ruling compared to complete exposure, makes it extremely important to map the entire range of partial fire exposures, that these effects can be quantified and incorporated in the design guides.

It is most likely so, that the performance and mode of failure that is ruling, differ between the two types of fire exposure. The degree of lateral displacement has been proved to attain a lot higher magnitude for partial fire exposure then for fire exposure on all faces. Furthermore the deflection concerning partial fire exposure will increase on a continuous basis throughout the fire scenario. However for the case of fire exposure on all faces the deflection will remain rather constant until failure occurs. Hence the cross-sectional stress will, in conformity with the deflection, enhance when partial fire exposure is regarded, and eventually the yield stress will be attained. This means that certain parts of the cross-section will be plasticized and accordingly not contribute to the stiffness of the structure. When the cross-sectional stress development has come this far a redistribution of the stresses will take place. As mentioned before the plasticizing reduces the stiffness and thus decreases the critical axial buckling load which now is a possible mode of failure.

As for the case of fire exposure on all faces the cross-sectional stress will barely increase during the fire scenario. The stiffness though will decrease more rapidly for this mode of fire exposure since the heat is penetrating the profile faster when all faces are exposed. Therefore the buckling phenomenon will eventually be reached and this is confirmed by the abruptly escalating deflection seen in, for instance, fig C2.

Accordingly the design guides of today, which all assume a constant temperature across the height of the cross-section, involve an approximation that is unacceptable and thus has to be corrected. Considering fire that exposes the entire structure, it is acceptable to assume constant cross-sectional temperatures, but as the effects from partial fire exposure are involved, the temperature distribution diverge significantly from the approximation. Following the results presented in this report, a set of parameter combinations have been found that imply a lower load-bearing capacity for 83%:s fire exposure on the profile then for 100%:s fire exposure.

Apparently an improvement of the design code is justified. In order to assess a profound description of the structural performance due to partial fire exposure, an extensive research intensification in this field is necessary.

REFERENCES

/1/ **Eurocode 3:** Design of Steel Structures, Part 1.2 Structural Fire Design. Draft prENV 1993-1-2, August 1993

/2/ **Eurocode 3:** Design of steel Structures, Part 1 General Rules and Rules for Buildings. November 1989.

/3/ **Yngve Anderberg:** Properties of materials at high temperatures steel. Rilem report 1983

/4/ **Yngve Anderberg:** SUPER-TEMPCALC, A Commercial And User-friendly Computer Program With Automatic Fem-Generation For Temperature Analysis Of Structures Exposed To Heat. Fire Safety Design AB, Lund 1991.

/5/ **Nils Erik Forsén:** STEELFIRE, Finit Element Program For Non liniear Analysis Of Steel Frames Exposed To Fire. Oslo, September 1983.

/6/ **G. M. E Cooke:** The Structural Response Of Steel I-Section Members Subject To Elevated Temperature Gradients Across The Section. London, September 1987.

/7/ **Sven-Erik Magnusson, Ove Pettersson and Jörgen Thor:** Brand Teknisk Dimensionering Av Stål Konstruktioner, 1974

/8/ **Björn Åsen:** An Experimental Study on Steel Column´s Behaviour at Elevated Temperatures, Trondheim 1985

/9/ **Arne Hillerborg:** Byggnadsmateriallära. Lund 1983

/10/ **Sven Thelandersson:** Stålkonstruktioner, Bärande Konstruktioner FK 2. Lund 1993.

/11/ **Yngve Anderberg, Nils Erik Forsén, Björn Aasen:** Measured and predicted behaviour of steel beams and columns in fire, Lund 1986

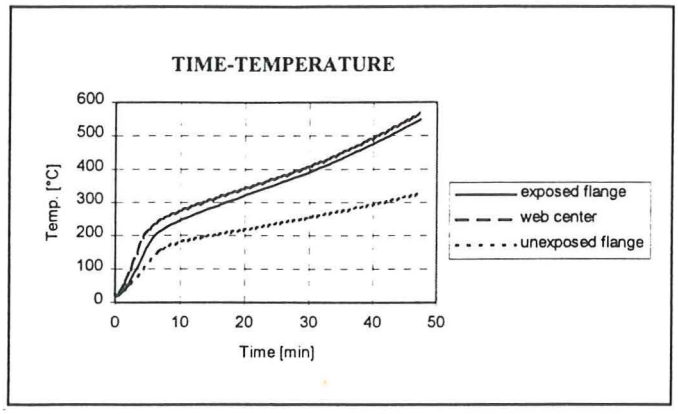

Fig A1 Time temperature development in the flanges and web center. Partial fire exposure (83%).

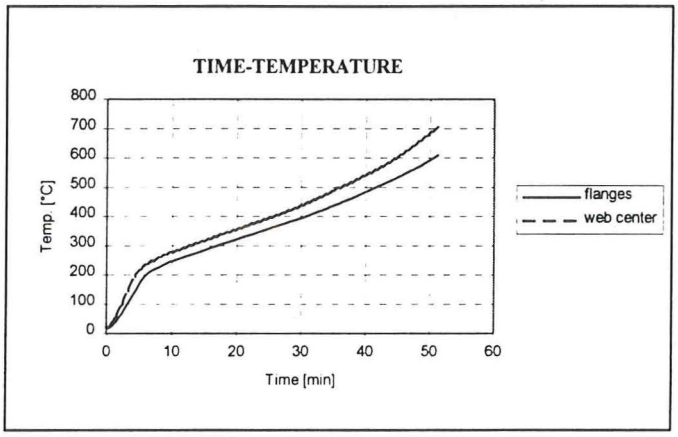

Fig A2 Time temperature development in the flanges and web center. Fire exposure on all faces (100%).

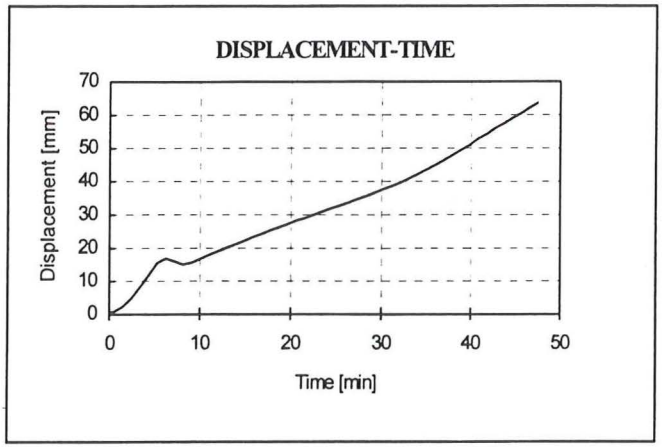

Fig A3 Lateral displacement as function of time at the top of an axially loaded steel column. Loading: 20% of critical axial buckling load. Slenderness equal to 0.5. Partial fire exposure (83%).

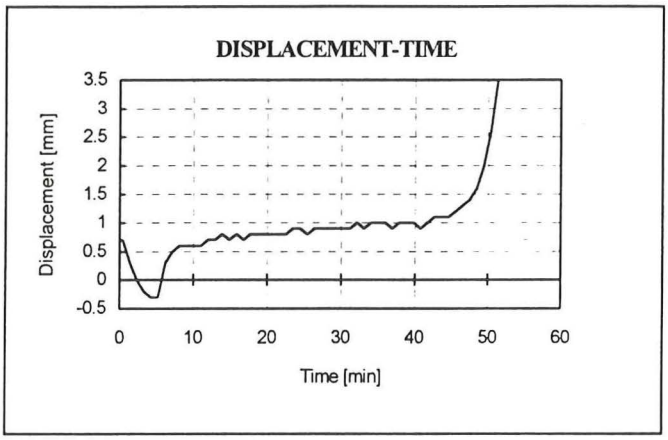

Fig A4 Lateral displacement as function of time at the top of an axially loaded steel column. Loading: 20% of critical axial buckling load. Slenderness equal to 0.5. Fire exposure on all faces (100%).

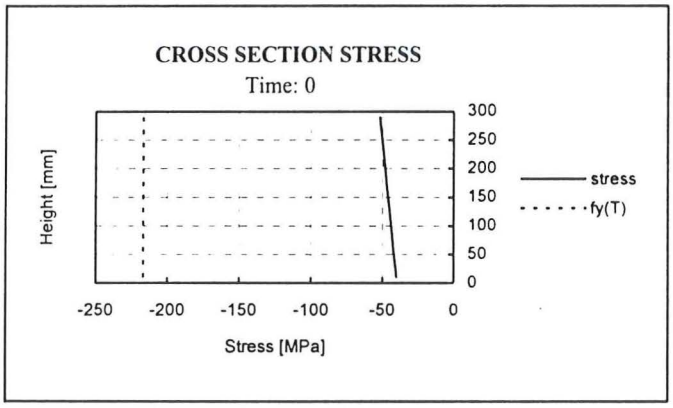

Fig A5 Cross section stress at the fixed end boundary condition, at room temperature. Loading: 20% of critical axial buckling load. Slenderness equal to 0.5.

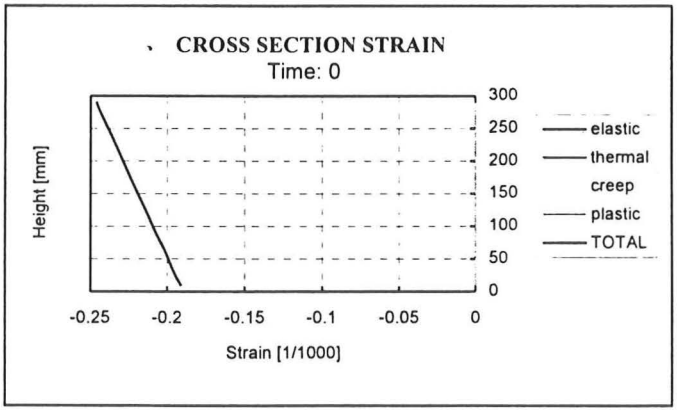

Fig A6 Cross section strain at the fixed end boundary condition, at room temperature. Loading: 20% of critical axial buckling load. Slenderness equal to 0.5.

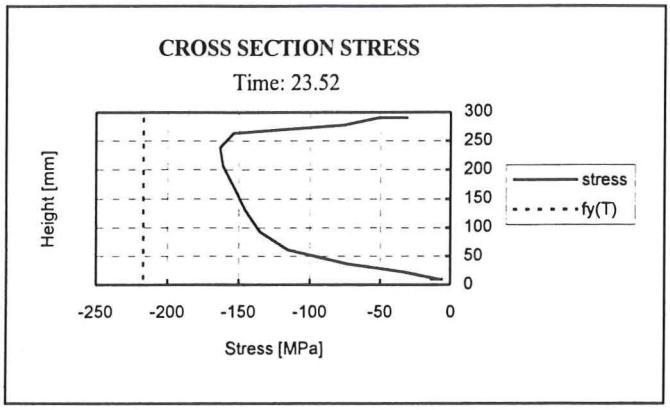

Fig A7 Cross section stress at the fixed end boundary condition, 23.52 minutes after initiation of temperature elevation. Loading: 20% of critical axial buckling load. Slenderness equal to 0.5. Partial fire exposure (83%).

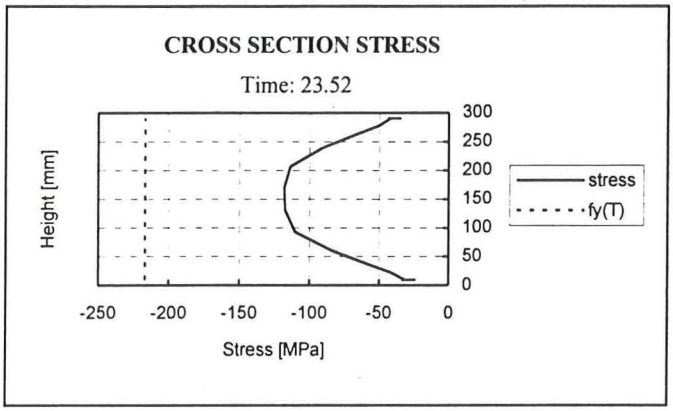

Fig A8 Cross section stress at the fixed end boundary condition, 23.52 minutes after initiation of temperature elevation. Loading: 20% of critical axial buckling load. Slenderness equal to 0.5. Fire exposure on all faces (100%).

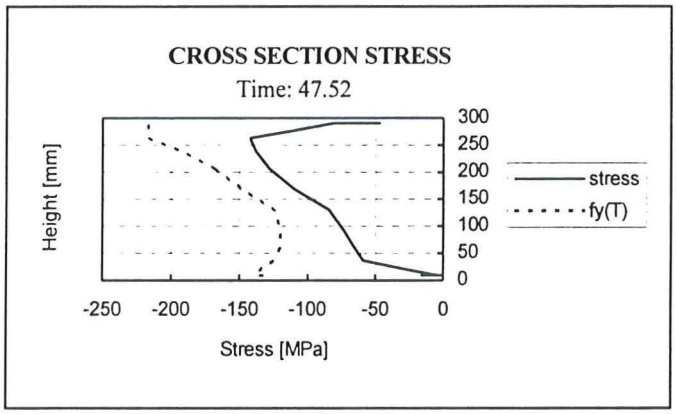

Fig A9 Cross section stress at the fixed end boundary condition, 47.52 minutes after initiation of temperature elevation. Loading: 20% of critical axial buckling load. Slenderness equal to 0.5. Partial fire exposure (83%).

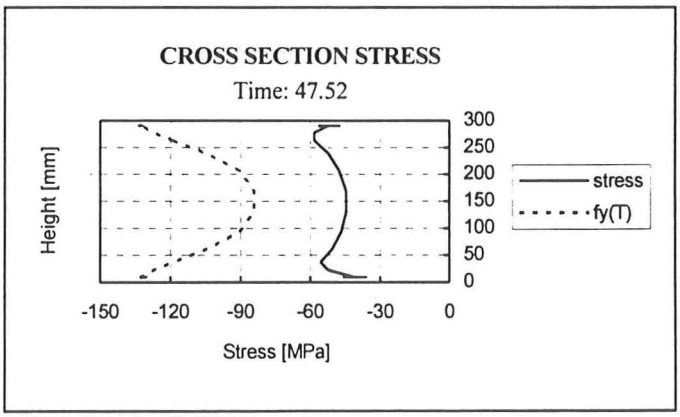

Fig A10 Cross section stress at the fixed end boundary condition, 47.52 minutes after initiation of temperature elevation. Loading: 20% of critical axial buckling load. Slenderness equal to 0.5. Fire exposure on all faces (100%).

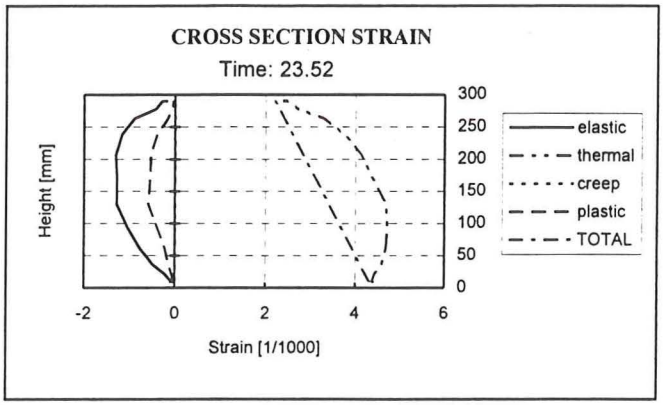

Fig A11 Cross section strain at the fixed end boundary condition, 23.52 minutes after initiation of temperature elevation. Loading: 20% of critical axial buckling load. Slenderness equal to 0.5. Partial fire exposure (83%).

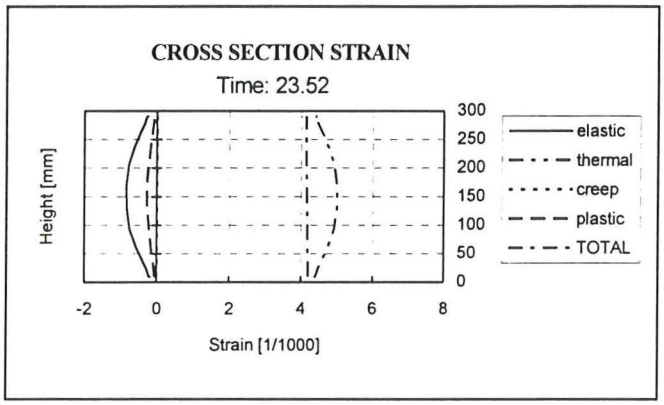

Fig A12 Cross section strain at the fixed end boundary condition, 23.52 minutes after initiation of temperature elevation. Loading: 20% of critical axial buckling load. Slenderness equal to 0.5. Fire exposure on all faces (100%).

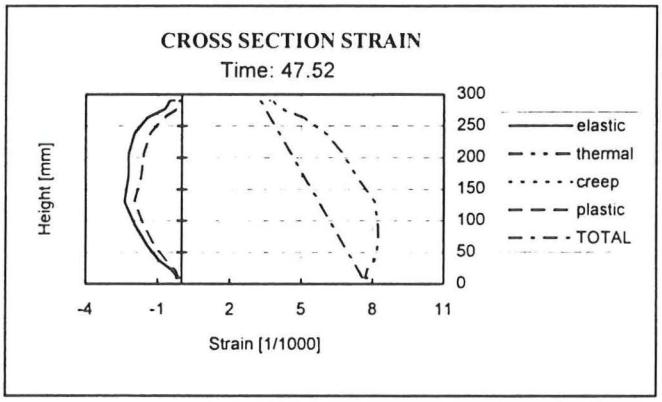

Fig A13 Cross section strain at the fixed end boundary condition, 47.52 minutes after initiation of temperature elevation. Loading: 20% of critical axial buckling load. Slenderness equal to 0.5. Partial fire exposure (83%).

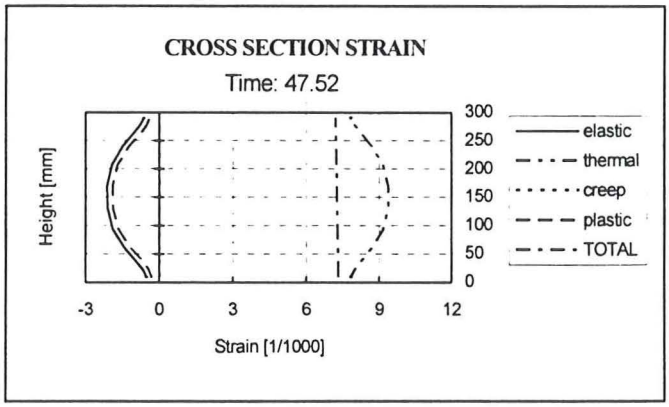

Fig A14 Cross section strain at the fixed end boundary condition, 47.52 minutes after initiation of temperature elevation. Loading: 20% of critical axial buckling load. Slenderness equal to 0.5. Fire exposure on all faces (100%).

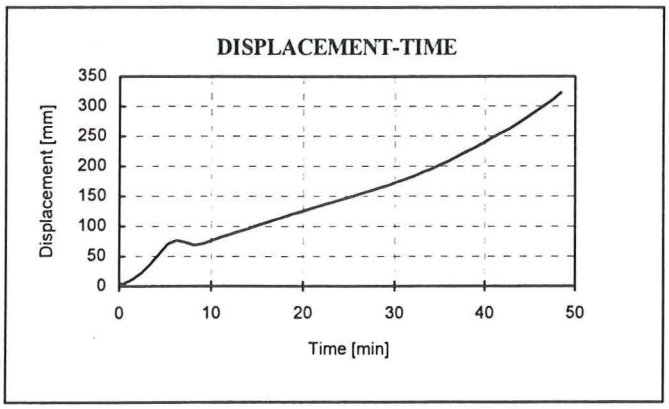

Fig A15 Lateral displacement as function of time at the top of an axially loaded steel column. Loading: 20% of critical axial buckling load. Slenderness equal to 1.0. Partial fire exposure (83%).

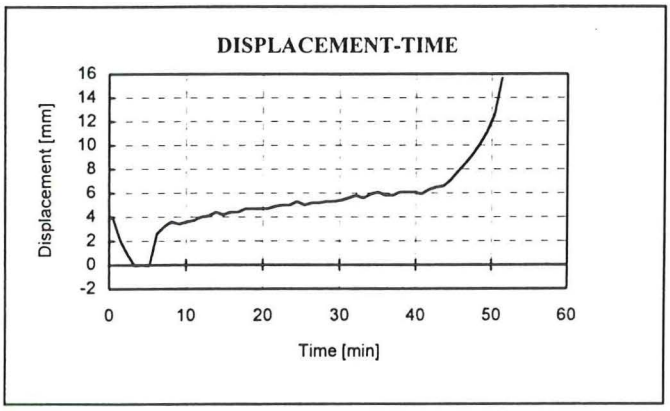

Fig A16 Lateral displacement as function of time at the top of an axially loaded steel column. Loading: 20% of critical axial buckling load. Slenderness equal to 1.0. Fire exposure on all faces (100%).

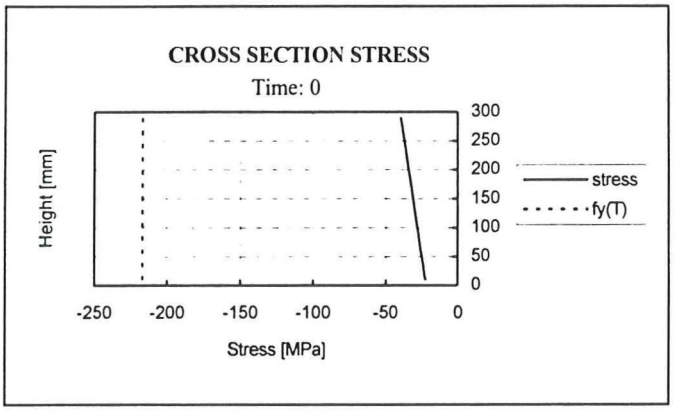

Fig A17 Cross section stress at the fixed end boundary condition, at room temperature. Loading: 20% of critical axial buckling load. Slenderness equal to 1.0.

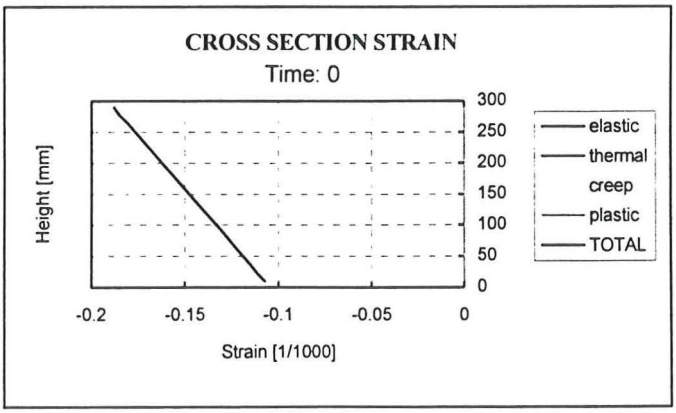

Fig A18 Cross section strain at the fixed end boundary condition, at room temperature. Loading: 20% of critical axial buckling load. Slenderness equal to 1.0.

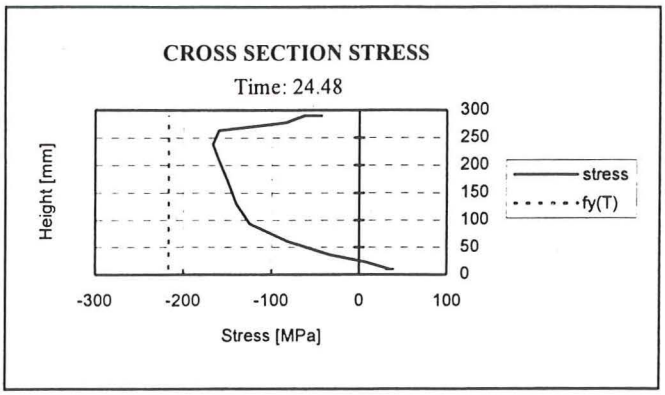

Fig A19 Cross section stress at the fixed end boundary condition, 24.48 minutes after initiation of temperature elevation. Loading: 20% of critical axial buckling load. Slenderness equal to 1.0. Partial fire exposure (83%).

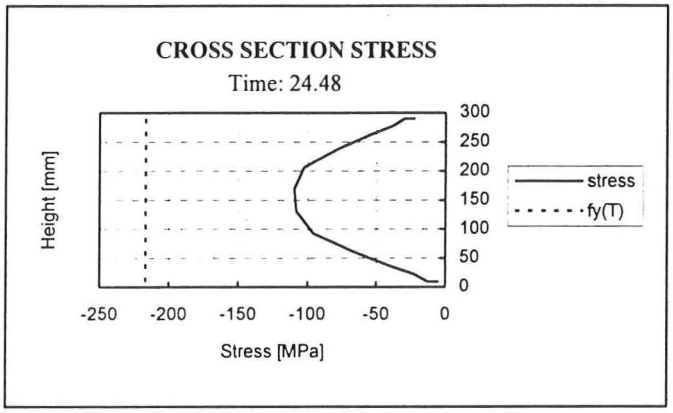

Fig A20 Cross section stress at the fixed end boundary condition, 24.48 minutes after initiation of temperature elevation. Loading: 20% of critical axial buckling load. Slenderness equal to 1.0. Fire exposure on all faces (100%).

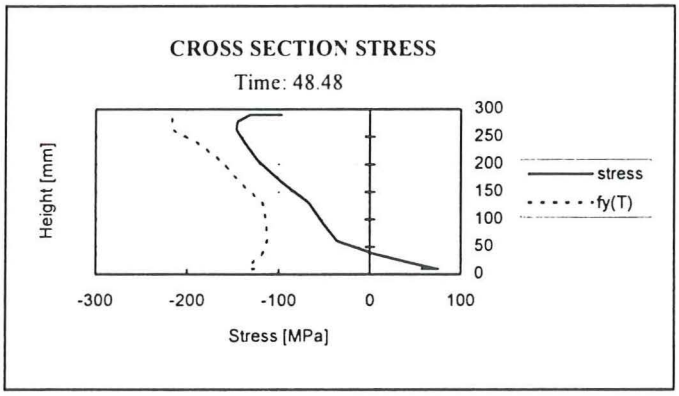

Fig A21 Cross section stress at the fixed end boundary condition, 48.48 minutes after initiation of temperature elevation. Loading: 20% of critical axial buckling load. Slenderness equal to 1.0. Partial fire exposure (83%).

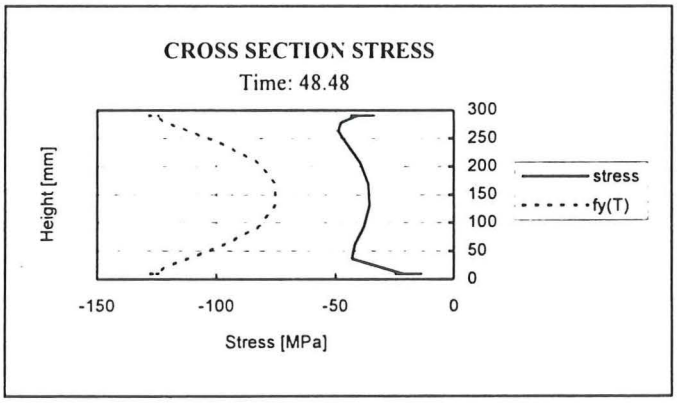

Fig A22 Cross section stress at the fixed end boundary condition, 48.48 minutes after initiation of temperature elevation. Loading: 20% of critical axial buckling load. Slenderness equal to 1.0. Fire exposure on all faces (100%).

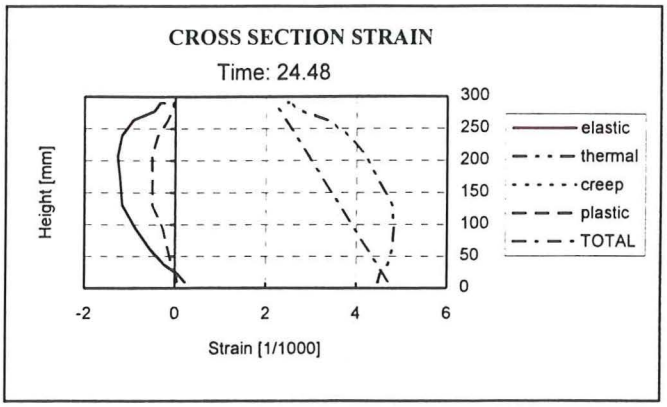

Fig A23 Cross section strain at the fixed end boundary condition, 24.48 minutes after initiation of temperature elevation. Loading: 20% of critical axial buckling load. Slenderness equal to 1.0. Partial fire exposure (83%).

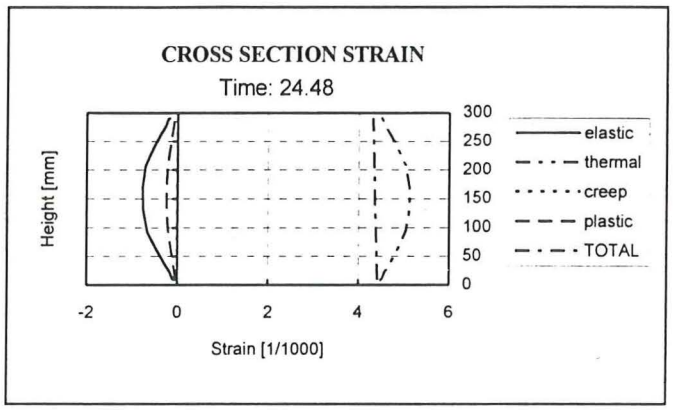

Fig A24 Cross section strain at the fixed end boundary condition, 24.48 minutes after initiation of temperature elevation. Loading: 20% of critical axial buckling load. Slenderness equal to 1.0. Fire exposure on all faces (100%).

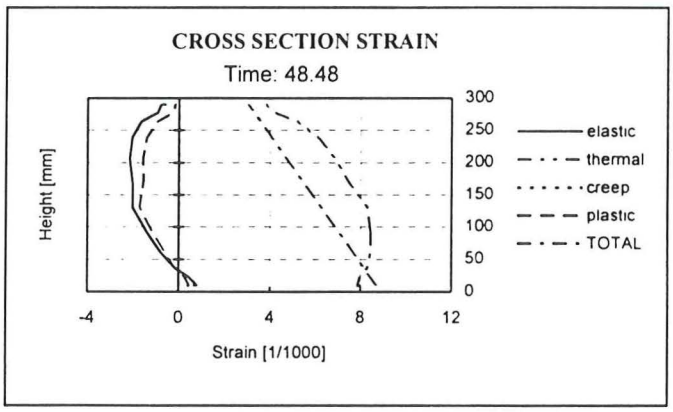

Fig A25 Cross section strain at the fixed end boundary condition, 48.48 minutes after initiation of temperature elevation. Loading: 20% of critical axial buckling load. Slenderness equal to 1.0. Partial fire exposure (83%).

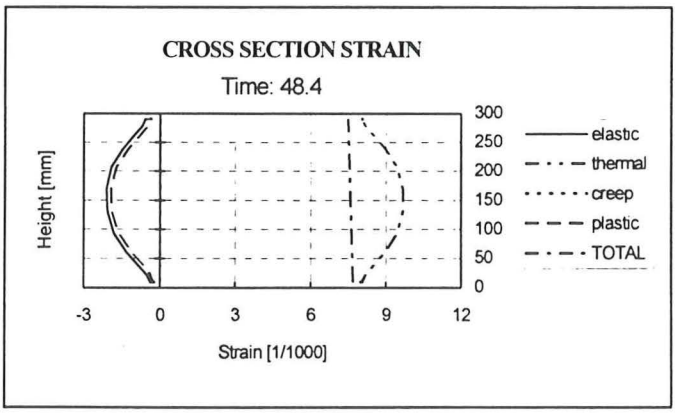

Fig A26 Cross section strain at the fixed end boundary condition, 48.48 minutes after initiation of temperature elevation. Loading: 20% of critical axial buckling load. Slenderness equal to 1.0. Fire exposure on all faces (100%).

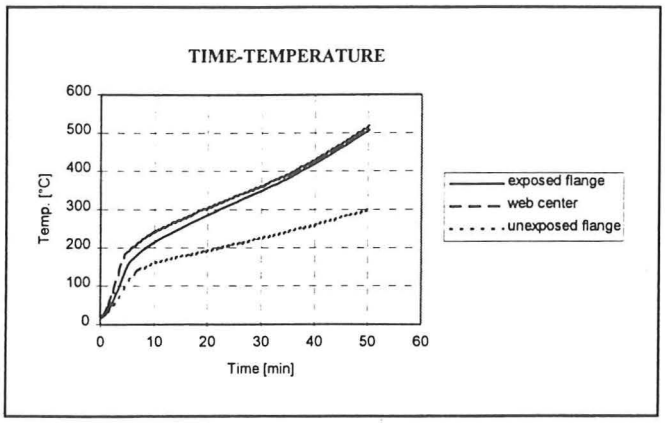

Fig B1 Time temperature development in the flanges and web center. Partial fire exposure (83%).

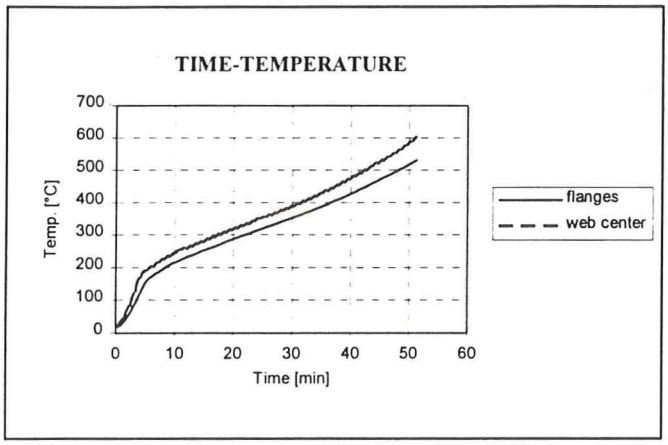

Fig B2 Time temperature development in the flanges and web center. Fire exposure on all faces (100%).

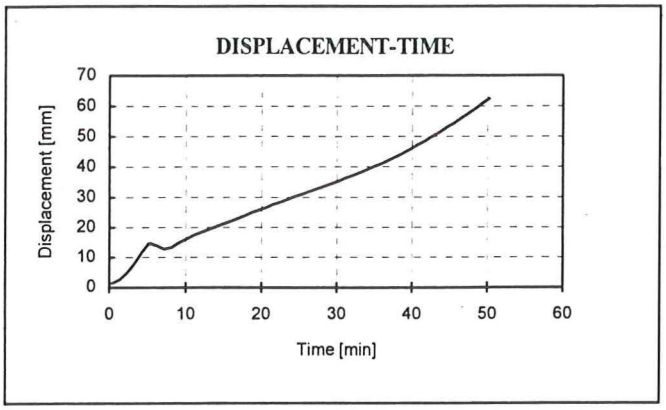

Fig B3 Lateral displacement as function of time at the top of an axially loaded steel column. Loading: 40% of critical axial buckling load. Slenderness equal to 0.5. Partial fire exposure (83%).

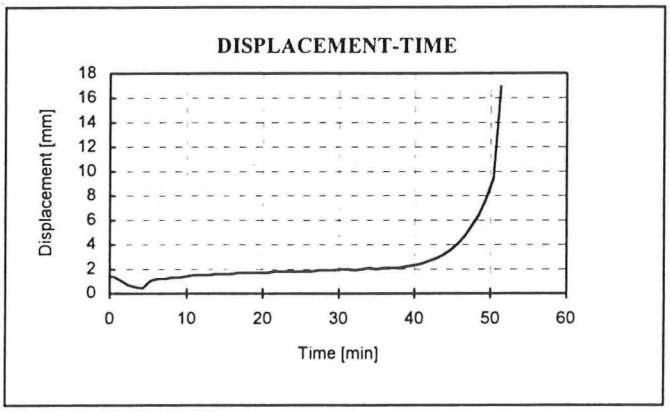

Fig B4 Lateral displacement as function of time at the top of an axially loaded steel column. Loading: 40% of critical axial buckling load. Slenderness equal to 0.5. Fire exposure on all faces (100%).

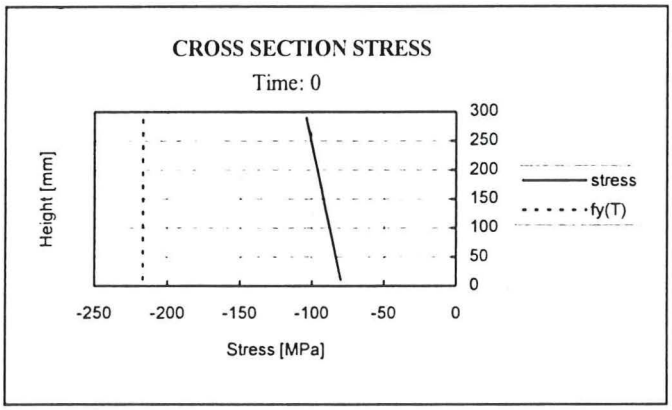

Fig B5 Cross section stress at the fixed end boundary condition, at room temperature. Loading: 40% of critical axial buckling load. Slenderness equal to 0.5.

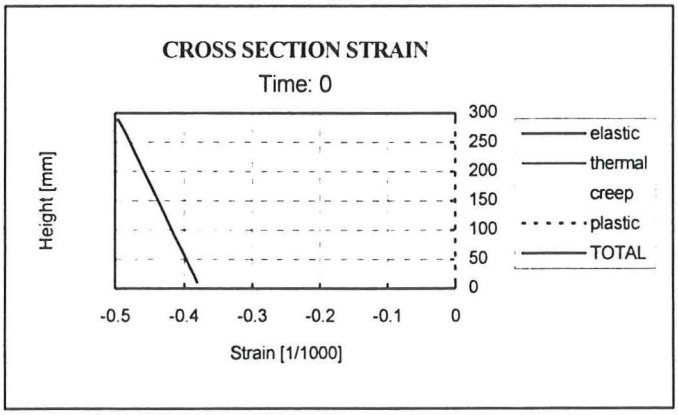

Fig B6 Cross section strain at the fixed end boundary condition, at room temperature. Loading: 40% of critical axial buckling load. Slenderness equal to 0.5.

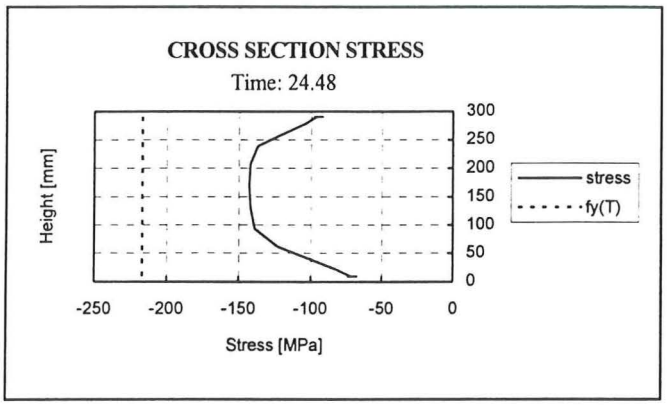

Fig B7 Cross section stress at the fixed end boundary condition, 24.48 minutes after initiation of temperature elevation. Loading: 40% of critical axial buckling load. Slenderness equal to 0.5. Partial fire exposure (83%).

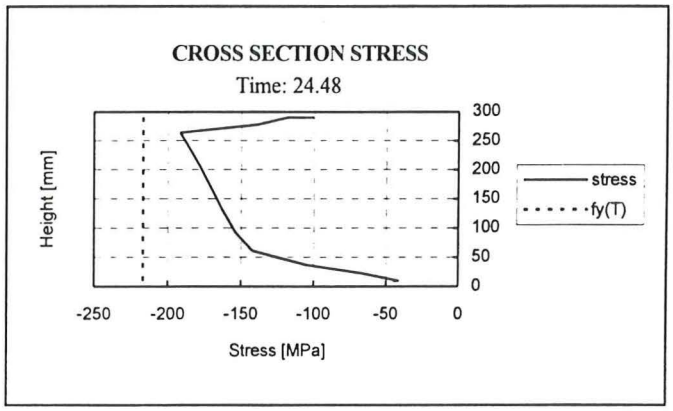

Fig B8 Cross section stress at the fixed end boundary condition, 24.48 minutes after initiation of temperature elevation. Loading: 40% of critical axial buckling load. Slenderness equal to 0.5. Fire exposure on all faces (100%).

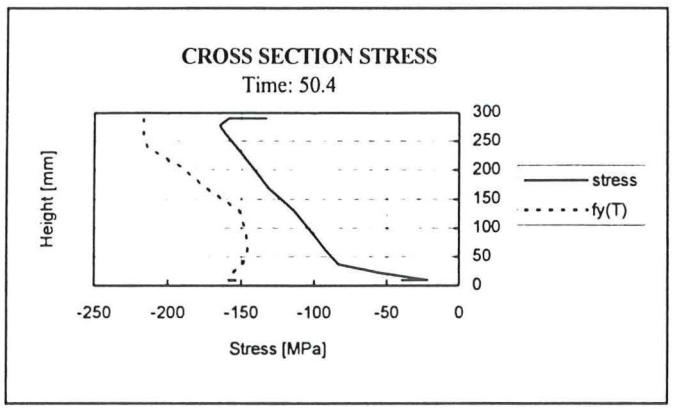

Fig B9 Cross section stress at the fixed end boundary condition, 50.4 minutes after initiation of temperature elevation. Loading: 40% of critical axial buckling load. Slenderness equal to 0.5. Partial fire exposure (83%).

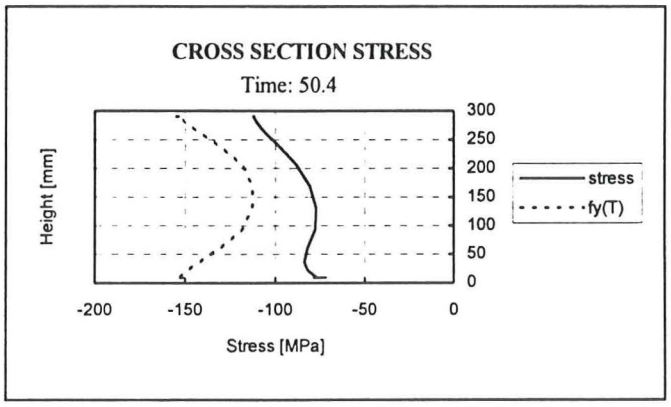

Fig B10 Cross section stress at the fixed end boundary condition, 50.4 minutes after initiation of temperature elevation. Loading: 40% of critical axial buckling load. Slenderness equal to 0.5. Fire exposure on all faces (100%).

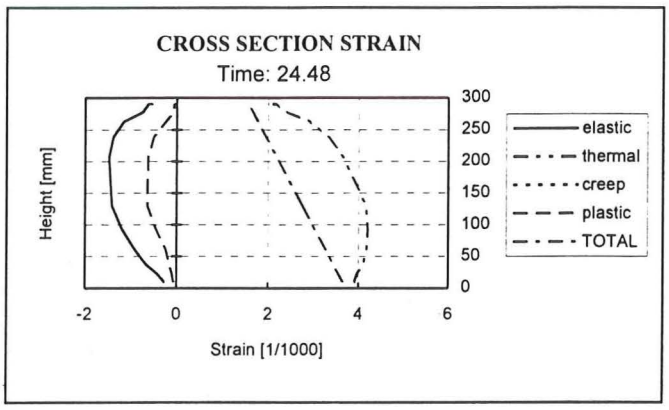

Fig B11 Cross section strain at the fixed end boundary condition, 24.4 minutes after initiation of temperature elevation. Loading: 40% of critical axial buckling load. Slenderness equal to 0.5. Partial fire exposure (83%).

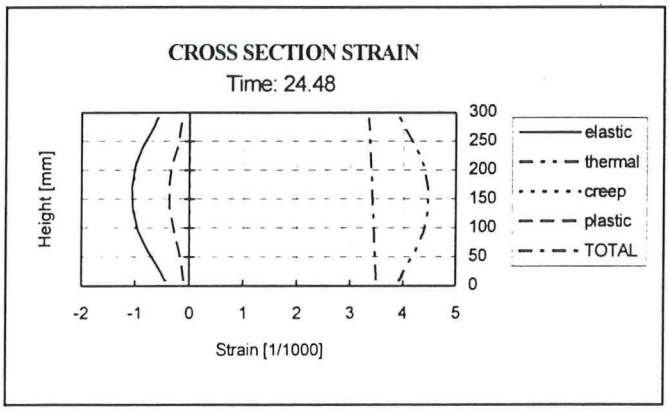

Fig B12 Cross section strain at the fixed end boundary condition, 24.4 minutes after initiation of temperature elevation. Loading: 40% of critical axial buckling load. Slenderness equal to 0.5. Fire exposure on all faces (100%).

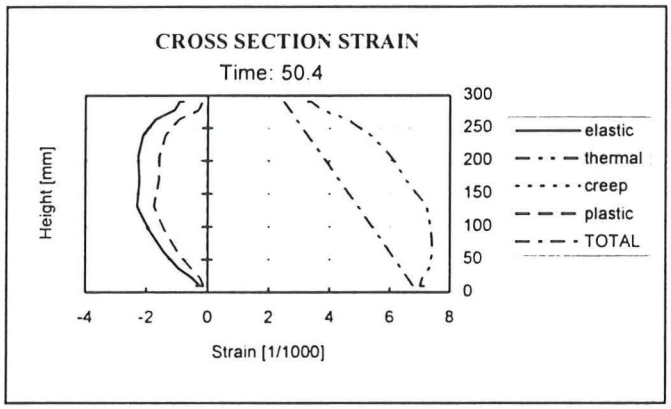

Fig B13 Cross section strain at the fixed end boundary condition, 50.4 minutes after initiation of temperature elevation. Loading: 40% of critical axial buckling load. Slenderness equal to 0.5. Partial fire exposure (83%).

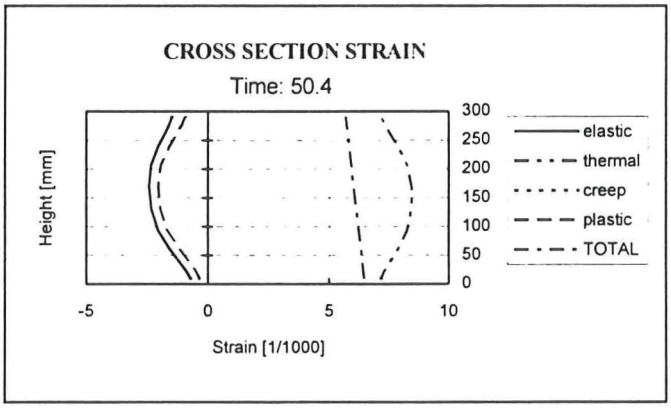

Fig B14 Cross section strain at the fixed end boundary condition, 50.4 minutes after initiation of temperature elevation. Loading: 40% of critical axial buckling load. Slenderness equal to 0.5. Fire exposure on all faces (100%).

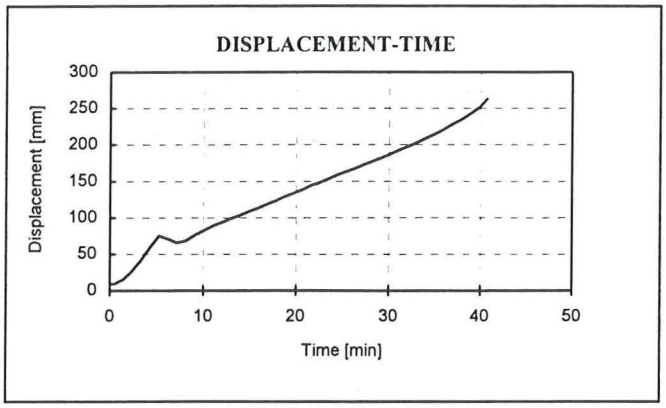

Fig B15 Lateral displacement as function of time at the top of an axially loaded steel column. Loading: 40% of critical axial buckling load. Slenderness equal to 1.0. Partial fire exposure (83%).

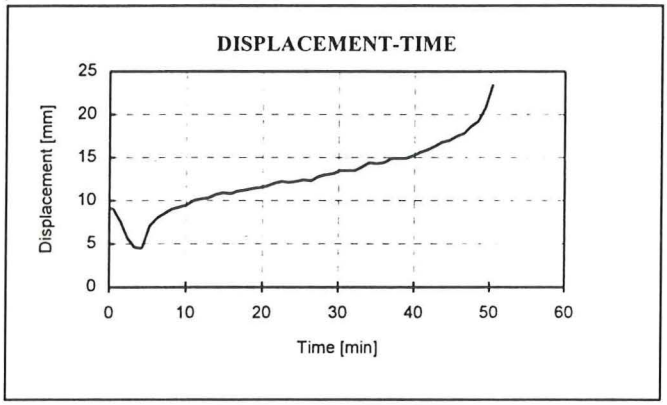

Fig B16 Lateral displacement as function of time at the top of an axially loaded steel column. Loading: 40% of critical axial buckling load. Slenderness equal to 1.0. Fire exposure on all faces (100%).

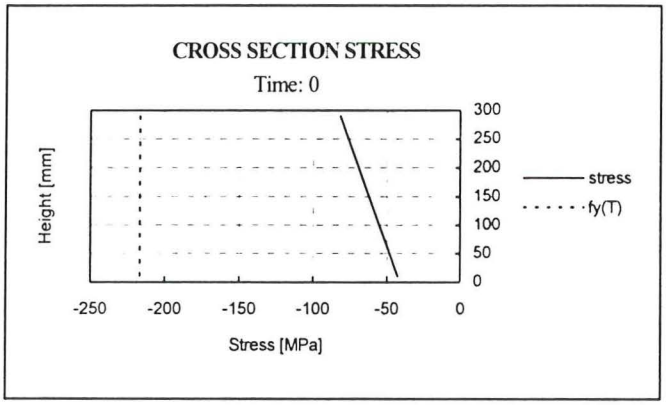

Fig B17 Cross section stress at the fixed end boundary condition, at room temperature. Loading: 40% of critical axial buckling load. Slenderness equal to 1.0.

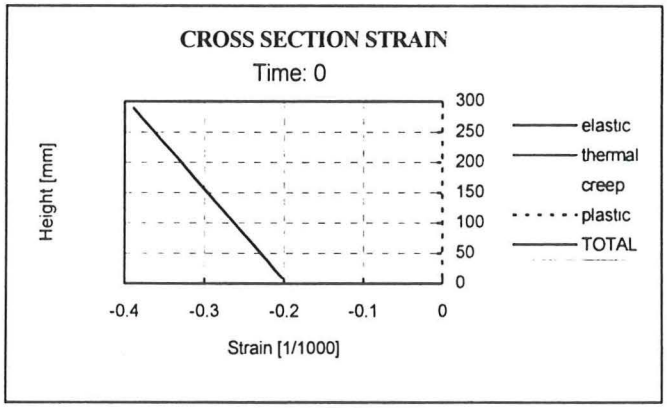

Fig B18 Cross section strain at the fixed end boundary condition, at room temperature. Loading: 40% of critical axial buckling load. Slenderness equal to 1.0.

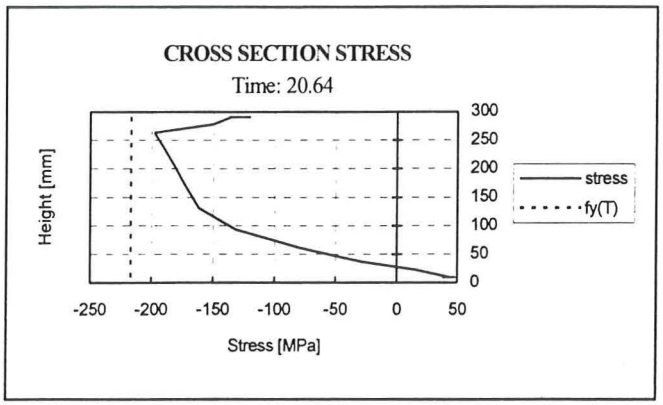

Fig B19 Cross section stress at the fixed end boundary condition, 20.64 minutes after initiation of temperature elevation. Loading: 40% of critical axial buckling load. Slenderness equal to 1.0. Partial fire exposure (83%).

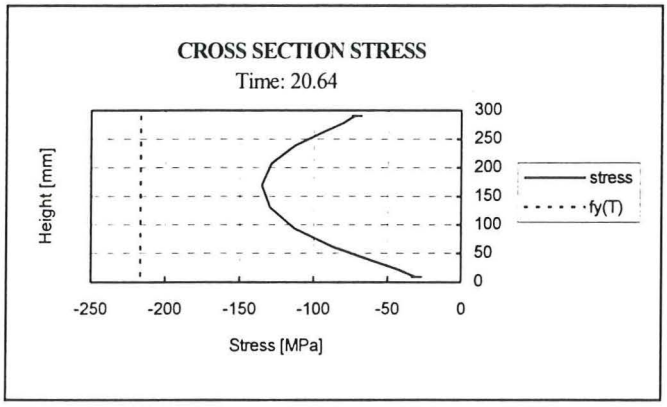

Fig B20 Cross section stress at the fixed end boundary condition, 20.64 minutes after initiation of temperature elevation. Loading: 40% of critical axial buckling load. Slenderness equal to 1.0. Fire exposure on all faces (100%).

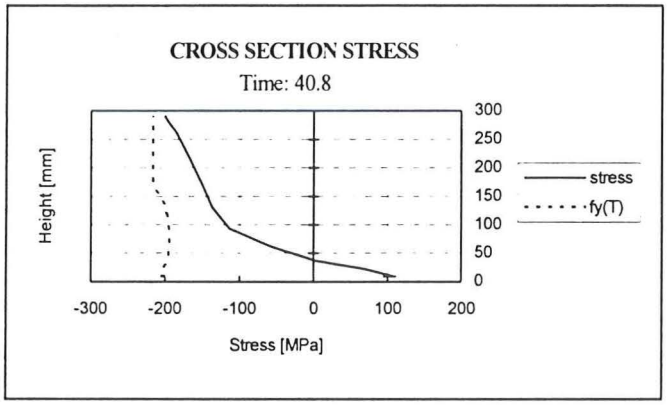

Fig B21 Cross section stress at the fixed end boundary condition, 40.8 minutes after initiation of temperature elevation. Loading: 40% of critical axial buckling load. Slenderness equal to 1.0. Partial fire exposure (83%).

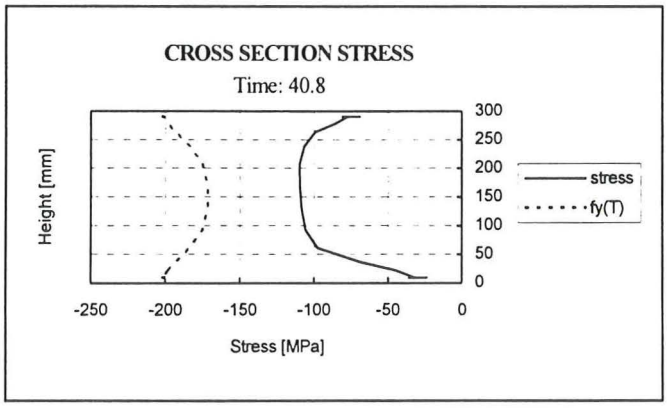

Fig B22 Cross section stress at the fixed end boundary condition, 40.8 minutes after initiation of temperature elevation. Loading: 40% of critical axial buckling load. Slenderness equal to 1.0. Fire exposure on all faces (100%).

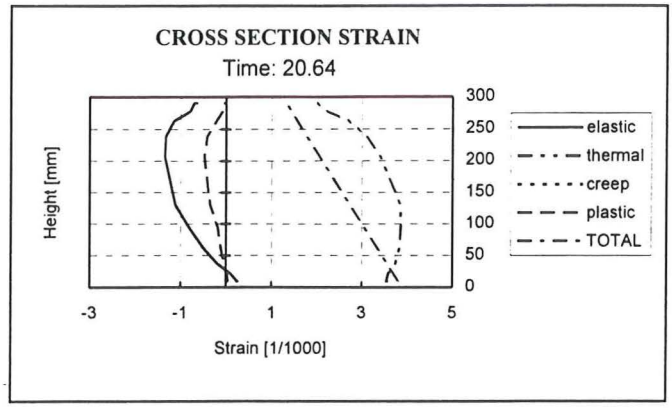

Fig B23 Cross section strain at the fixed end boundary condition, 20.64 minutes after initiation of temperature elevation. Loading: 40% of critical axial buckling load. Slenderness equal to 1.0. Partial fire exposure (83%).

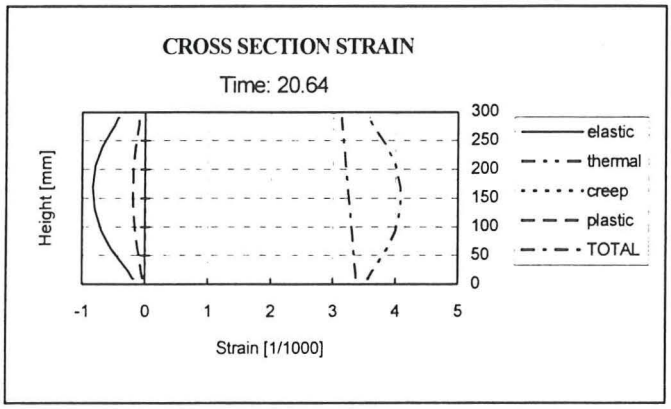

Fig B24 Cross section strain at the fixed end boundary condition, 20.64 minutes after initiation of temperature elevation. Loading: 40% of critical axial buckling load. Slenderness equal to 1.0. Fire exposure on all faces (100%).

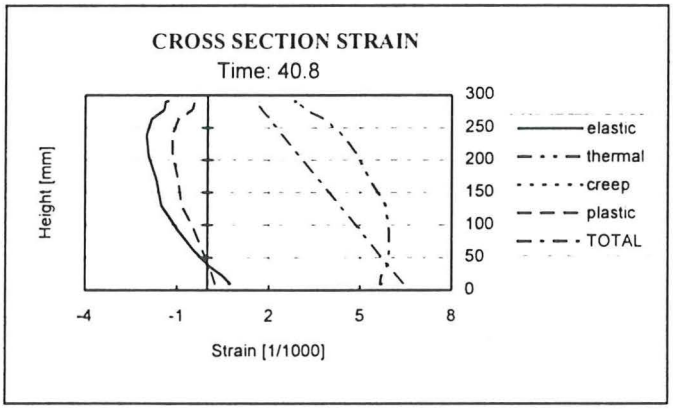

Fig B25 Cross section strain at the fixed end boundary condition, 40.8 minutes after initiation of temperature elevation. Loading: 40% of critical axial buckling load. Slenderness equal to 1.0. Partial fire exposure (83%).

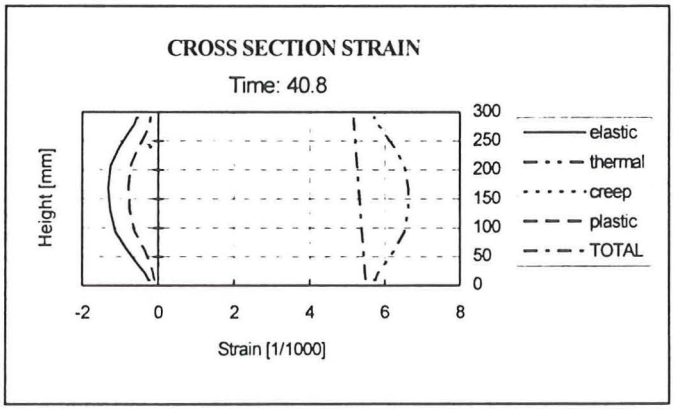

Fig B26 Cross section strain at the fixed end boundary condition, 40.8 minutes after initiation of temperature elevation. Loading: 40% of critical axial buckling load. Slenderness equal to 1.0. Fire exposure on all faces (100%).

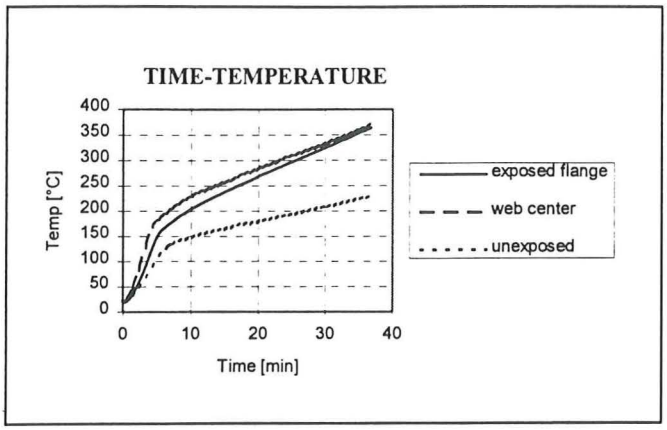

Fig C1 Time temperature development in the flanges and web center. Partial fire exposure (83%).

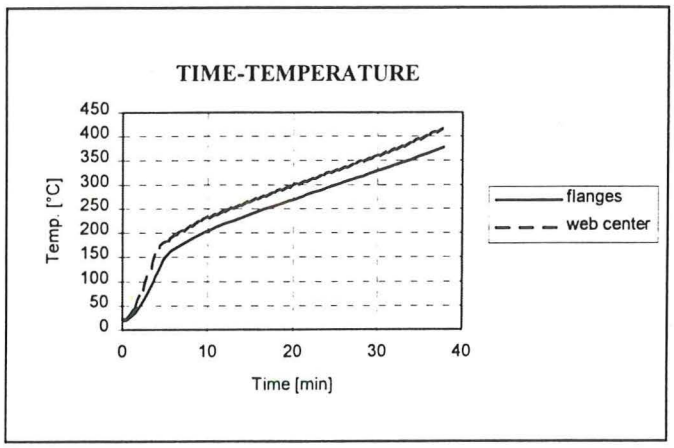

Fig C2 Time temperature development in the flanges and web center. Fire exposure on all faces (100%).

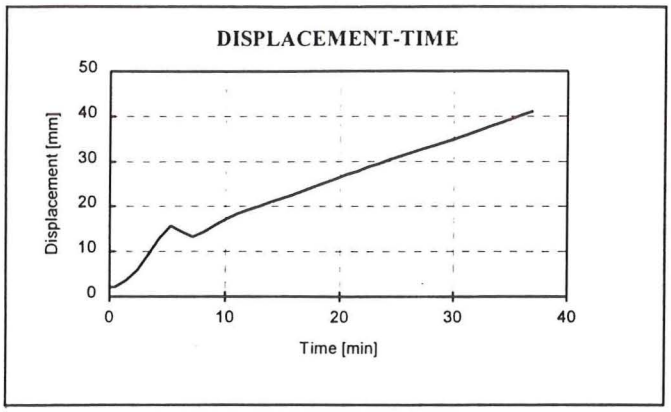

Fig C3 Lateral displacement as function of time at the top of an axially loaded steel column. Loading: 60% of critical axial buckling load. Slenderness equal to 0.5. Partial fire exposure (83%).

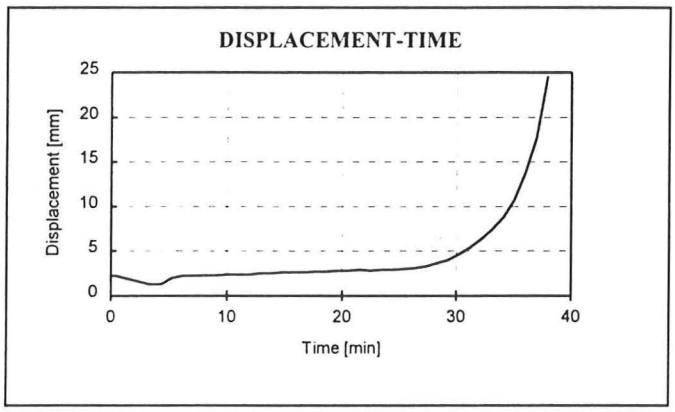

Fig C4 Lateral displacement as function of time at the top of an axially loaded steel column. Loading: 60% of critical axial buckling load. Slenderness equal to 0.5. Fire exposure on all faces (100%).

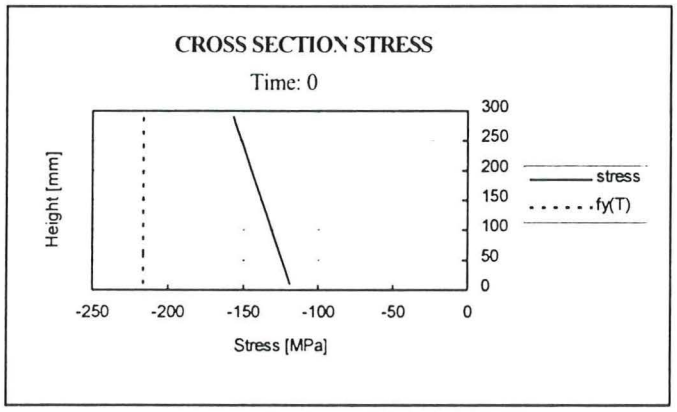

Fig C5 Cross section stress at the fixed end boundary condition, at room temperature. Loading: 60% of critical axial buckling load. Slenderness equal to 0.5.

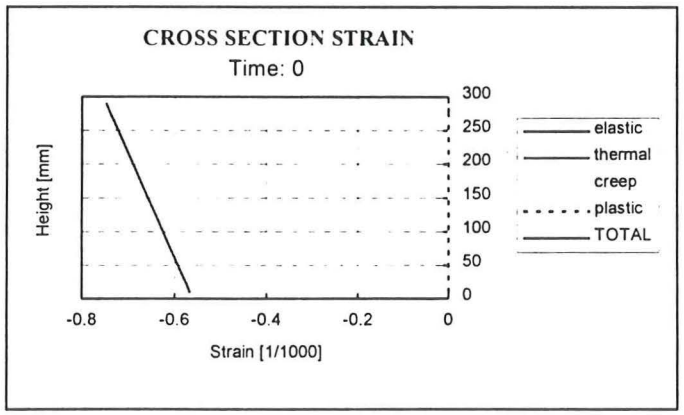

Fig C6 Cross section strain at the fixed end boundary condition, at room temperature. Loading: 60% of critical axial buckling load. Slenderness equal to 0.5.

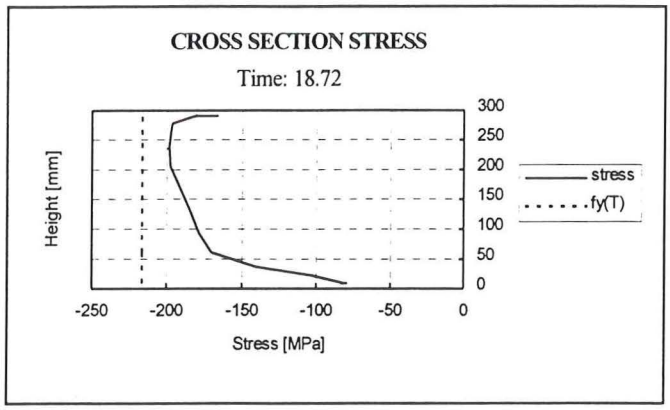

Fig C7 Cross section stress at the fixed end boundary condition, 18.72 minutes after initiation of temperature elevation. Loading: 60% of critical axial buckling load. Slenderness equal to 0.5. Partial fire exposure (83%).

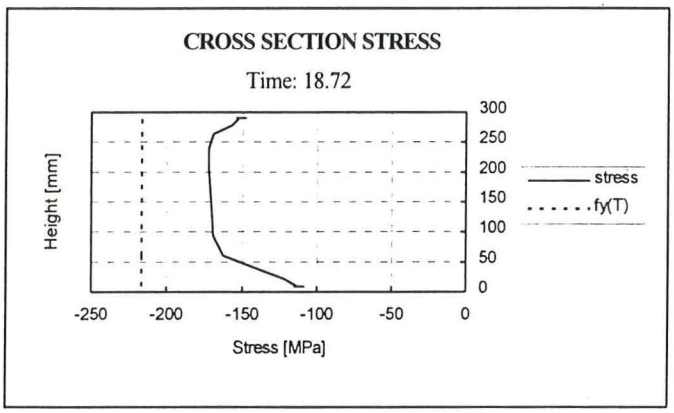

Fig C8 Cross section stress at the fixed end boundary condition, 18.72 minutes after initiation of temperature elevation. Loading: 60% of critical axial buckling load. Slenderness equal to 0.5. Fire exposure on all faces (100%).

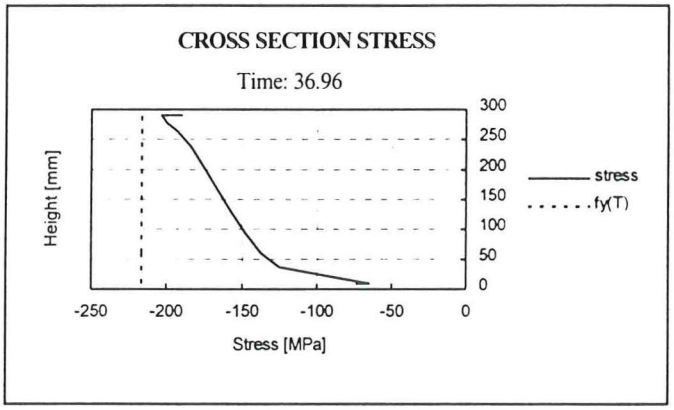

Fig C9 Cross section stress at the fixed end boundary condition, 36.96 minutes after initiation of temperature elevation. Loading: 60% of critical axial buckling load. Slenderness equal to 0.5. Partial fire exposure (83%).

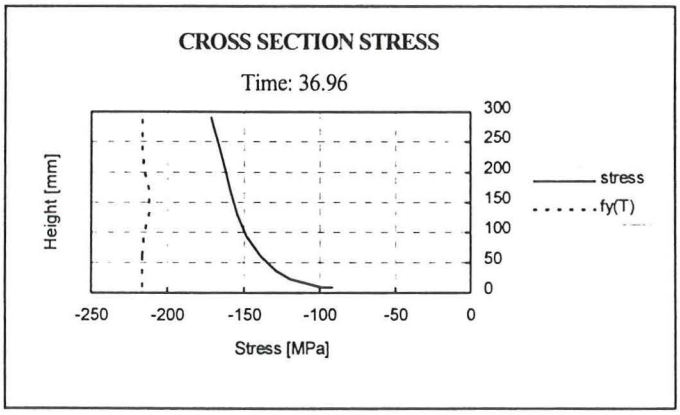

Fig C10 Cross section stress at the fixed end boundary condition, 36.96 minutes after initiation of temperature elevation. Loading: 60% of critical axial buckling load. Slenderness equal to 0.5. Fire exposure on all faces (100%).

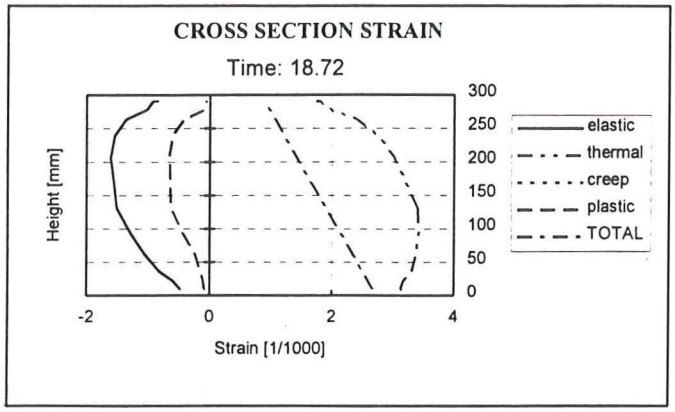

Fig C11 Cross section strain at the fixed end boundary condition, 18.72 minutes after initiation of temperature elevation. Loading: 60% of critical axial buckling load. Slenderness equal to 0.5. Partial fire exposure (83%).

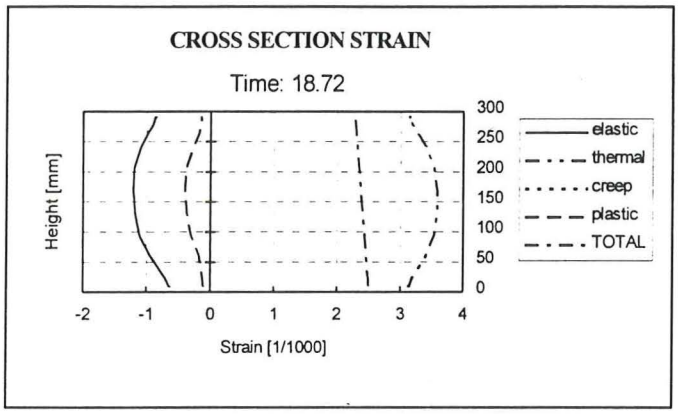

Fig C12 Cross section strain at the fixed end boundary condition, 18.72 minutes after initiation of temperature elevation. Loading: 60% of critical axial buckling load. Slenderness equal to 0.5. Fire exposure on all faces (100%).

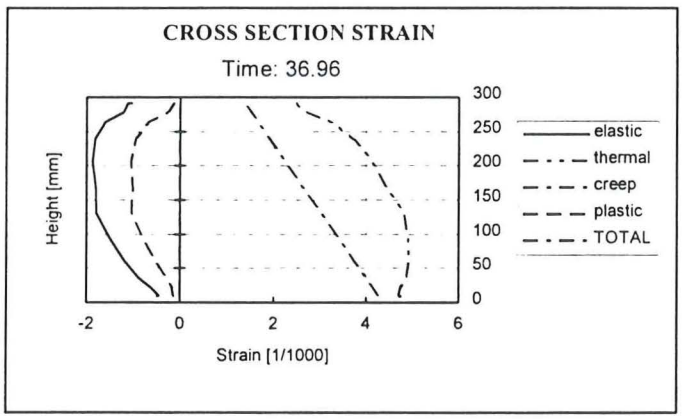

Fig C13 Cross section strain at the fixed end boundary condition, 36.96 minutes after initiation of temperature elevation. Loading: 60% of critical axial buckling load. Slenderness equal to 0.5. Partial fire exposure (83%).

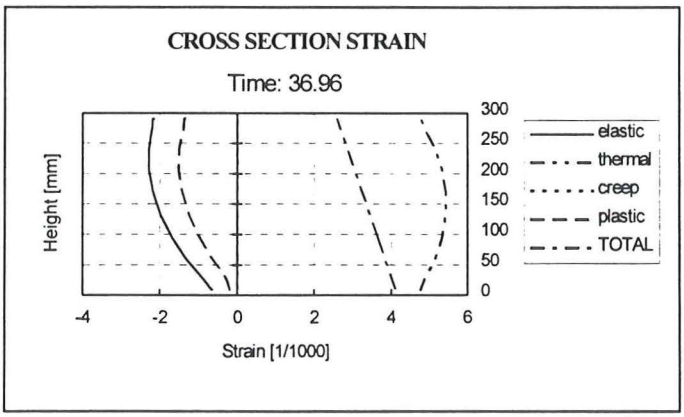

Fig C14 Cross section strain at the fixed end boundary condition, 36.96 minutes after initiation of temperature elevation. Loading: 60% of critical axial buckling load. Slenderness equal to 0.5. Fire exposure on all faces (100%).

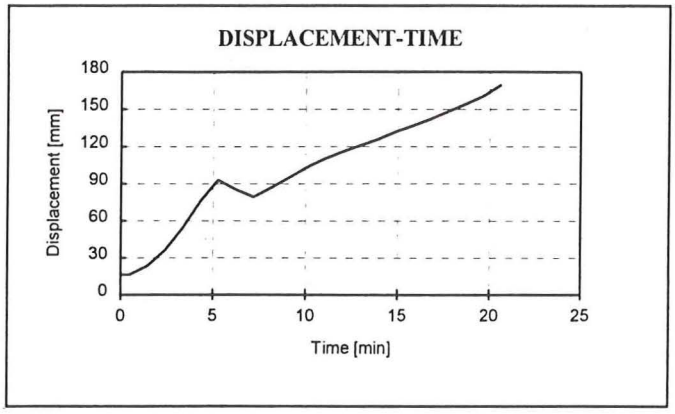

Fig C15 Lateral displacement as function of time at the top of an axially loaded steel column. Loading: 60% of critical axial buckling load. Slenderness equal to 1.0. Partial fire exposure (83%).

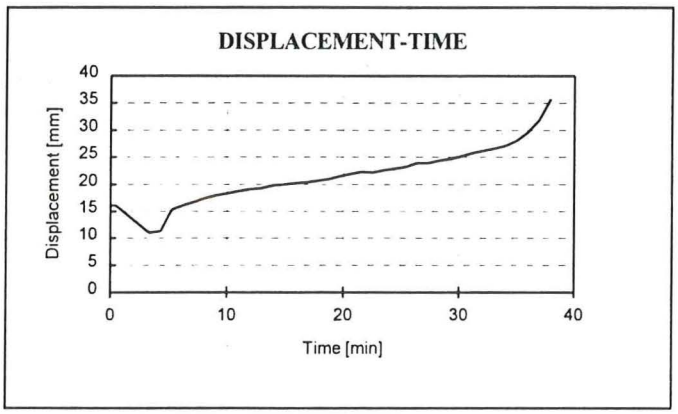

Fig C16 Lateral displacement as function of time at the top of an axially loaded steel column. Loading: 60% of critical axial buckling load. Slenderness equal to 1.0. Fire exposure on all faces (100%).

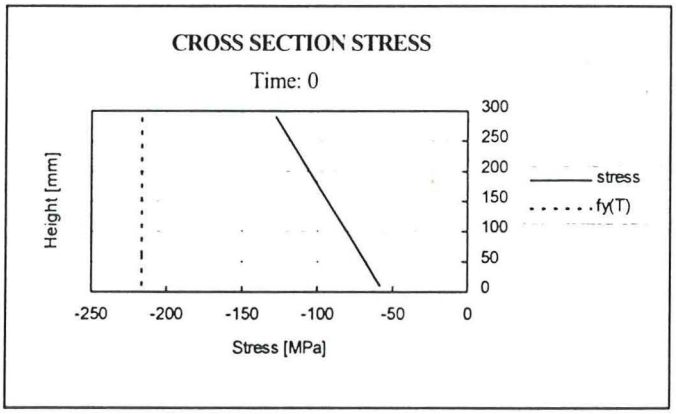

Fig C17 Crossection stress at the fixed end boundary condition, at room temperature. Loading: 60% of critical axial buckling load. Slenderness equal to 1.0.

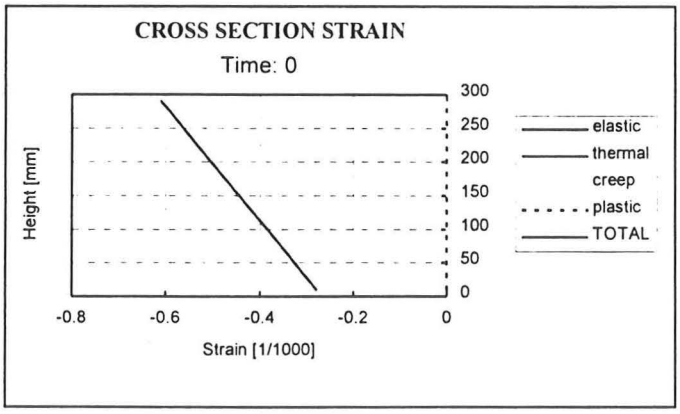

Fig C18 Cross section strain at the fixed end boundary condition, at room temperature. Loading: 60% of critical axial buckling load. Slenderness equal to 1.0.

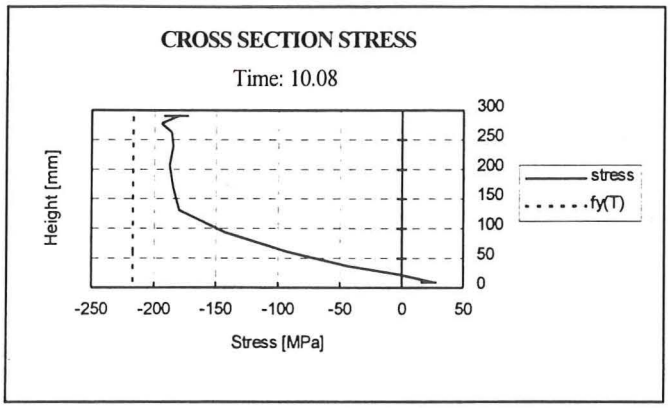

Fig C19 Cross section stress at the fixed end boundary condition, 10.08 minutes after initiation of temperature elevation. Loading: 60% of critical axial buckling load. Slenderness equal to 1.0. Partial fire exposure (83%).

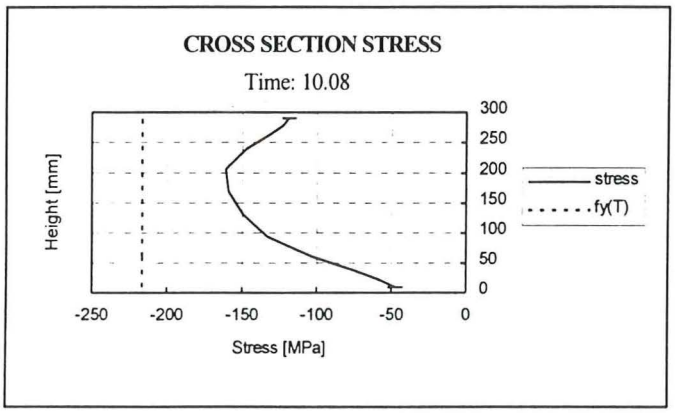

Fig C20 Cross section stress at the fixed end boundary condition, 10.08 minutes after initiation of temperature elevation. Loading: 60% of critical axial buckling load. Slenderness equal to 1.0. Fire exposure on all faces (100%).

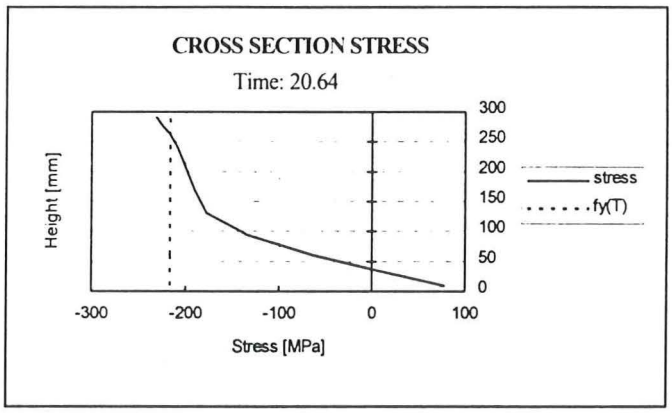

Fig C21 Cross section stress at the fixed end boundary condition, 20.64 minutes after initiation of temperature elevation. Loading: 60% of critical axial buckling load. Slenderness equal to 1.0. Partial fire exposure (83%).

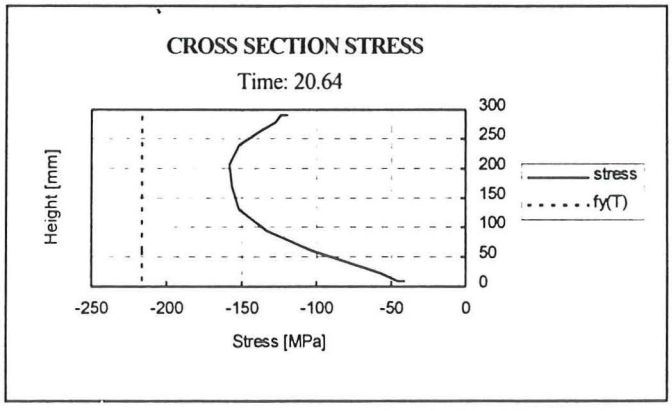

Fig C22 Cross section stress at the fixed end boundary condition, 20.64 minutes after initiation of temperature elevation. Loading: 60% of critical axial buckling load. Slenderness equal to 1.0. Fire exposure on all faces (100%).

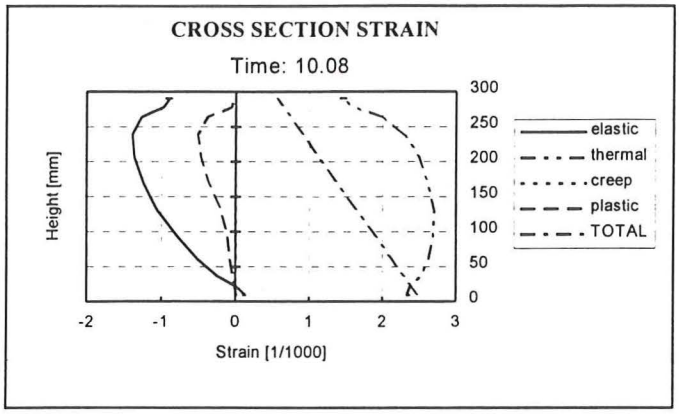

Fig C23 Cross section strain at the fixed end boundary condition, 10.08 minutes after initiation of temperature elevation. Loading: 60% of critical axial buckling load. Slenderness equal to 1.0. Partial fire exposure (83%).

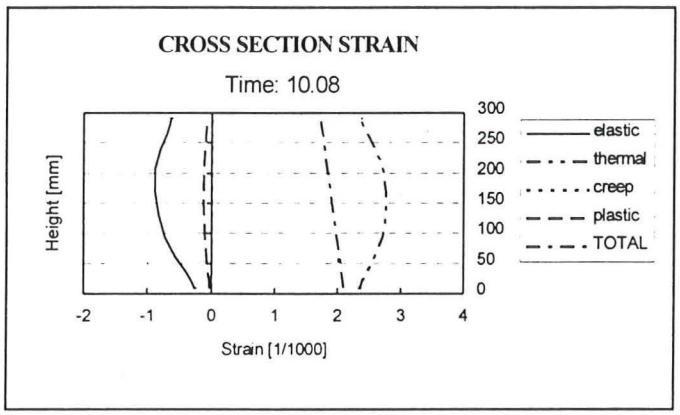

Fig C24 Cross section strain at the fixed end boundary condition, 10.08 minutes after initiation of temperature elevation. Loading: 60% of critical axial buckling load. Slenderness equal to 1.0. Fire exposure on all faces (100%).

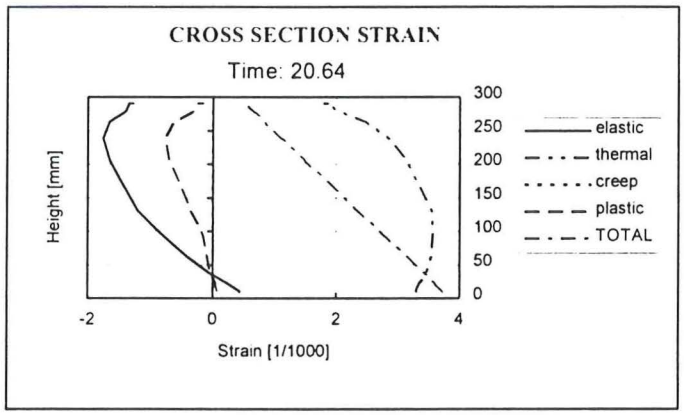

Fig C25 Cross section strain at the fixed end boundary condition, 20.64 minutes after initiation of temperature elevation. Loading: 60% of critical axial buckling load. Slenderness equal to 1.0. Partial fire exposure (83%).

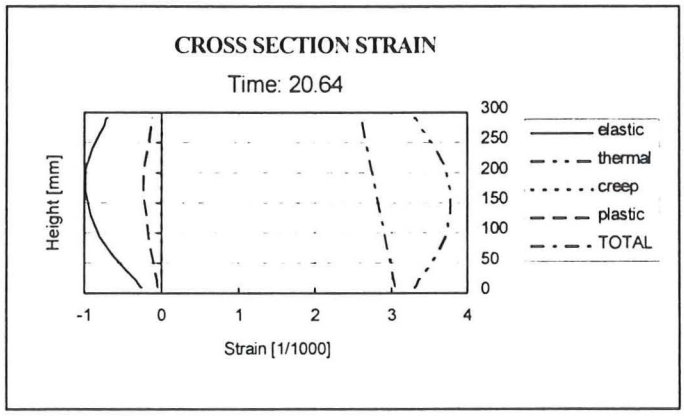

Fig C26 Cross section strain at the fixed end boundary condition, 20.64 minutes after initiation of temperature elevation. Loading: 60% of critical axial buckling load. Slenderness equal to 1.0. Fire exposure on all faces (100%).

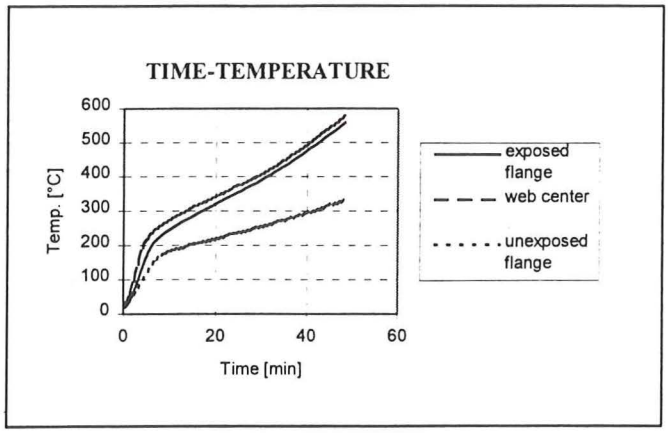

Fig D1 Time temperature develpoment in the flanges and web center. Partial fire exposure (83%).

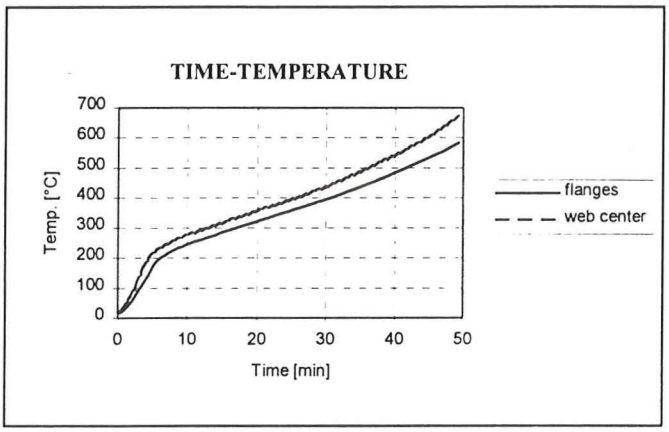

Fig D2 Time temperature develpoment in the flanges and web center. Fire exposure on all faces (100%).

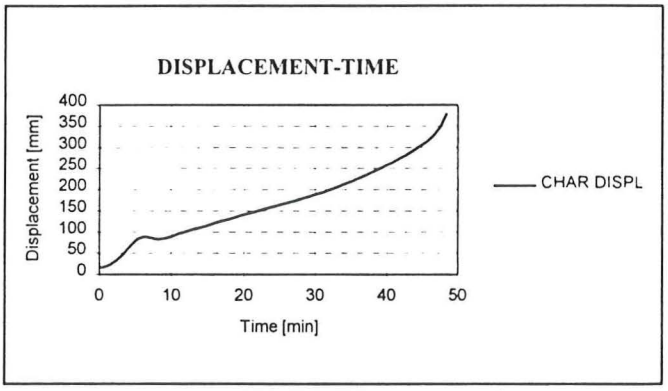

Fig D3 Lateral displacement as function of time at the top of an axially loaded steel column. Loading: 20% of critical axial buckling load. Slenderness equal to 1.0. Additional eccentricity. Partial fire exposure (83%).

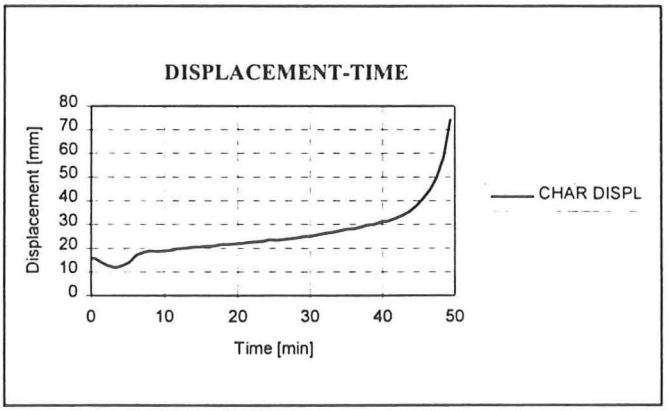

Fig D4 Lateral displacement as function of time at the top of an axially loaded steel column. Loading: 20% of critical axial buckling load. Slenderness equal to 1.0. Additional eccentricity. Fire exposure on all faces (100%).

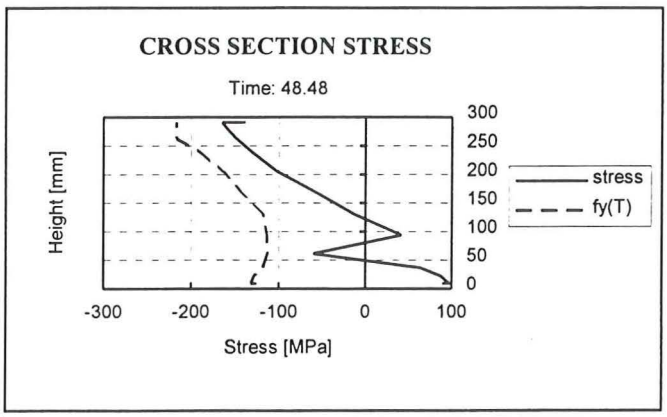

Fig D5 Crossection stress at the fixed end boundary condition, 48.48 minutes after initiation of temperature elevation. Loading: 20% of critical axial buckling load. Slenderness equal to 1.0. Additional eccentricity. Partial fire exposure (83%).

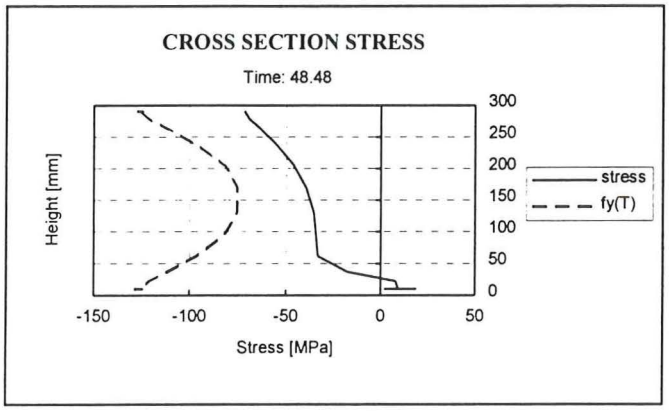

Fig D6 Crossection stress at the fixed end boundary condition, 48.48 minutes after initiation of temperature elevation. Loading: 20% of critical axial buckling load. Slenderness equal to 1.0. Additional eccentricity. Fire exposure on all faces (100%).

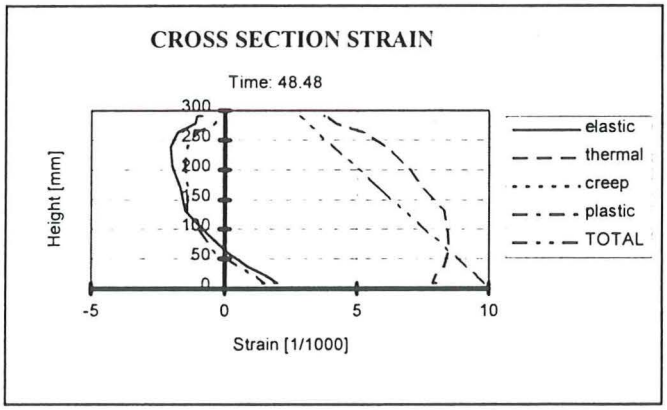

Fig D7 Crossection strain at the fixed end boundary condition, 48.48 minutes after initiation of temperature elevation. Loading: 20% of critical axial buckling load. Slenderness equal to 1.0. Additional eccentricity. Partial fire exposure (83%).

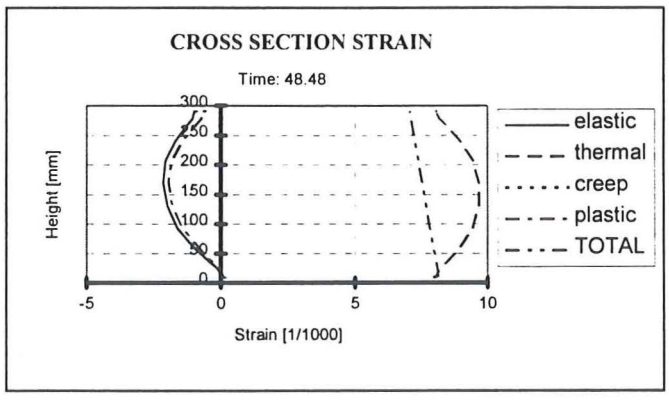

Fig D8 Crossection strain at the fixed end boundary condition, 48.48 minutes after initiation of temperature elevation. Loading: 20% of critical axial buckling load. Slenderness equal to 1.0. Additional eccentricity. Fire exposure on all faces (100%).

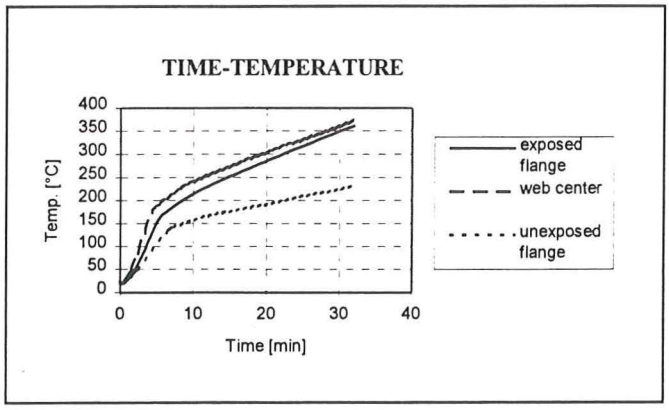

Fig E1 Time temperature develpoment in the flanges and web center. Additional eccentricity. Partial fire exposure (83%).

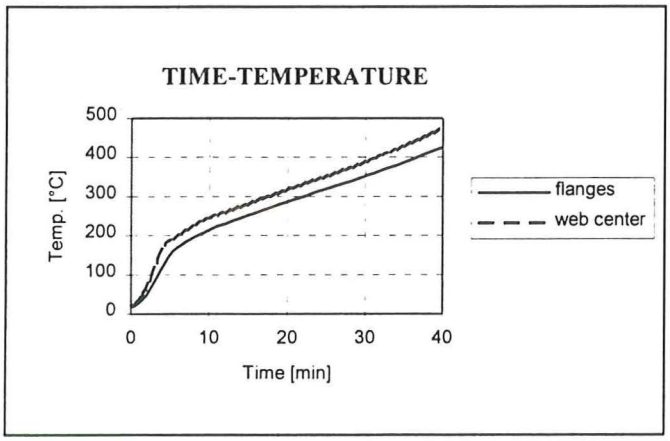

Fig E2 Time temperature develpoment in the flanges and web center. Additional eccentricity. Fire exposure on all faces (100%).

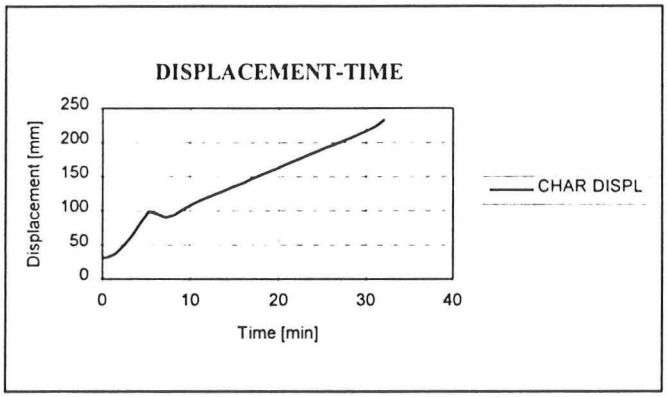

Fig E3 Lateral displacement as function of time at the top of an axially loaded steel column. Loading: 40% of critical axial buckling load. Slenderness equal to 1.0. Additional eccentricity. Partial fire exposure (83%).

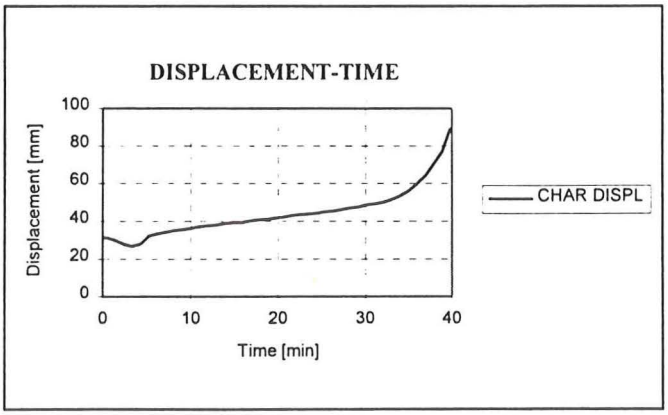

Fig E4 Lateral displacement as function of time at the top of an axially loaded steel column. Loading: 40% of critical axial buckling load. Slenderness equal to 1.0. Additional eccentricity. Fire exposure on all faces (100%).

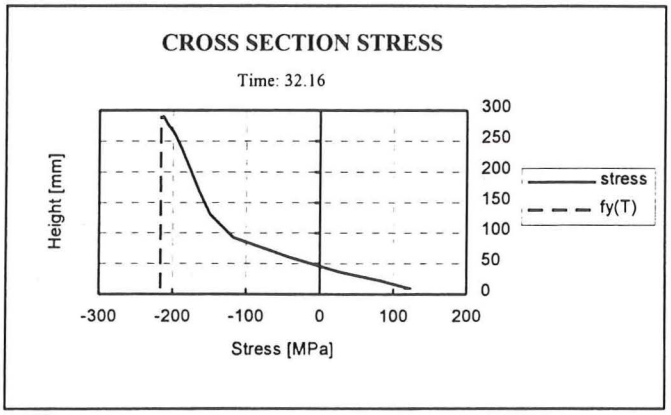

Fig E5 Crossection stress at the fixed end boundary condition, 32.16 minutes after initiation of temperature elevation. Loading: 40% of critical axial buckling load. Slenderness equal to 1.0. Additional eccentricity. Partial fire exposure (83%).

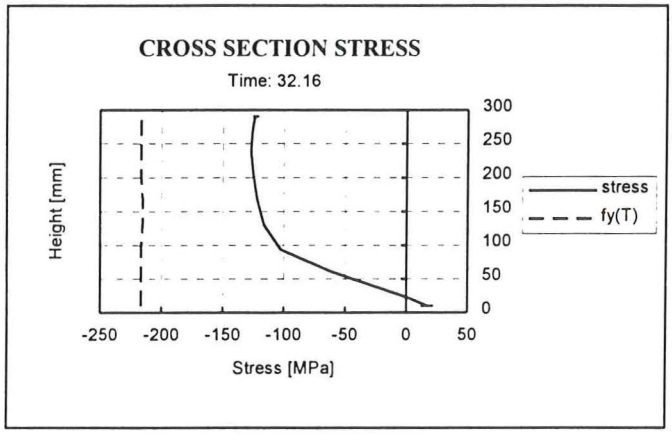

Fig E6 Crossection stress at the fixed end boundary condition, 32.16 minutes after initiation of temperature elevation. Loading: 40% of critical axial buckling load. Slenderness equal to 1.0. Additional eccentricity. Fire exposure on all faces (100%).

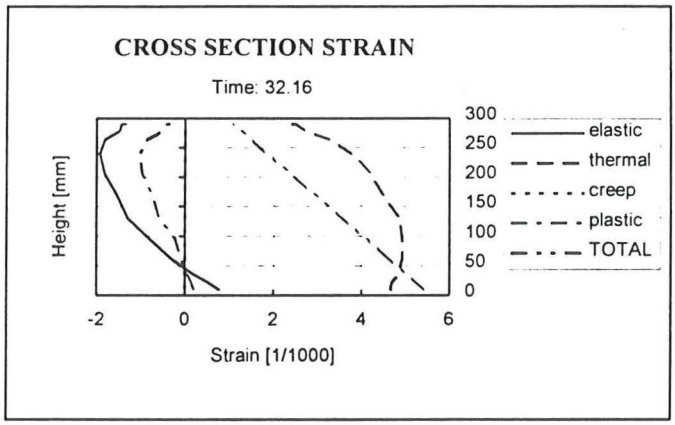

Fig E7 Crossection strain at the fixed end boundary condition, 32.16 minutes after initiation of temperature elevation. Loading: 40% of critical axial buckling load. Slenderness equal to 1.0. Additional eccentricity. Partial fire exposure (83%).

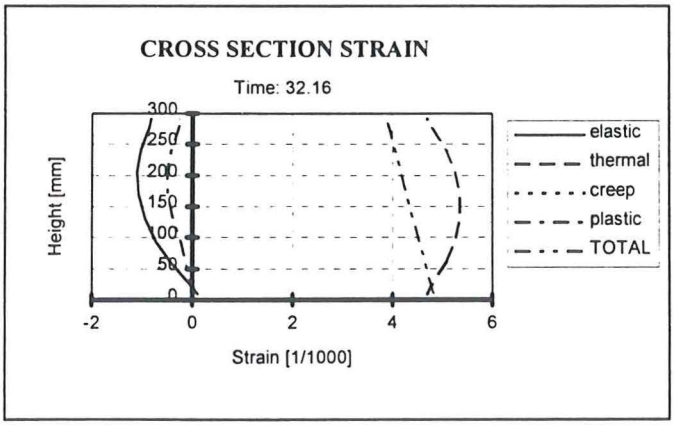

Fig E8 Crossection strain at the fixed end boundary condition, 32.16 minutes after initiation of temperature elevation. Loading: 40% of critical axial buckling load. Slenderness equal to 1.0. Additional eccentricity. Fire exposure on all faces (100%).

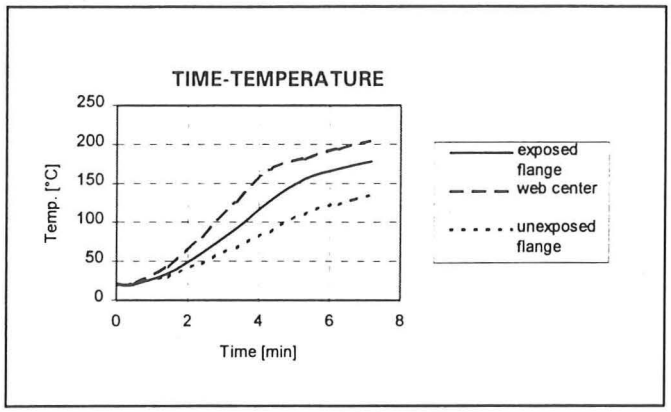

Fig F1 Time temperature develpoment in the flanges and web center. Partial fire exposure (83%).

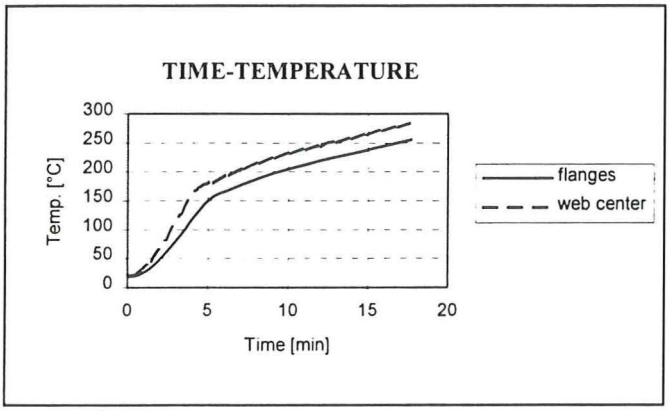

Fig F2 Time temperature develpoment in the flanges and web center. Fire exposure on all faces (100%).

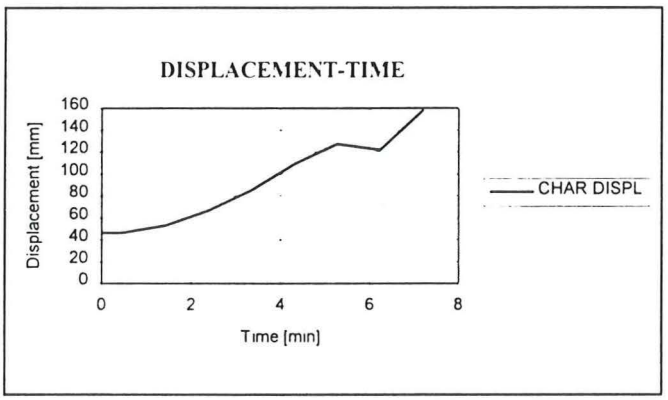

Fig F3 Lateral displacement as function of time at the top of an axially loaded steel column. Loading: 60% of critical axial buckling load. Slenderness equal to 1.0. Additional eccentricity. Partial fire exposure (83%).

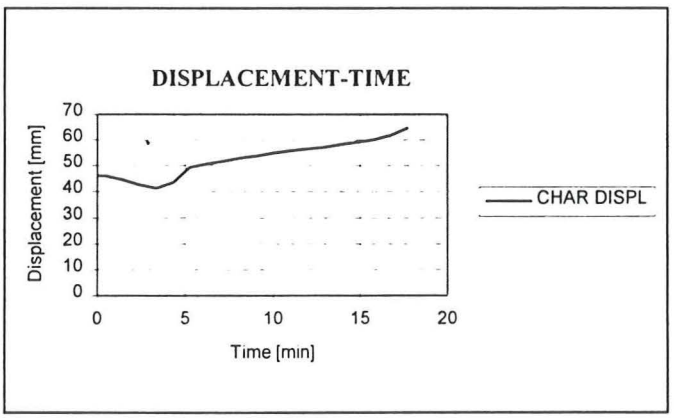

Fig F4 Lateral displacement as function of time at the top of an axially loaded steel column. Loading: 60% of critical axial buckling load. Slenderness equal to 1.0. Additional eccentricity. Fire exposure on all faces (100%).

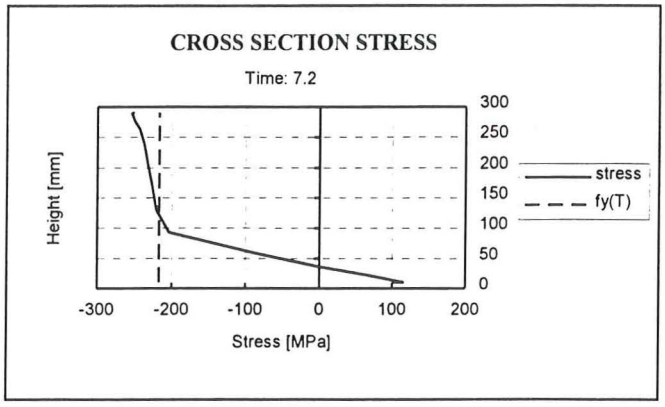

Fig F5 Crossection stress at the fixed end boundary condition, 7.2 minutes after initiation of temperature elevation. Loading: 60% of critical axial buckling load. Slenderness equal to 1.0. Additional eccentricity. Partial fire exposure (83%).

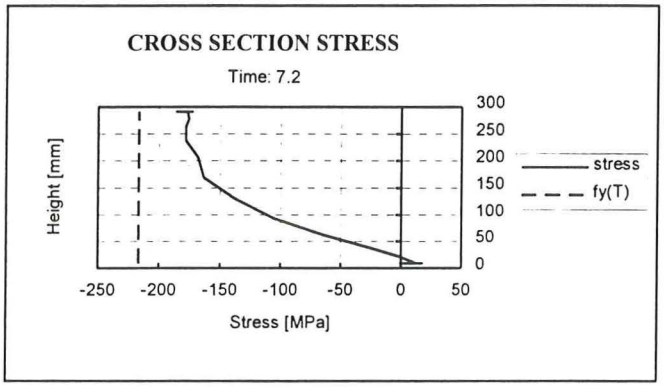

Fig F6 Crossection stress at the fixed end boundary condition, 7.2 minutes after initiation of temperature elevation. Loading: 60% of critical axial buckling load. Slenderness equal to 1.0. Additional eccentricity. Fire exposure on all faces (100%).

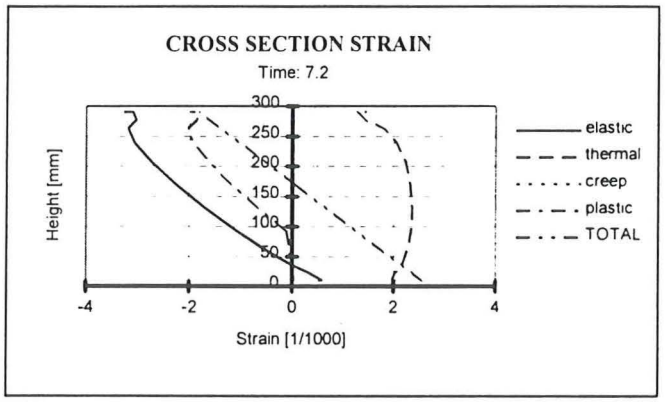

Fig F7 Crossection strain at the fixed end boundary condition, 7.2 minutes after initiation of temperature elevation. Loading: 60% of critical axial buckling load. Slenderness equal to 1.0. Additional eccentricity. Partial fire exposure (83%).

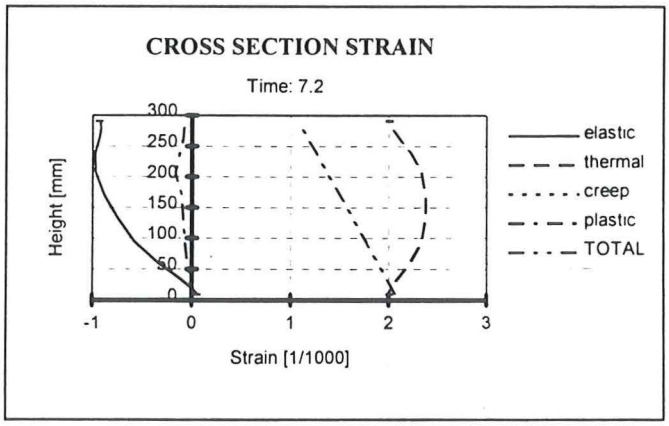

Fig F8 Crossection strain at the fixed end boundary condition, 7.2 minutes after initiation of temperature elevation. Loading: 60% of critical axial buckling load. Slenderness equal to 1.0. Additional eccentricity. Fire exposure on all faces (100%).

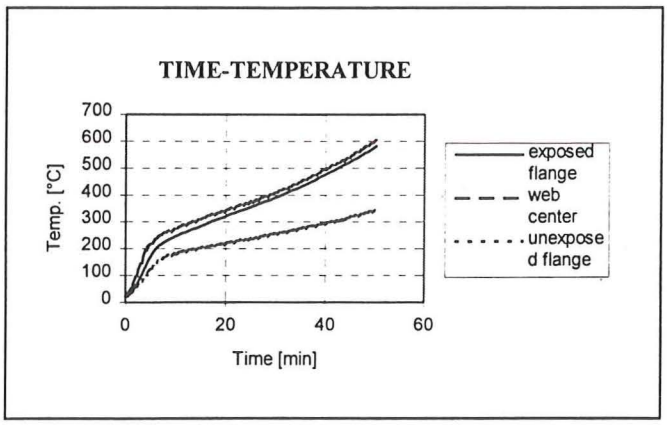

Fig G1 Time temperature develpoment in the flanges and web center. Partial fire exposure (83%).

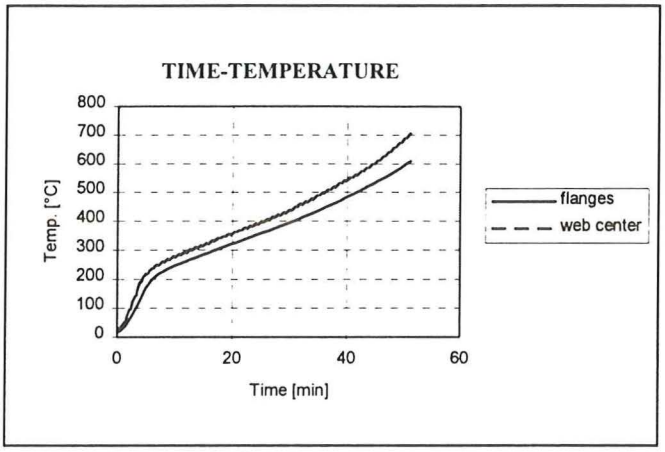

Fig G2 Time temperature develpoment in the flanges and web center. Fire exposure on all faces (100%).

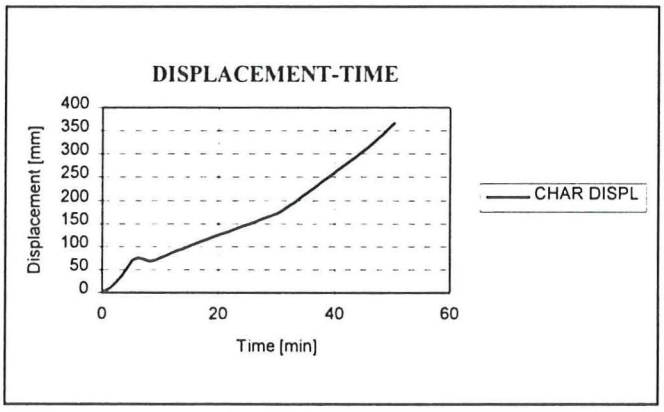

Fig G3 Lateral displacement as function of time at the top of an axially loaded steel column. Loading: 20% of critical axial buckling load. Slenderness equal to 1.0. Restrained elongation. Partial fire exposure (83%).

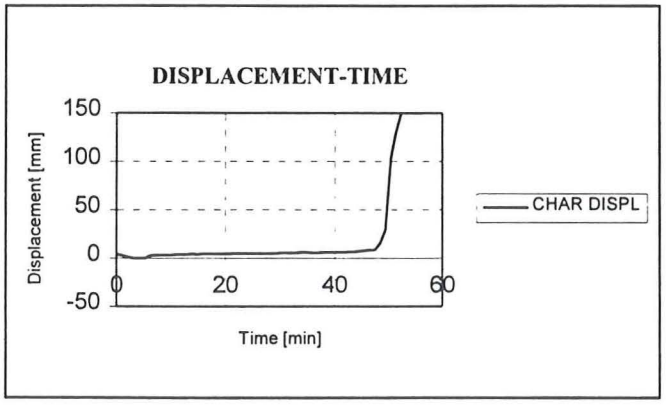

Fig G4 Lateral displacement as function of time at the top of an axially loaded steel column. Loading: 20% of critical axial buckling load. Slenderness equal to 1.0. Restrained elongation. Fire exposure on all faces (100%).

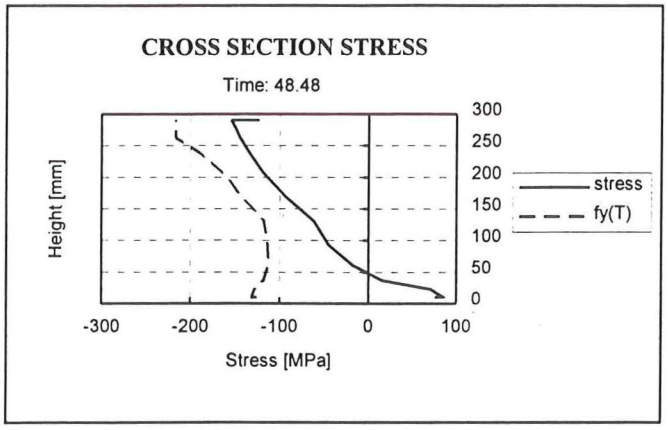

Fig G5 Crossection stress at the fixed end boundary condition, 48.48 minutes after initiation of temperature elevation. Loading: 20% of critical axial buckling load. Slenderness equal to 1.0. Restrained elongation. Partial fire exposure (83%).

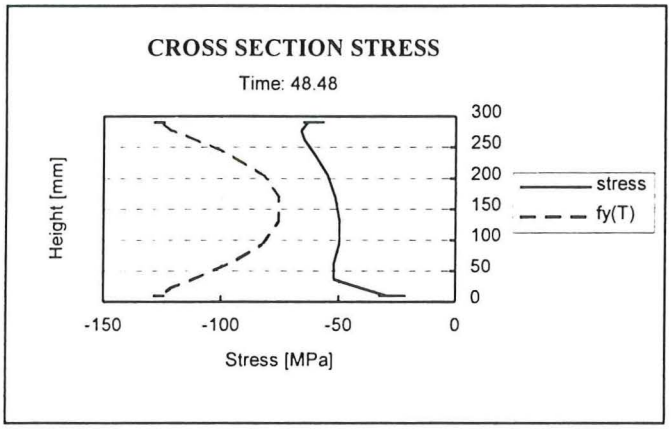

Fig G6 Crossection stress at the fixed end boundary condition, 48.48 minutes after initiation of temperature elevation. Loading: 20% of critical axial buckling load. Slenderness equal to 1.0. Restrained elonation. Fire exposure on all faces (100%).

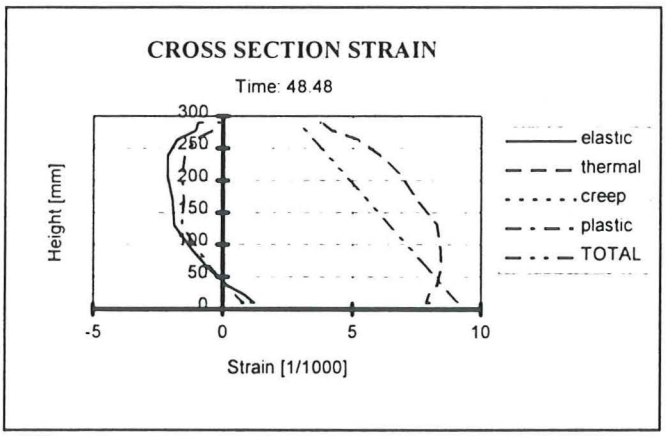

Fig G7 Crossection strain at the fixed end boundary condition, 48.48 minutes after initiation of temperature elevation. Loading: 20% of critical axial buckling load. Slenderness equal to 1.0. Restrained elongation. Partial fire exposure (83%).

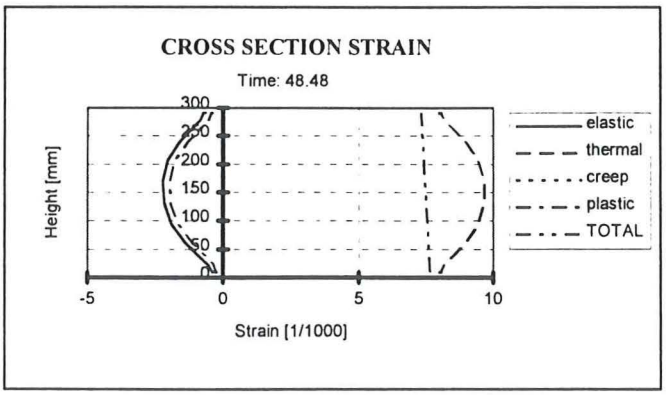

Fig G8 Crossection strain at the fixed end boundary condition, 48.48 minutes after initiation of temperature elevation. Loading: 20% of critical axial buckling load. Slenderness equal to 1.0. Restrained elongation. Fire exposure on all faces (100%).

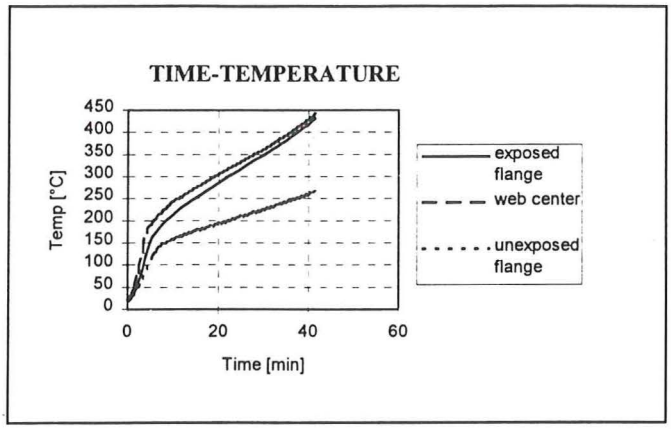

Fig H1 Time temperature develpoment in the flanges and web center. Partial fire exposure (83%).

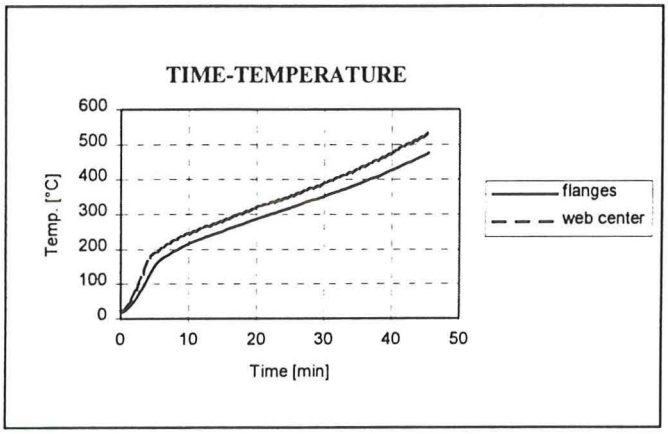

Fig H2 Time temperature develpoment in the flanges and web center. Fire exposure on all faces (100%).

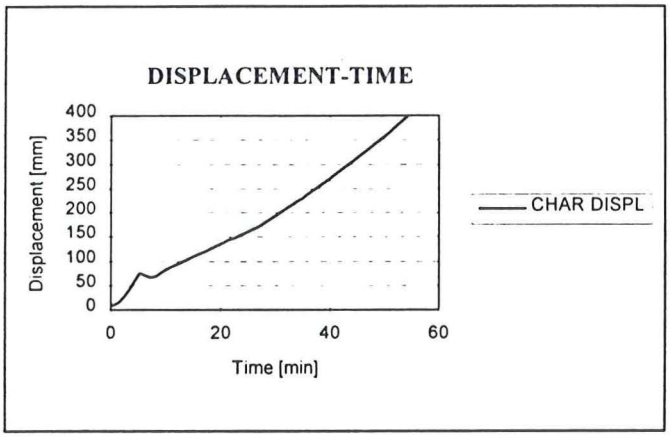

Fig H3 Lateral displacement as function of time at the top of an axially loaded steel column. Loading: 40% of critical axial buckling load. Slenderness equal to 1.0. Restrained elongation. Partial fire exposure (83%).

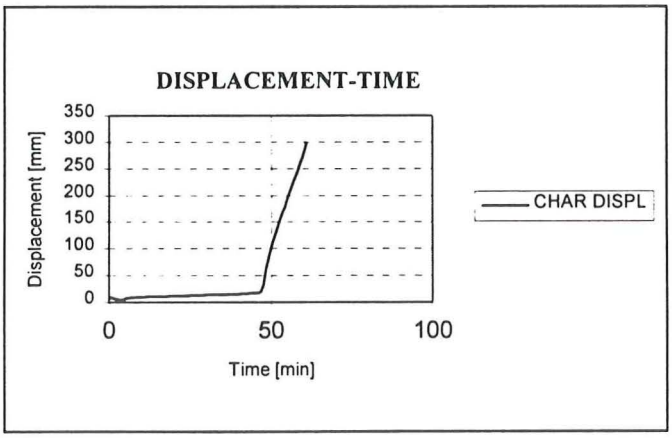

Fig H4 Lateral displacement as function of time at the top of an axially loaded steel column. Loading: 40% of critical axial buckling load. Slenderness equal to 1.0. Restrained elongation. Fire exposure on all faces (100%).

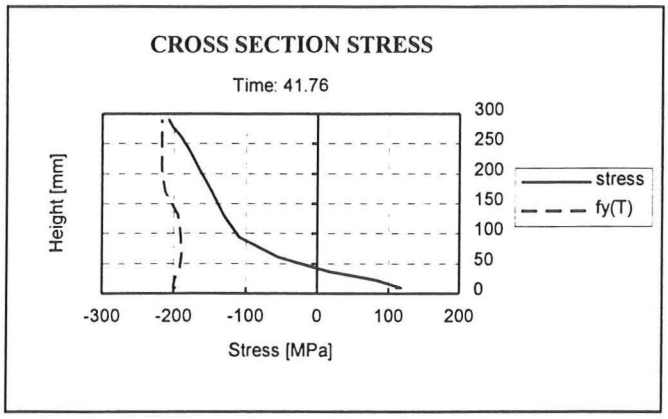

Fig H5 Crossection stress at the fixed end boundary condition, 41.76 minutes after initiation of temperature elevation. Loading: 40% of critical axial buckling load. Slenderness equal to 1.0. Restrained elongation. Partial fire exposure (83%).

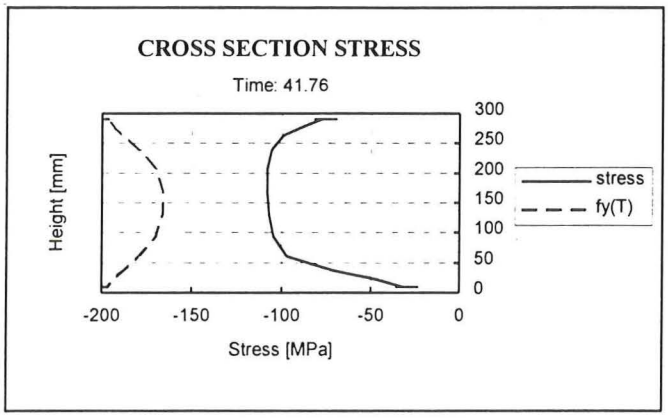

Fig H6 Crossection stress at the fixed end boundary condition, 41.76 minutes after initiation of temperature elevation. Loading: 40% of critical axial buckling load. Slenderness equal to 1.0. Restrained elonation. Fire exposure on all faces (100%).

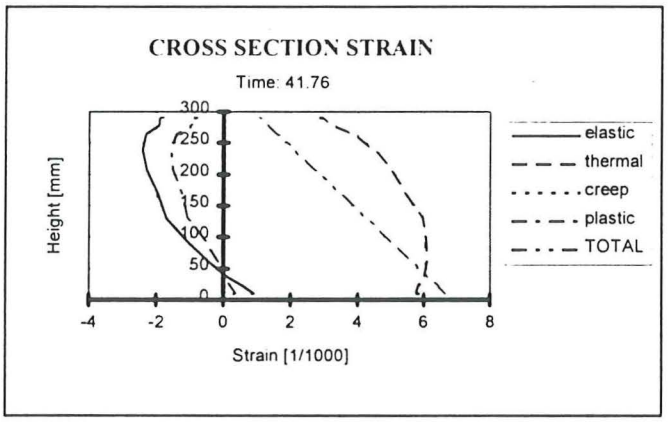

Fig H7 Crossection strain at the fixed end boundary condition, 41.76 minutes after initiation of temperature elevation. Loading: 40% of critical axial buckling load. Slenderness equal to 1.0. Restrained elongation. Partial fire exposure (83%).

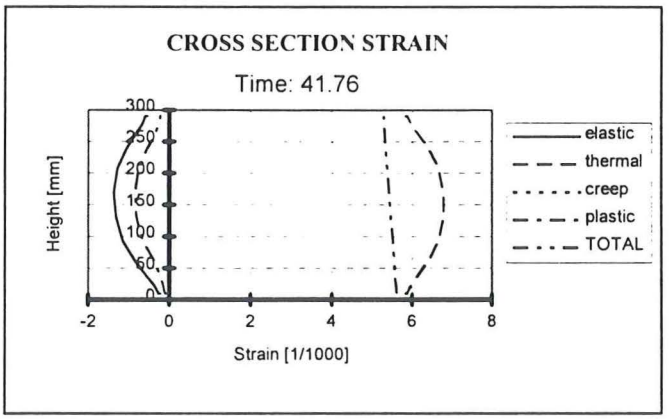

Fig H8 Crossection strain at the fixed end boundary condition, 41.76 minutes after initiation of temperature elevation. Loading: 40% of critical axial buckling load. Slenderness equal to 1.0. Restrained elonation. Fire exposure on all faces (100%).

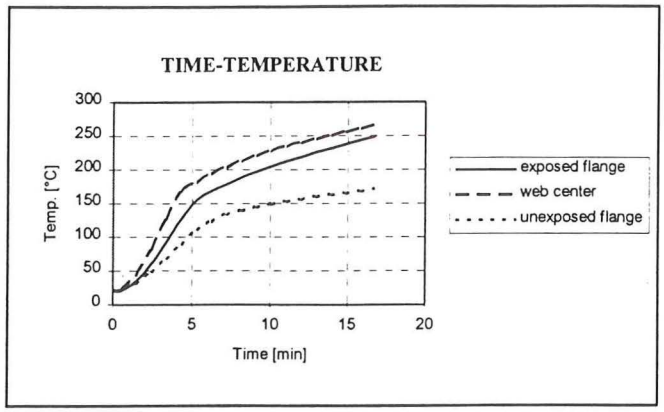

Fig I1 Time temperature develpoment in the flanges and web center. Partial fire exposure (83%).

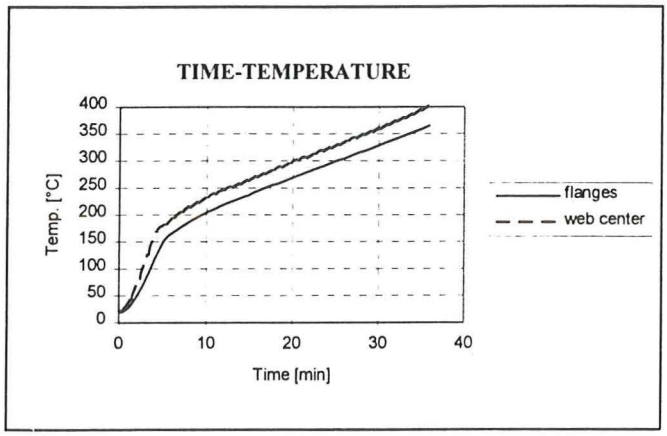

Fig I2 Time temperature develpoment in the flanges and web center. Fire exposure on all faces (100%).

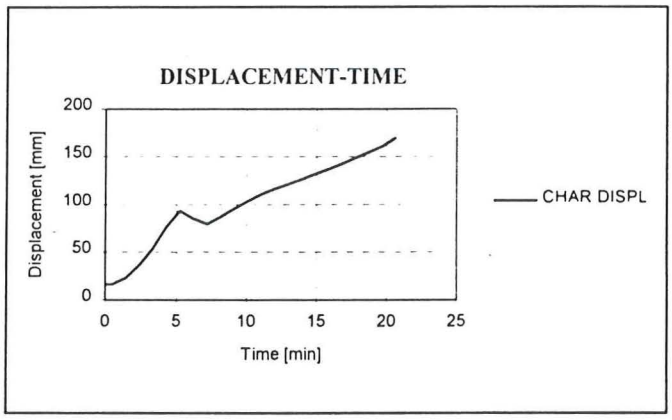

Fig I3 Lateral displacement as function of time at the top of an axially loaded steel column. Loading: 60% of critical axial buckling load. Slenderness equal to 1.0. Restrained elongation. Partial fire exposure (83%).

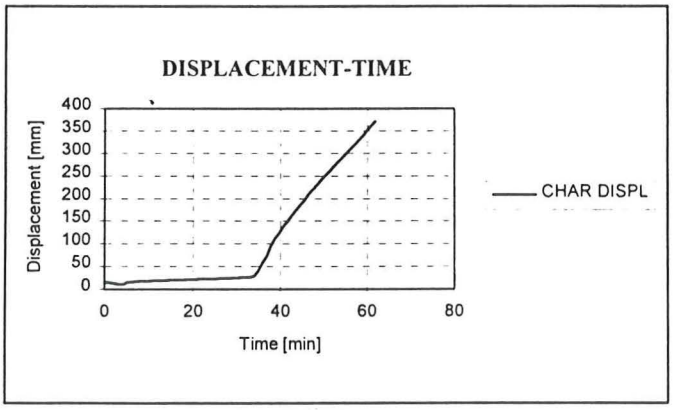

Fig I4 Lateral displacement as function of time at the top of an axially loaded steel column. Loading: 60% of critical axial buckling load. Slenderness equal to 1.0. Restrained elongation. Fire exposure on all faces (100%).

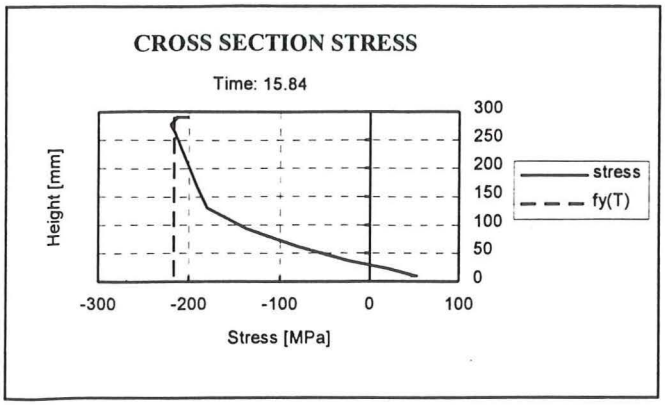

Fig I5 Crossection stress at the fixed end boundary condition, 15.84 minutes after initiation of temperature elevation. Loading: 60% of critical axial buckling load. Slenderness equal to 1.0. Restrained elongation. Partial fire exposure (83%).

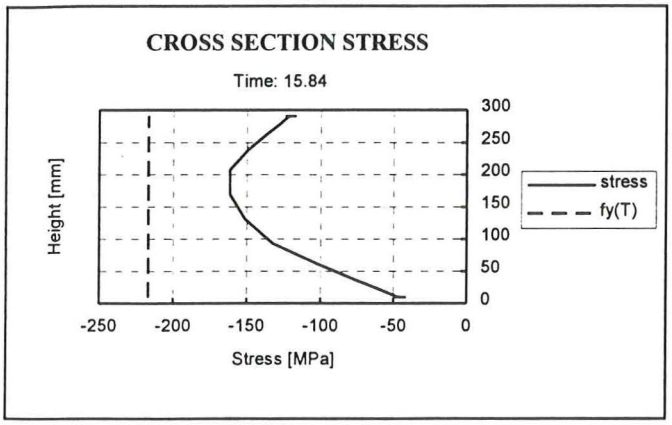

Fig I6 Crossection stress at the fixed end boundary condition, 15.84 minutes after initiation of temperature elevation. Loading: 60% of critical axial buckling load. Slenderness equal to 1.0. Restrained elongation. Fire exposure on all faces (100%).

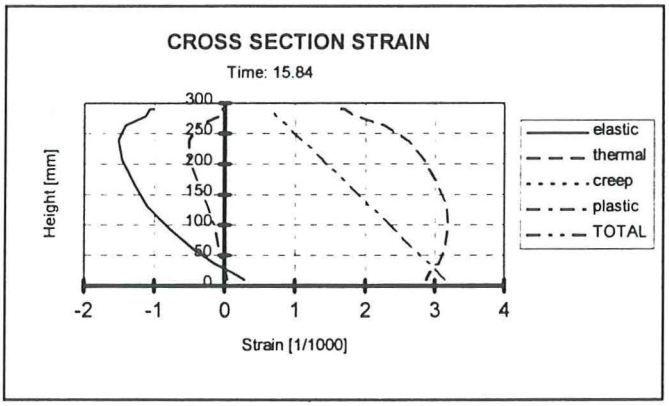

Fig I7 Crossection strain at the fixed end boundary condition, 15.84 minutes after initiation of temperature elevation. Loading: 60% of critical axial buckling load. Slenderness equal to 1.0. Restrained elongation. Partial fire exposure (83%).

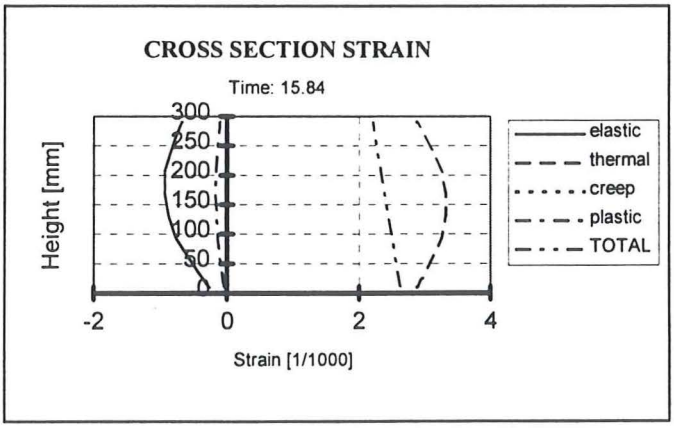

Fig I8 Crossection strain at the fixed end boundary condition, 15.84 minutes after initiation of temperature elevation. Loading: 60% of critical axial buckling load. Slenderness equal to 1.0. Restrained elonation. Fire exposure on all faces (100%).